POLITECNICO
MILANO 1863

POLITECNICO DI MILANO

Department of Electrical Engineering

Master of Science (MSc) in Electrical Engineering

Track: Smart Grids

Modeling of LVDC Distribution System: An Assessment of Control, Power Quality, and DC Faults

Supervisor: Prof. Morris Brenna

Co-Supervisor: Prof. Enrico Ragaini

Masters Dissertation of:

Faheem Ghazanfar

Matricola: 883082

Academic Year 2018-2019

Dedicated to

my respected family members, who have had a gigantic influence on my life, my success, and my abundance.

Acknowledgments

The author would like to thank Professor Morris Brenna and Professor Enrico Ragaini who have supported me with great patience and knowledge throughout this dissertation. They consistently allowed research and guidelines to write this thesis, to be my own work but always steered me in the right direction whenever I needed.

Abstract

The main objective of this dissertation is to design, control, and perform power quality studies in the VSC-LVDC domain. A major proportion of the investigation focuses on the poorly damped controllers and instability which linked to DC side resonance. Initially, a graphical tuning method is used to modeled two-terminal VSC-LVDC connection to find centroids of stability regions in the controller parameter space.

Time-domain simulation models are implemented in the Simulink environment. The model integrates analytical equations that describe the behavior of the network components and power flow calculations. Meanwhile, the power quality measurements and harmonic pollution on the DC network are analyzed. Further, the network behavior during transients is analyzed and verified that the proposed model is stable during large-scale perturbations.

Finally, the studies are performed in LVDC network faults, with the main objective of proposing advanced control strategies that can offer robust performance during steady-state and transient conditions, while improved power flow and direct voltage handling capabilities. The advantageous properties of the proposed controllers are proven through simulations under different fault conditions, in which their performance compared to their conventional counterparts are shown.

Keywords: LVDC, VSC, Control, Power quality, Transient, Fault

Sommario

L'obiettivo principale di questa tesi è progettare, controllare ed eseguire studi sulla qualità dell'alimentazione nel dominio VSC-LVDC. Una parte importante dell'indagine si concentra sui controller scarsamente smorzati e sull'instabilità collegati alla risonanza del lato DC. Inizialmente, viene utilizzato un metodo di ottimizzazione grafico per modellare la connessione VSC-LVDC a due terminali per trovare i centroidi delle regioni di stabilità nello spazio dei parametri del controller.

I modelli di simulazione nel dominio del tempo sono implementati nell'ambiente Simulink. Il modello integra equazioni analitiche che descrivono il comportamento dei componenti di rete e i calcoli del flusso di potenza. Nel frattempo, vengono analizzate le misurazioni della qualità dell'alimentazione e l'inquinamento armonico sulla rete DC. Inoltre, il comportamento della rete durante i transitori viene analizzato e verificato che il modello proposto sia stabile durante le perturbazioni su larga scala.

Infine, gli studi vengono condotti su guasti della rete LVDC, con l'obiettivo principale di proporre strategie di controllo avanzate in grado di offrire prestazioni affidabili in condizioni di regime e transitorio, migliorando al contempo il flusso di potenza e le capacità di gestione della tensione diretta. Le proprietà vantaggiose dei controller proposti sono dimostrate attraverso simulazioni in diverse condizioni di errore, in cui sono mostrate le loro prestazioni rispetto alle loro controparti convenzionali.

Parole chiave: LVDC, VSC, Controllo, Qualità dell'alimentazione, Transitorio, Guasto

Contents

List of Figures

List of Tables

Introduction

Environmental changes and global warming concerns initiated a path towards the renewable generation, in the form of PV and wind farms power plants. Furthermore, the increasing popularity of small-scale generation (DGs) and plug-in hybrid electric vehicles (PHEV) causes perturbation in the existing LVAC network. In addition, the number of power electronic devices, such as induction cookers, washing machines with inverter control and LED lamps, has increased rapidly in residential homes. Last, but not least, the traditional AC distribution systems have played a key role in electricity distribution for the last century. Consequent, smoothing peaks of power generation & matching generation with loads, advanced network management & control over the small-scale generation, and aging of the traditional electricity distribution network offers an opportunity to implement new solutions in which reliability and power quality of distribution systems are taken to the next level.

To cope with the growing concerns, a worldwide move toward smart grids has started, with their increasing number of communication and measurement devices in the network with an objective of distributed generations and load management. Along with the benefits (higher efficiency, lower power losses, higher power transfer capabilities of cables, ease of synchronization, and higher reliability, etc.) of DC distribution system as compared to their counterpart traditional AC distribution system. Hence, the DC microgrids is an approach that brings new features and benefits to the distribution network which enables efficient integration of renewable energy reserves (DERs) and permits advanced management of load.

In consideration of the prevailing technical, and societal context, an LVDC distribution network might be a realistic and effective solution for future electricity distribution.

This dissertation addresses a power distribution solution developed at Politecnico di Milano, based on DC technology and power electronics devices: a low-voltage direct current (LVDC) distribution network (± 500 Vdc with 1.1 MVA power capacity). The concept of the LVDC distribution network is based on two voltage sourced converters (VSC). The proposed concept has techno-economic potential, as mentioned in chapter 2. This network is different from the traditional LVAC distribution network, and therefore, special attention has to be paid on power quality, protection and safety issues in the system. The impact of the low-voltage DC (LVDC) distribution system on reliability, life cycle costs have been calculated, and the system has been shown to be economically advantageous. Moreover, the modeling of a grid-connected and customer-end inverter along with the filtering have been discussed. Furthermore, a comprehensive analysis of the power quality, network transient behavior, and LVDC network faults are presented in the dissertation.

The details of each chapter of this dissertation are the following:

Chapter 1: Introduce the state of the art LVDC microgrids. It provides all-inclusive details about LVDC network topology, voltage standards, different power electronic conversion devices, DC cables, and protection devices to form a DC grid.

Chapter 2: It provides techno-economic benefits and real-time applications of DC distribution system. A comparison between traditional LVAC and LVDC distribution systems has made based on power losses, personnel safety, maximum power transfer capacity of the cable, ease of synchronization, efficiency, and reliability of the distribution systems.

Chapter 3: LVDC modeling, operation, and control section deal with the network basic components, voltage sourced converters (VSCs) operation, power transfer capability of the system, and the network control scheme. The control strategy of each individual control loop (inner current loop, phase-locked loop, active and reactive power, and voltage loop) have modeled.

Chapter 4: In this section, the network transient and dynamic state stability have analyzed in time-domain with the help of the Simulink tool. Fast Fourier Transform (FFT) analysis tool in the Powergui module is used for inverter-end power quality analysis. It also

shows the actual measurements of the AC side bus and DC side bus voltages and currents of the network under normal operation.

Chapter 5: Last section, the study based on the types of DC network faults, grounding schemes for DC network, and available protection devices for LVDC network. Along with possible LVDC network faults (pole to pole, pole to the ground, DC side capacitor failure, and customer-end inverter AC bus faults) has studied.

In the last part of the dissertation, the summarises of most relevant results, and suggestions for possible further studies are discussed.

CHAPTER 1

State of the Art LVDC Distribution System

This chapter has concerned with the state of art in the LVDC distribution system. It begins with LVDC network topology, types of power electronics conversion, grounding and protection, types of cables, power quality, DC microgrids, distribution generation, energy storage systems and main advantages of DC network which drives toward the development of the Low Voltage Direct Current (LVDC) distribution system.

In general, the LVDC distribution system combines generation, power electronics, DC distribution, and protections. These are the key enablers for grid services to ensure flawless operation and compatibility within the network. The main objectives behind the development of LVDC distribution network; to Improve the power quality & security of supply experienced by the electricity end-users, economical electricity distribution, flexibility, robust point of common coupling (PCC) for small scale generations, and develop infrastructure for interactive & intelligent distribution network [1]. The main advantages of DC distribution systems are:

- **System Efficiency:** The system efficiency is higher than the AC distribution system because of the reduction of conversion losses of inverters between DC output source and loads.

- **Easier Composition:** There is no need for synchronization (frequency & phase), no skin effect and reactive power in the DC system.
- **Integration with Renewable Energy Sources (RES):** In DC system, distributed energy sources such as photovoltaic (PV), and fuel cells generate DC energy thus the first conversion stage (AC/DC) is neglected and saves between 2.5% to 10% of developed energy. Hence, It offers simple integration of renewable energy sources with the DC network.
- **Environmental Benefits:** Electricity production poses a strong impact on the environment, which is responsible for a major portion of carbon dioxide (CO_2) emission. By increasing the use of renewable energy sources to produce emission-free electricity would also be a solution to global warming and the reduction in fossil fuels [2].
- **Power Quality:** The DC system is simpler, less power conversion units as compared to AC distribution system and due to the absence of reactive current component, the same active power drawn by the load results lower current magnitude, and lower losses. So, the power quality is much higher than the AC distribution system.
- **Reduction of Unnecessary Loss:** The DC distribution system is simple and can avoid many conversion steps. Due to the absence of reactive current component, the same active power is drawn by the load results in lower current magnitude, so lower system losses as compared to the conventional AC distribution system.

1.1 LVDC Distribution Concept

The LVDC distribution system is the last section of the electricity distribution network. It replaces the medium voltage (MV) network branches, provides higher transmission capacity as compared with the low voltage AC distribution line and have almost similar components such as cables & protection devices. Furthermore, the LVDC distribution system is based on power electronics device [3]. To apply DC distribution into existing AC distribution system, few conditions such as topologies, connections types of the system, and power electronic converters should be considered in advanced.

1.1.1 Network Topology

Electrical distribution networks can be divided into radial or ring structure. In a radial network, loads are supplied via one route however in ring networks loads have more than one route of supply. The low voltage networks are nearly built-in radial form. The ring structure improves the reliability & continuity of service to end-users during fault situations since it is possible to provide electricity through several routes.

Typical LVDC distribution system constructs of AC grid, 3-phase transformer, power electronic converters and DC link between the converters. The transformer uses to step down the voltage, to provide isolation from the AC grid and minimize the voltage drop in the low voltage system. The topology of the LVDC distribution system can have different configuration according to location and number of end-users. In the most common topology, the AC/DC conversion unit is always located near the traditional grid. The distribution system can be either a wide LVDC distribution district or HVDC link type network according to the DC/AC conversion unit location. The wide LVDC distribution district can be compared to existing LVAC network topology with multiple branches. In this case, there is no need for separate 3-phase AC network because the AC lines have been replaced with DC lines.

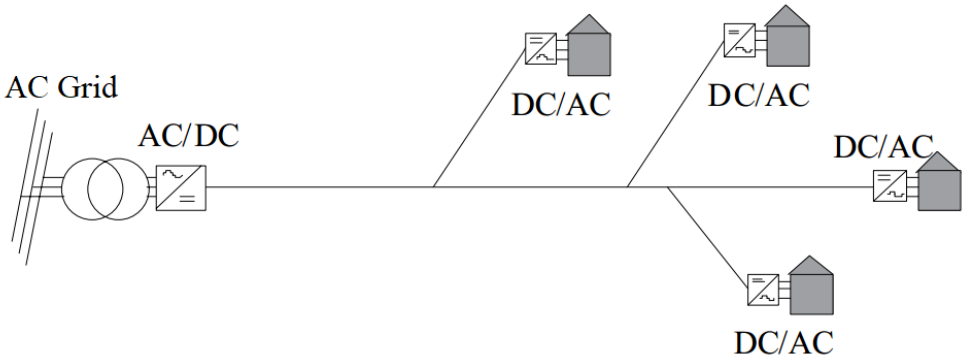

Figure 1.1 - Wide LVDC distribution network [4]

The HVDC link type network constructs of single DC line which interconnects with two separate AC networks. In this kind of network, the end-users are connected to a common 3-phase LVAC network. The DC link must be connected to customer AC network via a

transformer to ensure suitability with the existing AC system. LVDC link distribution system is shown in figure 1.2:

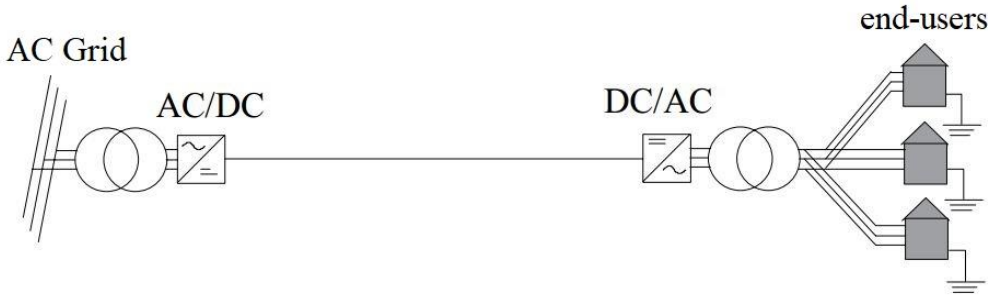

Figure 1.2 - HVDC link type network [4]

1.1.2 System Connections

The LVDC distribution can be implemented with two different connection types of power electronic converters and the structure of DC conductors. There are two basic implementations of LVDC distribution system; unipolar and bipolar. For efficient power transmission in LVDC network, unipolar or bipolar distribution system has chosen based on the number of conductors and possible voltage level.

Unipolar Connections: As seen in figure 1.3, the unipolar LVDC distribution system have two conductors; one is an outgoing conductor and the other is return conductor for current. In this case, there is one voltage level for power transmission which is below 1500 Vdc according to the low voltage directive (LVD 73/23/ECC) and the international standard IEC-60038 [5]. As we know, the unipolar system has just one voltage level, so all the end-users are connected between the positive and negative pole.

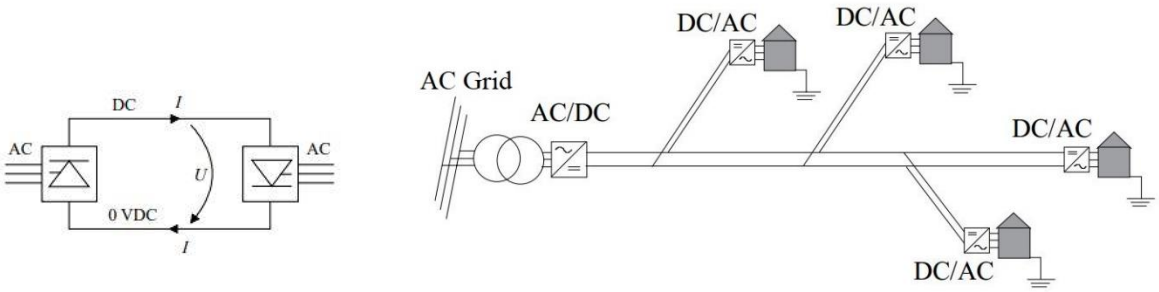

(a) (b)

Figure 1.3 - Unipolar LVDC distribution system connection [6],[4]

The advantages of the unipolar system [7]:

- no asymmetry between poles
- simple system structure

The main disadvantage of the unipolar system, there is no redundancy in the system which means a single fault leads to whole system shutdown. The possible use of higher voltage level leads to some disadvantages:

- higher costs of converters
- fewer applicable product availability
- safety risks
- higher switching and conduction losses in IGBTs [8]

Bipolar Connections: The bipolar distribution system consists of two unipolar systems which are connected in series. In a bipolar system, the customers can be connected between different voltage levels (+750Vdc, 0V, -750Vdc) with four possible ways. The connection alternatives are 1) between a positive pole, 2) between a negative pole, 3) between positive and negative poles and 4) between positive and negative poles with neutral connection [4]. Hence, bipolar connections offer the maximum ± 750 VDC as permissible by the low voltage directive (LVD 73/23/ECC) and the international standard IEC-60038 [5].

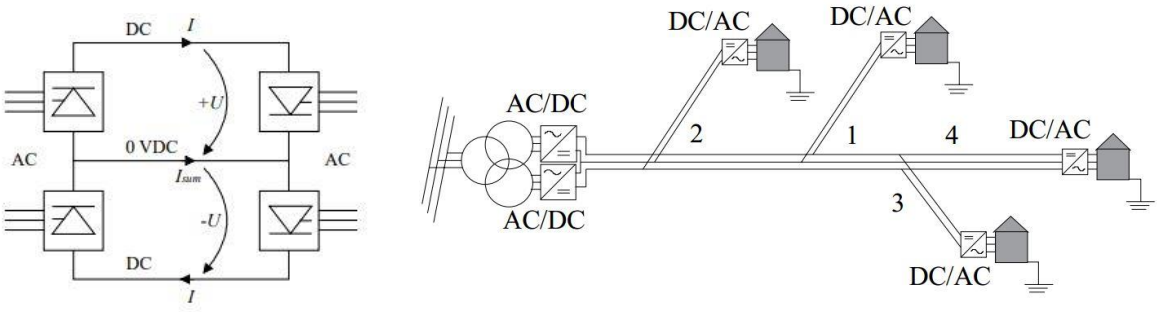

(a) (b)

Figure 1.4 - Bipolar LVDC distribution system connection [6][4]

The advantages of the bipolar LVDC distribution system [7]:

- redundancy
- lower voltage level provides; reduced safety risks and better products availability

The main disadvantage of a bipolar system is that electricity consumption varies extensively among end-users, thus the bipolar LVDC distribution network becomes asymmetrical due to network structure. The overvoltage occurs as a result of the neutral wire current superposition. It causes voltage stress on the switches of the line converter and leads to converter failure [8]. The possible use of a lower voltage level leads to some disadvantages:

- complex system
- unbalanced load between poles

1.1.3 Classification of Voltage Standards

The European Union low-voltage directive (LVD 73/23/ECC) and the international standard IEC-60038 defines the boundaries for low voltage DC distribution system. According to these standards, the LVDC distribution system has a voltage level below 1500 Vdc [9].

The selected voltage level for LVDC distribution system is inevitably related to the power rating of the different elements (DG, ESS, & loads, etc) in the network. Different voltages are optimal among different applications while optimizing efficiency, safety, and compatibility with existing AC distribution systems. Each level of DC voltage has unique standards and codes according to their applications.

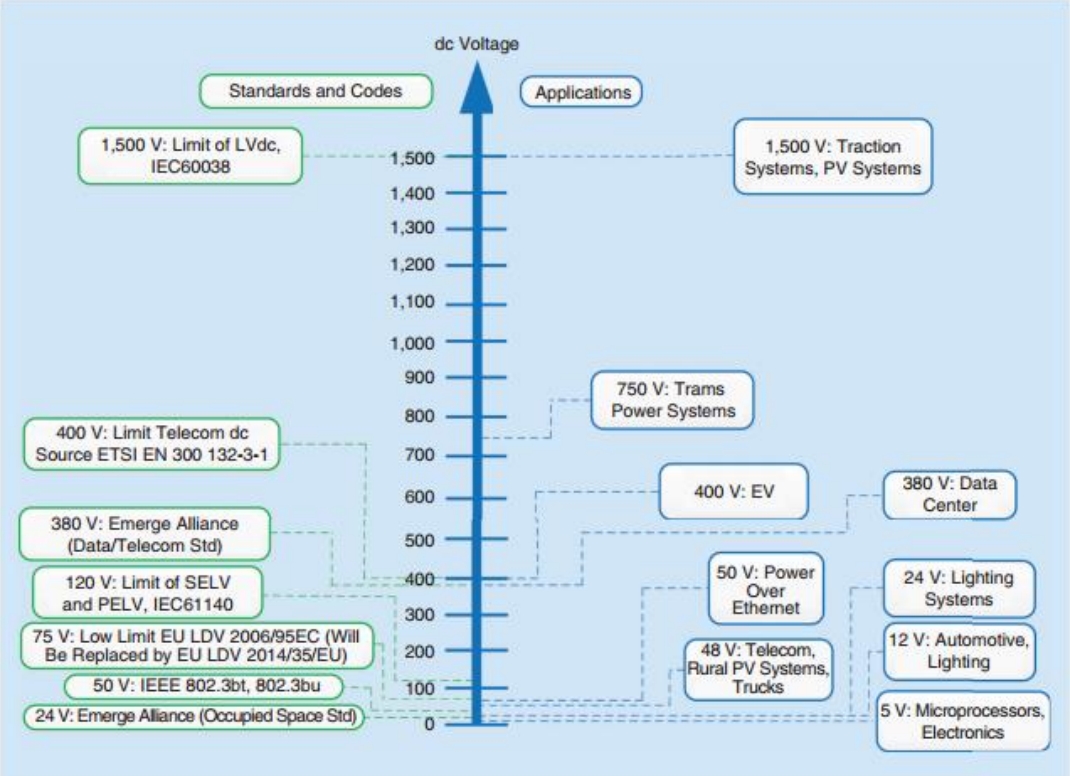

Figure 1.5 - Collection of standards, codes, & applications using LVDC [10]

As seen in figure 1.5, the highest efficiency was achieved by using a bipolar LVDC distribution network with a voltage level ±750 VDC [8]. The following table shows the advantages of different DC voltage levels. As we can see in table 1.1, the voltage below 120 Vdc is known as extra LV and there is no need for a protection system against indirect contacts.

Voltage Level (DC)	Advantages
≥565 V	Direct interconnection with the three-phase,400 Vac grid
380-400 V	Standard in data center industry
325 V	Minimum modification required for loads with input rectifier
230 V	Compatibility with purely resistive loads
120 V	The limit for extra LV definition, no need for protection system against indirect contacts
48 V	Standard in the telecommunication industry
24 V	Emerge Alliance occupied space standard
12 V	Standard in the automotive industry

Table 1.1 - Advantages of LVDC distribution voltage levels [10]

1.2 Power Electronics Conversion

The development in power electronics and smart grids have increased due to their attractiveness for improving the quality of power supply and flexibility in power flow control. The structure of distribution networks is changing, and the power transmission is bidirectional between power plants and customers. The number of small-scale power generation units, energy storage systems, and electric vehicles are increasing, and almost all the generations and loads are operating at DC voltage. The LVDC distribution network enables easy connection of distributed generation to the grid and in most cases, power conversion is required to match the different voltage levels with the grid voltage [11].

For every interconnection point to the AC network, an AC to DC conversion is required. However, every end-user connected to the LVDC network, an electricity supply is provided via DC to AC inverter or DC to DC converter if the end-user can exploit the DC supply. Furthermore, power electronics enables the customer-end voltage quality [12].

AC to DC (Converter): This process is known as rectification; to convert AC voltage and current into DC voltage and current. It is used to connect the AC system with DC system. Depending on the DC network structure and desired functionalities, the following requirements are set for the rectifier [13]:

- unidirectional/bidirectional power flow
- DC voltage & power control
- high energy efficiency
- remote control and monitoring

DC to AC (Inverter): It has the function of turning the direct current into alternating current by controlling and stabilizing frequency and waveform. Typically, it's known as a customer-end inverter (CEI), solely responsible for the customer-end power supply. Hence, it should meet the voltage quality and electrical safety requirements. The following requirements are set for the CEI [13]:

- high energy efficiency
- low EMI
- short circuit current supply
- complies with voltage quality standards
- complies with electrical safety and EMI standards

DC to DC (Converter): An electromechanical device uses to convert direct current from one voltage level into another voltage level. The functions provided by DC/DC converters are [14];

- step-up the DC voltage
- step-down the DC voltage
- galvanic isolation between DC and customer-end AC network

There are two different types of DC to DC converter uses in the LVDC;

Buck Converter: A DC/DC buck converter is a step-down converter which generates a lower output voltage from a higher DC input voltage.

Boost Converter: A DC/DC boost converter is a step-up converter with an output voltage greater than its input voltage. Usually, it is used to step-up the output voltage of photovoltaic power plants to connect with the main DC distribution system.

1.3 Grounding and Protection

The fundamental purpose of the grounding & protection in the LVDC distribution system is to protect both the equipment and humans against over-voltages and over-currents. The protection limits the fault current or voltage magnitudes or exposure time at a safe level.

Typically, over-currents are due to; overload or faults. Both overvoltage and overcurrent may result due to malfunctioning of the equipment or due to environmental phenomena or human errors. The protection system is constituted by the earthing system, circuit breakers/fuses, converter-based protection, galvanic isolation and additional equipment such as Insulation monitoring devices and surge protection devices [7].

According to the standard IEC60364-1, LVDC grounding schemes are classified into TN (TN-S, TN-C, & TN-C-S), TT and IT. The first letter indicates the system grounding state and the second letter indicates the equipment grounding state. T, I, N represents direct grounded, ungrounded or grounded with high resistances, and grounded through system grounding point (PEN and PE+N) [15]. The main benefits of using different earthing schemes are that the system is bound to earth potential and risks of floating potentials are reduced, hence no need for insulation monitoring devices.

In the earthed system, the worst case is when a fault occurs between pole and earth. The touch voltage increases based on supply voltage, fault location, and fault resistance. The acceptable touch voltage for the DC system is ≤120 Vdc, defines by standard IEC 60364-4-41. When a fault occurs close to the inverter the fault resistance is almost zero, which causes a very high touch voltage, and completely against the safety norms.

Different grounding schemes have different consequences on network operation and fault behavior. In case of a ground fault, general-purpose converters are not able to limit fault currents in DC short circuit condition, therefore, fast protection devices needed [16]. The LVDC network requires the following types of protection [17]:

- Overcurrent protection
- Short circuit protection
- Earth fault protection

The protection devices used in the LVDC system are; circuit breakers, fuses, insulation monitoring devices (IMD) and residual current devices (RCD's). The fuses used for overcurrent protection. In case, the ungrounded LVDC (IT) system, short circuit protection cannot be used for earth fault protection because of a small proportion of fault current. Hence, such a system required an insulation monitor device for ground faults.

There is a different kind of circuit breakers uses for the protection of LVDC distribution system such as; electro-mechanical circuit breaker (MCB & MCCB), solid-state circuit breakers, and hybrid DC circuit breakers. The molded case circuit breaker has used for short circuit protection. It can be placed either DC or AC side of the converter. If it used on the AC side, it can also protect against switching faults in the converter. Solid-state circuit breakers (SSCB) can interrupt the DC fault currents 900 times faster than mechanical circuit breakers. Apart from very high switching speed, it has on-state losses. Hence, the hybrid DC circuit breakers have been proposed recently to cope with the on-state losses in solid-state circuit breakers (SSCB). However, DC hybrid circuit breakers are not widely used as compare to electro-mechanical and SSCB due to their immaturity for LVDC[18].

There are different protection devices uses in the customer-end AC network to protect human and electric fire, known as residual current devices. The IEC-60479 standard defines the effects of current on human body w.r.t time. It specifies that 30 mA residual current devices can be used between and customer-end AC network for human safety. During double fault conditions, the residual current device separates customer network from DC network. In the case of ungrounded IT system, 300 mA residual current device can be used against fire protection [17]. In general, the degradation of material and fire risk is much higher in DC than AC due to the DC arcs. The residual current devices that normally used in the AC network to interrupt and limit fault currents at the safe level are not standardized [18].

1.4 Cables in LVDC System

In the LVDC distribution system, cables transmit energy from the rectifier to inverter. There are different factors to be considered in the selection of cable: transmitted power, line length, short circuit currents, allowed losses, voltage drop, and economic requirements.

The rated current of the system is calculated according to the power demand and it should be lower than the cable rated current. Voltage drop is an important parameter in the distribution line, it is a difference between the voltage at the beginning of the line and the end of the line. It becomes more significant as the line length increases. Consequently, the cable cross-section selection is mainly based on voltage drops.

According to the comparison [19], the existing AC cables can be used in the LVDC system despite the differences between AC and DC distribution systems. When an existing LVAC cable uses under DC provide a maximum power capacity of $\sqrt{2}$ times that of an AC system and minimize the system losses (as the lack of skin & proximity effects, and no dielectric losses). There are two main types of cables; PILC (Paper insulated lead covered) 4-core cable and XLPE (Cross-linked polyethylene) 3-core cable uses in LV distribution network. The cable selections are primarily based on the LVDC distribution system topology and earthing scheme [20].

The low voltage underground cables can be used in an unearthed DC system if the voltage across the conductors is not greater than 1500 Vdc, and the voltage between the conductors & earth is not higher than 900 Vdc. So, the bipolar LVDC network configuration allows the use of traditional low voltage underground cables. The power transfer capability of such a bipolar LVDC distribution network (+750 Vdc, 0Vdc, -750 Vdc) is around four times of traditional 400 Vac system, limited by the thermal capacity of the cables [21]. Furthermore, the power transfer distance is around seven times that of a traditional 400 VAC system. According to the standard IEC 60364, for circuits supplied at nominal voltage up to 1500 Vdc, the allowed voltage ripples in DC voltage is 10% [22].

1.5 Power Quality in DC Distribution Networks

The purpose of LV distribution network is to supply electricity to the end-users with adequate power quality. Power quality is an important factor to ensure the performance of the DC distribution network, however, poor quality can produce malfunction or damage electrical and electronic equipment. There are two different types of DC generation: distributed generators such as PV cells or energy storage system that produces DC voltage

and conversion from AC/DC (single-phase or three-phase rectifiers) that produces DC voltage with ripple content caused by the AC input section to the DC output. As seen in figure 1.6, the graph of DC voltage produced by different power resources and the effects of the ripples.

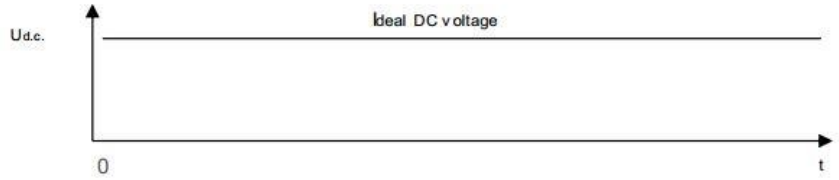

(a)

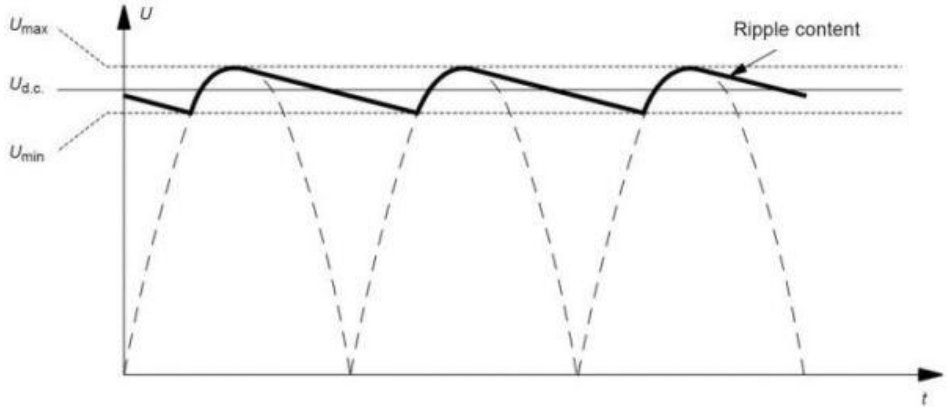

(b)

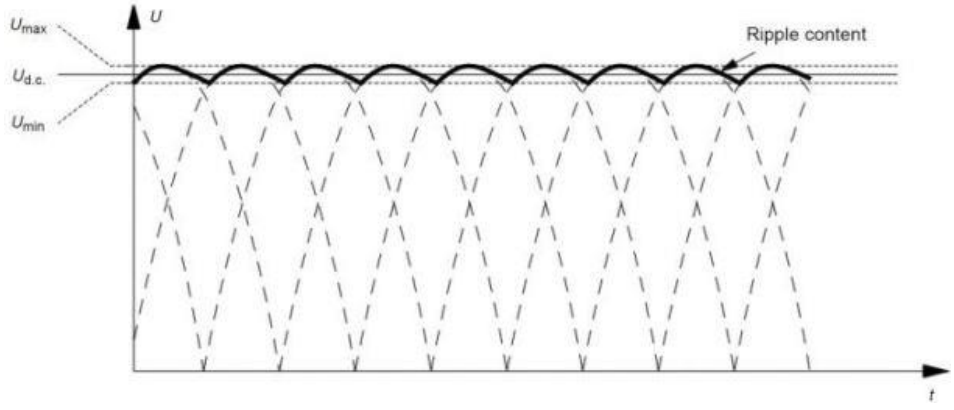

(c)

Figure 1.6 - DC voltage shapes produced by different power sources: (a) Ideal DC voltage, (b) single-phase AC/DC conversion, and (c) three-phase AC/DC conversion

According to the European standard EN-50160 and IEC 61000-4-30 which defines the power quality phenomena in the LVDC distribution network:

- supply voltage deviations
- voltage unbalance
- ripple/harmonics
- voltage swells & voltage dips
- supply voltage interruptions
- rapid voltage changes and flicker

Voltage dips, voltage swells, and supply voltage interruptions are basically caused by faults and switching of the load. According to European Standard EN 50155, the electrical and electronic equipment is expected to operate within the range 0.7–1.25 of nominal voltage and duration time is less than one second (t < 1 s), when the range is 0.6–1.4 of the nominal voltage & duration time (t < 0.1 s) less than 100 milliseconds, and up to 10 milliseconds during a voltage interruption [23]. As seen in figure 1.7, In the compliant zone, the voltage variations do not cause malfunctioning of the equipment.

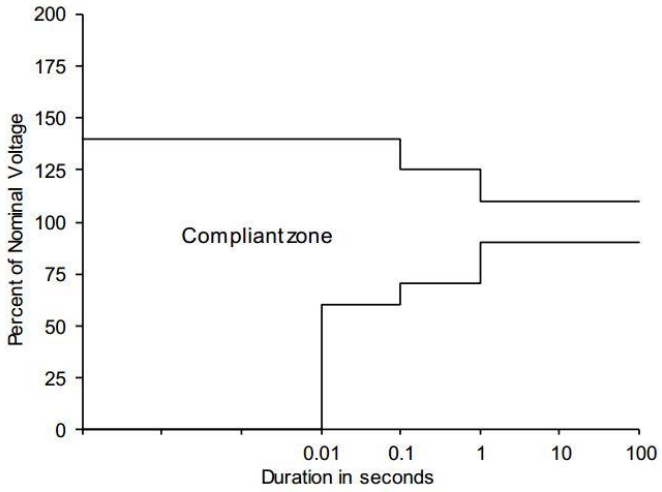

Figure 1.7 - Voltage tolerance of equipment for railway applications

Rapid voltage changes (RVC) is known as the abrupt transition between two rms steady-state voltages and during which the rms value does not exceed the dip/swell threshold. The maximum delta should be less than ±10% of the nominal voltage, otherwise, the event should be classified as a voltage dip or as a voltage swell.

Voltage ripples are superimposed AC voltage on a DC voltage; defined as the quantity derived by removing the direct component from pulsating quantity. The main sources are ripple produced by AC/DC conversion, battery charging, and ripple generated from equipment absorbing pulsating currents. Voltage ripple can produce additional heating and increase losses. The ripple limits are changes according to applications; as ±15% of nominal voltage in railway applications and ±10% in the DC power system on ships according to IEEE standard 1662-2008.

Electromagnetic Interference (EMI): It can take the form of conducted and radiated emissions. The types of emission that travel through electrical conductors, wires, and components are known as conducted emission while radiated emission travels through the air as magnetic fields or radio waves [24]. These emissions are generated during the current flowing through the electrical and electronic equipment. Hence, power supplies, inverters and in general all power electronics are sources of EMI. To limit the EMI within the acceptable range, different filters are implemented accordingly to the type of emission. These interferences cause the malfunction of electronic equipment such as unnecessary tripping of protection devices and inaccurate operation of telecommunication equipment if the amount of emissions does not comply with electromagnetic compatibility standards.

1.6 LVDC Microgrids

The growing concern about climate change and carbon emissions (EU plan for low carbon economy by 2050) have directed the research towards the development & integration of renewable energy sources (RES) to reduce fossil fuel usage and enhance the future energy sustainability. The European framework to cut carbon emission around 80–95% by 2050 and proposed to accomplish at least 27% renewable energy usage by 2030 [25]. The incorporation of distributed energy reserves (DER) such as wind turbines, photovoltaic (PV) and energy storage systems (ESS) has demonstrated significant potential to reduce CO_2 emission.

Microgrid (MG) is a group of interconnected loads and distributed energy sources with defined electrical boundaries forming a local electric power system at a distribution voltage level, that acts as a single entity and able to operate either in grid-connected or island mode. The microgrids shall be classified into isolated microgrids or non-isolated microgrids.

The classifications based on the availability of a wider electric power system, characteristics of local DERs, load pattern, power quality, and reliability of microgrid. In order to avoid the unnecessary power conversion stages, simplicity of control system, exponential growth in the development of renewable energy resources (RES), energy storage system (ESS) and electric vehicles infrastructure led to the concept of LVDC microgrids [26].

The main characteristics of DC microgrids are [27]:

- distribution system becomes simple as the main control variable is the DC voltage at the point of common coupling (PCC), which maintained dynamically adjusting the set-points of voltage and current according to load variation.
- each power supply connected with the DC microgrid can be operated autonomously because it only controls DC voltage.
- during the fault at the AC grid, the DC grid system is switched to stand-alone operation in which the generated power is supplied to the loads.
- renewable energy resources (RES) accompanied by an energy storage system can be used to create a more efficient microgrid as both generation and storage have DC nature.
- the overall system cost and losses can be reduced because only one AC grid-connected inverter is needed.

There are two different kinds of operations adopted by microgrids; grid-connected and island mode. During the normal operation, all the loads fed by tradition grid and the distributed generation presents in the network. When an event occurs on a traditional grid, the microgrid operates in island mode and all the loads supplied by the distributed generations. Islanded operations lead to various economic and technical issues such as power quality, voltage regulation, and network security and stability. In island mode, load shedding approach should be implemented to disconnect non-critical loads for the security of the grid. As soon as the traditional grid becomes normal there is a transition to connect microgrid with the main grid. A typical microgrid has shown in figure 1.8.

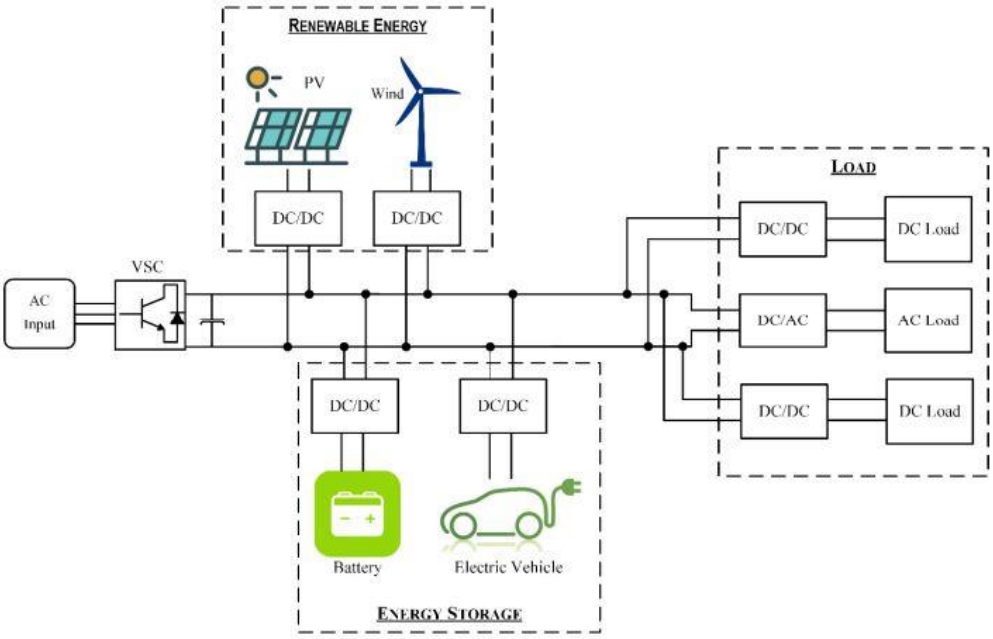

Figure 1.8 - DC microgrid distribution system

Distributed Generation (DG): The distribution generation sources such as photovoltaic (PV) and fuel cells produce DC, and easily connected to a DC distribution system directly, or through a DC/DC converter. Microturbines generating high-frequency AC are easy to connect with a DC system than an AC system, where a synchronized sinusoidal AC current is required [28]. The electric power output of a wind turbine can be kept at a maximum if the speed of the turbine is adjustable. If the shaft is connected to the generator through a gearbox, the ability to vary the speed is restricted. Therefore, to increase the speed range, an AC/DC/AC converter can be used, which is an expensive solution, but a cheaper and simpler solution is to connect an AC/DC converter with DC grid [28],[29]. DC distribution system makes it simple and easy to integrate renewable energy resources and energy storage system, either standby power generation, which is used only when there is a fault on the utility grid or distributed generation (DG) which are operated more or less continuously. To connect an energy source to a DC system only the voltage has to be controlled [28].

Energy Storage System: The basic function of ESS to converts electrical energy into some form of energy that can be stored and released as needed. There are different types of energy storage technologies such as mechanical (pumped hydro, compressed air, flywheels), electromagnetic (capacitor, supercapacitor, and superconductive magnetic energy storage system), chemical (batteries: lead-acid, Li-ion, NiCd/NiMH, etc.), and thermal. The ESS selection varies w.r.t power density and energy ratings, response time, weight, volume, and operating temperature. Some energy storage technologies need power electronic units to adapt their output voltage or current to the required output waveform. In LVDC, ESS must adapt its DC output voltage w.r.t to the grid voltage.

An energy storage system can be used for power-intensive application or energy-intensive applications. There are two main applications of energy storage system: transport and utility sector. In transport applications, time range varies from seconds to hundreds of minutes and power range from kilowatts to tens of megawatts, however, in utility applications, time range varies from minutes to hours and power range from megawatts to gigawatts [30].

The intermittent nature of renewable energy resources (RES) causes issues of power quality, network security & stability. In order to cope with renewable forecast and demand-side management, an energy storage system (ESS) can be used to support voltage regulation and renewable management (hosting capacity).

CHAPTER 2

Benefits & Applications of DC System

In 1883, Edison was proposed first time the DC power distribution system for lighting purposes. Due to the limited advancements in DC technology, DC distribution systems were considered inefficient for power transmission over long distances. In 1886, Sprague proposed alternating current (AC) distribution systems along with the invention of transformers and induction machines. These innovations made AC distribution systems more attractive because it could transmit power efficiently over long distances. Hence, AC distribution system became common and was universally opted for electric power distribution. Later in the 1960s, the advent of the semiconductor industry-led towards the introduction of power electronic converters (PECs) that were key components of DC distribution systems. Further research in semiconductor technology made PECs more efficient, reliable, cheaper, and size compactness enhanced the benefits and application of DC distribution system.

This chapter deals with the benefits and applications of DC distribution system, comparison between AC and DC distribution system, cables and maximum transmissible power, ease of synchronization. The authors also analyzed the efficiency, reliability, safety, protection, and stability of the LVDC distribution system. At the end of the chapter, the

applications (electric traction, PV system, battery energy storage system, electric vehicles, data center, ships, and many industrial applications) of the direct current distribution has been discussed.

2.1 Benefits of DC Distribution System

The DC distribution systems have many fundamental advantages over AC distributions such as higher efficiency, reliability, integration with renewable energy reserves (renewable energy resources and energy storage systems). It has reduced installation costs as it requires less power conversion stages, less copper, and small space. Moreover, DC systems have no reactive power and frequency stabilization issues, which enables ease of synchronization [31].

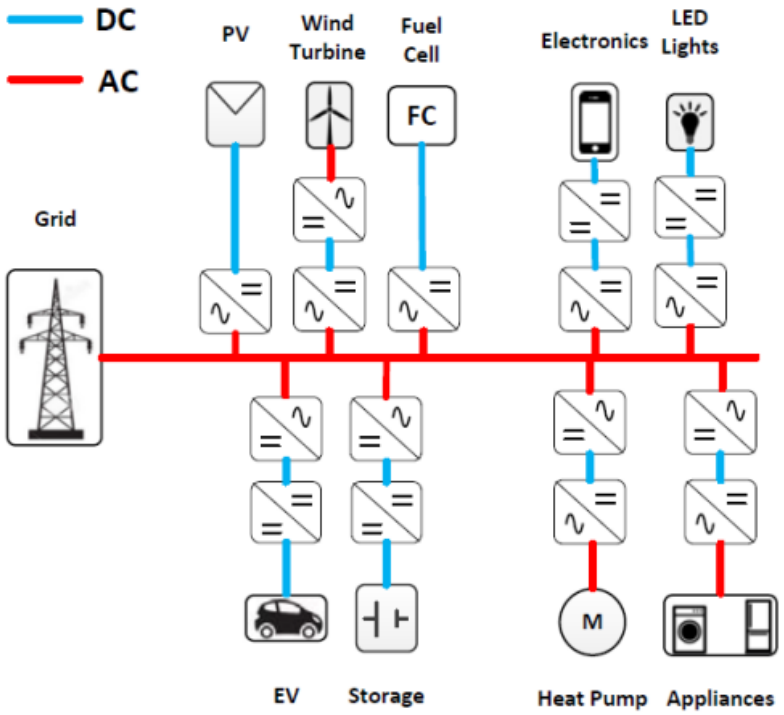

Figure 2.1 - Conversion stages in the AC distribution system [32]

A low voltage distribution network is traditionally based on a three-phase 400 Vac system. In low voltage, transformers (20/0.4 kV) installed the nearest possible location of the customer in order to avoid distribution losses. The distribution voltage level selection has a strong impact on power transmission capacity in the LV network. The use of a higher voltage level increases the transmission capacity of an aerial or underground cable with the same cross-section area. However, the power transfer capacity of the DC system is much higher than the AC system at the same voltage level. As the inductance of the transmission line does not have an impact in the steady-state condition, therefore, the voltage drop in the line is small in the DC system. There is also no skin effect, so transmission line resistance and voltage drop also decrease in the DC system [33].

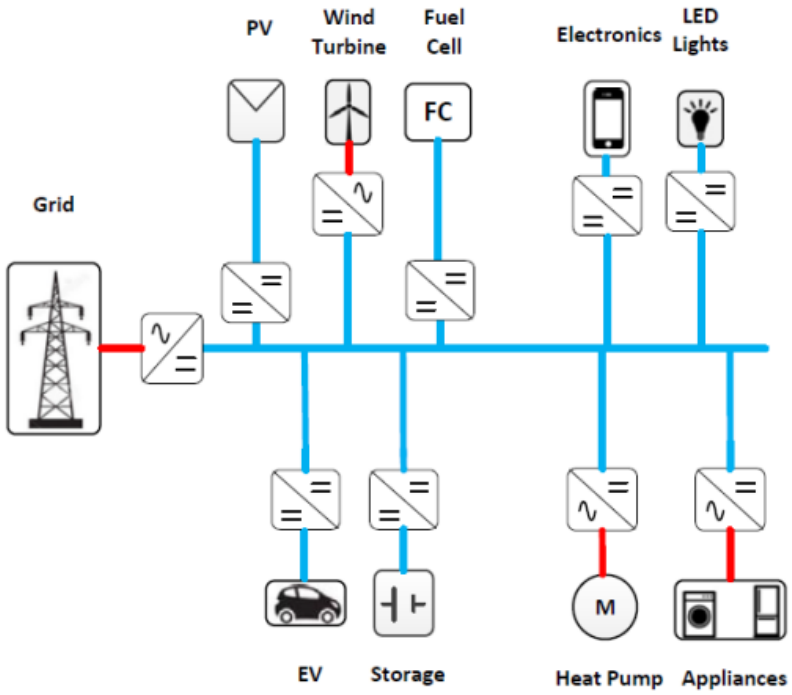

Figure 2.2 - Conversion stages in the DC distribution system [32]

2.1.1 Efficiency and Power Losses

The efficiency of DC systems is higher than the AC distribution system as the number of power conversion stages are lower in the DC system. In the figure (2.1& 2.2), the architecture of distribution systems, the residential and commercial loads comprise of an

electronic load that required DC power. To supply these loads by using a conventional AC distribution system, a power electronic converter is required to convert AC to DC. The power conversion from AC to DC results in additional power losses, usually 4 to 15% of the input power. As a result, the total system losses become relatively high as the number of power converters increase. In the DC system, the number of rectifier stages reduced and thereby improved the overall system efficiency [31].

The absence of reactive power and skin effect improved the efficiency of the DC distribution system as compared to an AC distribution system. In an AC system, skin effect increases the effective resistance of the wires and results in higher distribution losses. As there is no reactive power in a DC system, the apparent and active powers are equal which results in the reduction of power losses in the system. According to Lawrence Berkley, national laboratory studies on DC distribution stated that the DC distribution consumed 28% less power as compared with the AC system uses in the data center [31].

2.1.2 Electric Shock and Personnel Protection

The effect of an electric shock depends on the current magnitude, duration of current, current path, type of voltage (AC or DC). Direct current is less dangerous than alternating current [34]. According to a general principle, the human body is more sensitive to time-variable stresses as compared with continuous. The following graph shows the hazardous zones of AC vs DC and the time of current flow throughout the human body.

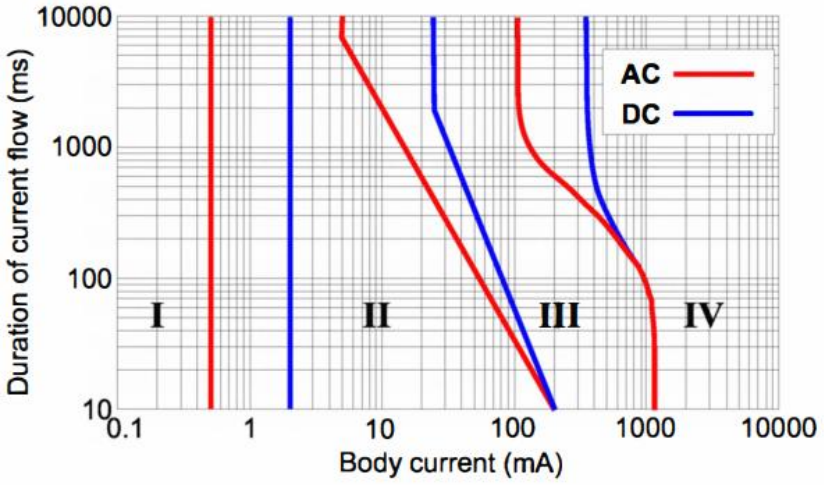

Figure 2.3 - Characteristic curve of body current, IEC/TR 60479-5 [35]

The graph divided into four regions based on the effects of current (AC & DC) on the human body:

- Region I = No effect
- Region II = A little pain but no dangerous effects
- Region III = Muscular contraction and respiratory compromise which are reversible
- Region IV = Critical effects such as ventricular fibrillation

Among all the possible effects of electric shock, ventricular fibrillation is most dangerous. Therefore, proper protection needed to prevent any casualties in the human body. It can be observed from the graph that the magnitude of safe operating current limits for DC is higher than AC. As a result, DC is safe to operate than AC [35].

There are different types of grounding (positive line grounding, negative line grounding, and mid-point line grounding) connections in LVDC distribution systems. The grounding provides personal safety, reduces equipment damage, and interruptions during short circuit and earth faults. According to [35], France Telecom and Emerson network power have selected and highly recommend high resistance mid-point grounding for 400 Vdc distribution system. As this kind of grounding provides better personal safety (by limiting fault current to harmless levels) as compared with other grounding methods for higher DC voltages.

2.1.3 Cable Maximum Power Transfer Capacity

The maximum power transfer capacity depends on the voltage level, maximum current, and the feeder length. The maximum power supplied by the cable is determined by two factors: the current in the cable equal to the maximum allowed current for the insulation, and the voltage drop equal to a given limit (provided by the manufacturer). The transmissible power for different systems are [36]:

- DC with two conductors: $Pdc2 = Vdc2 \times Idc2$ (2.1)
- DC with three conductors: $Pdc3 = 2 \times Vdc3 \times Idc3$ (2.2)
- Traditional AC system: $Pac = \sqrt{3} \times Vac \times Iac \times cos\varphi$ (2.3)

According to [28], 3-phase grounded AC distribution system required five wires (three-phases, one neutral and one ground wire) and DC distribution system required three wires (one positive pole, one negative pole, and one ground wire). Here an existing five-wire AC cable in a DC retrofit system can be used in two different configurations. In the first configuration, two wires for positive pole, two wires for negative pole and one wire for ground. In the second configuration, one wire for positive pole, one for negative pole, two for neutral and one for ground.

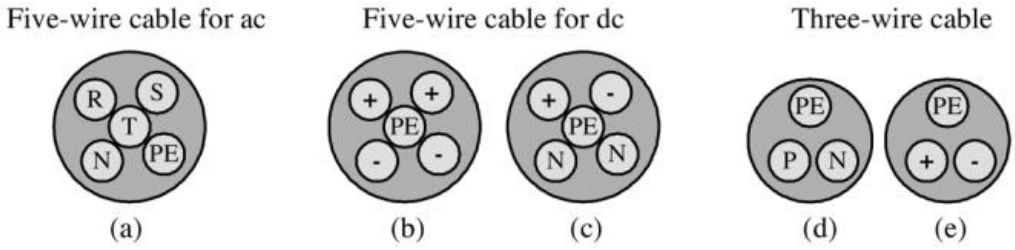

Figure 2.4 – Use of cables in DC retrofit system [28]

These two configurations are compared with an AC system with five wires size of 1.5 mm^2, voltage 450/750 V, and current 10A. The loads are assumed to have an average power factor equals 0.9 (AC only) and the DC load voltage equals to the peak value of the AC voltage. The maximum power transfer in each configuration is shown in table 2.1:

	AC (a)	**DC (b)**	**DC (c)**	**DC (d)**	**DC (e)**
Urms (V)	230	325	650	230	325
Irms (A)	10	20	10	10	10
P (W)	6210	6500	6500	2185	3250

Table 2.1 - Comparison of different cable configurations [28]

The comparison between AC and DC with 3 conductors shows that DC can transfer 1.28 times higher power than AC three-phase system. The same results have obtained in case of 2 conductors DC distribution system [36]. The relationship between AC and DC power is shown in equations 2.4 & 2.5:

$$\frac{Pdc3}{Pac} = \frac{2 \times Vdc3}{\sqrt{3} \times Vac \times cos\varphi} \quad (2.4) \qquad \frac{Pdc2}{Pac} = \frac{Vdc2}{\sqrt{3} \times Vac \times cos\varphi} \quad (2.5)$$

However, the maximum current that can flow in a power line limited by two constraints: the thermal limit of the cable and the maximum voltage drop along the line. According to [36], a comparison between the three solutions (Vac = 400 V, Vdc3 = 400 V, Vdc2 = 800 V) taking into account both the thermal and the maximum voltage drop limits by using a copper cable (3x95 + 50mm^2). The graph shows the maximum power transfer is a function of the line length. It can be observed that the power transfer is constant until a certain point and after this point, there is a reduction in power transfer. The main constraint is the line thermal limit (the flat part of the curves) and above which the main constraint is the maximum voltage drop (decreasing part of the curves).

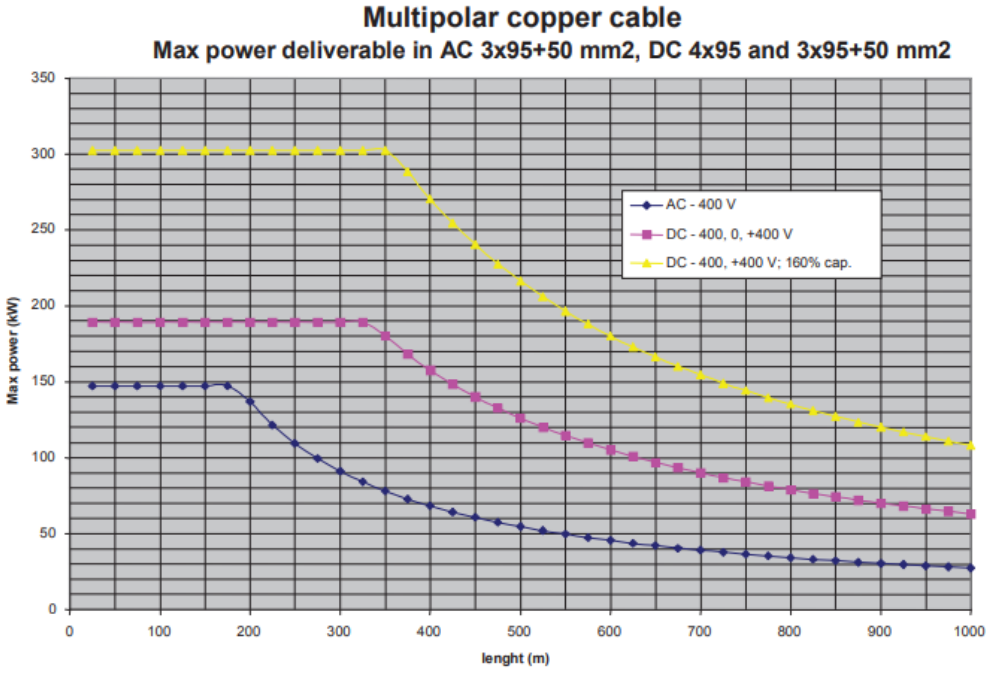

Figure 2.5 - Maximum transmissible power in AC, 3&2 wired DC system [36]

Furthermore, it can be observed that the line length is a fundamental constraint for line thermal limits. By increasing the length of the line, the DC solutions can transmit an amount of electric power up to 2.2÷3.9 times than AC distribution system. It can be concluded that with the same length of the distribution network, the DC solutions can supply a bigger load and transfer a higher amount of power.

2.1.4 Ease of Synchronization

The elimination of synchronization is a significant advantage of a DC system when compared with traditional AC system. AC current sources must be carefully synchronized before they can be connected at the point of common coupling. A failure to synchronize can result in catastrophic current and forces, as two sources work against one another. As a result, the impacts starting from voltage variation, the shutdown of the power system and at worst there can be significant damage to the generation, distribution and control components. The possible solutions to prevent these events required the primary and secondary voltage control along-with special control schemes. The control scheme becomes more and more complex with the increase in the number of distributed energy resources [37].

However, the DC system is exempted of from complex synchronization issue as it has constant voltages. Even using multiple sources in parallel within a DC system does not require any control. Therefore, a DC distribution system is the best solution for distributed energy generations such a PV, wind, and energy storage system [37].

2.1.5 Economic Analysis

The DC distribution systems cost less than the AC distribution system. In case, the use of higher-level DC voltage further reduces the system costs and improves the system efficiency, thus reducing the operational costs of the system. Power electronic converters are a major component of the system cost. The reduction in the number of the conversion stages using a high voltage DC system eliminates the need for these converters which greatly reduces the system cost. Furthermore, the smaller floor space is required as the number of conversion stages are reduced which further reduces the cost. On the other hand, the amount of copper required to limit the copper losses decreases. It is inversely proportional to the square of the voltage [31]. According to study [38], a 380V DC system as compared to an

AC system required 15% less capital cost due to the reduced power conversion and 33% less floor space, which contributes to the reduced cost: it also has 36% lower lifetime cost. Furthermore, the conductor cost in the DC distribution system can be 10-15% of the total hardware cost and further increasing the DC bus voltage level can represent less than 5% savings in the total hardware costs.

In the renovation example [4], a traditional 20/0.4 kV system and ± 750 Vdc bipolar LVDC distribution system uses to compare the total system costs. The total power of the system is 220.1 kW, consumed by 33 customers. All customers are assumed to be domestic customers. The traditional 20/0.4 kV system built with an MV branch and six LV districts. The total length of MV and LV lines are 4.1 and 6.0 km, respectively. The ±750Vdc bipolar distribution system constructs one wide DC distribution district which AC/DC conversion has made at the beginning of the MV branch and DC/AC conversions are made at customer ends. The price estimation of power electronic converters is 1500 € for 10 kVA converter (DC/AC) and 2000 € for 50 kVA converter (AC/DC). The adequate unit sizes are assumed, as seen in table 2.2.

Parameters	**Value**
Lifetime (years)	40
The lifetime of a power electronics device, 1st generation (years)	10
The lifetime of power electronic devices, 2nd generation (years)	15
Interest rate (%)	5
Power factor	0.97
Time of load growth in the supply network (years)	40
Time of load growth in the LV network and branch line (years)	10
Peak operating time of losses (hours)	1000
The efficiency of power electronics devices (%)	0.96
Interruption time in permanent fault (hour)	1

Table 2.2 - Calculation parameters for distribution systems [4]

System	Traditional 20/0.4 kV System [k€)	Bipolar ± 750Vdc System [k€]
Investment costs - network	168.41	85.60
Investment costs - power electronic devices	0.00	160.27
Power losses costs - network	16.27	15.23
Power losses costs - power electronic devices	0.00	20.61
Outages costs	118.32	0.20
Maintenance and repair costs	25.25	6.05
Total costs	328.25	288.06

Table 2.3 - Costs of traditional AC and LVDC distribution system [4]

As seen in Table 2.3, the cost of the LVDC bipolar system reduces nearly half as compared with the traditional AC system, further, smaller cables size and reduction in the number of the transformers. The outages cost of LVDC system is also very low. However, the investment cost is 46% higher in the LVDC system because the investment cost of power electronics is high. Finally, the total cost reduces by 12% in the LVDC distribution system [4].

2.1.6 Reliability

The reliability of any distribution system depends on the system architecture and the level of redundancy. In the DC distribution system, the increase in system voltage level causes electrical stress on systems components (breakers, power electronics switches, etc.), thereby reduce the reliability of the system. As mentioned in [39], the capacitor life is inversely proportional of bus voltage, as the bus voltage increases, the capacitor life decreases. In DC systems, higher voltage level system required smaller capacitances, because the capacitance is inversely proportional to the square of voltage for the same amount of power. Hence, the precise selection of capacitors w.r.t to adequate voltage level and series/parallel combination of capacitors can improve the system reliability.

In [40], the DC power supplies are less-prone to failures as compared with AC uninterruptable power supplies (UPS). The reliability of any given system can be calculated based on mean time between failure (MTBF) and mean time to repair (MTTR) of the system components.

$$A = \frac{MTBF}{(MTBF + MTTR)} \tag{2.6}$$

$$U = \frac{MTBF}{(MTBF + MTTR)} \tag{2.7}$$

$$R(t) = e^{-t/MTBF} \tag{2.8}$$

where, A = Availability, U = Unavailability, and R(t) is the time-dependent reliability function. It has exposed in figure 2.6, the reliability and availability of the DC UPS system are 10 times higher than the AC UPS system (based on comparison of power system for 10000 UPS and 23000 DC systems).

Figure 2.6 - Reliability field data of AC and DC power supply [41]

In telecom and data center, DC distribution systems are more reliable than conventional AC systems despite the fact that components experience higher electrical stresses [42]. The analysis [38] stated that the data center with 380 Vdc distribution is 1000% more reliable than AC tier IV distribution due to the elimination of the extra conversion stages.

2.2 Applications of DC Distribution System

DC distribution can be seen in figure 1.5, each level of DC voltage has unique applications and their own standards. The application of DC distribution system is mainly in the electric traction system, PV plants, battery energy storage system, charging stations, data center, ships, auxiliary services, and industrial applications.

Furthermore, thanks to the several benefits of the LVDC distribution system, which has discussed in section 2.1, thus it allows DC system for other large-scale applications such as rural and urban networks (suitable for new construction and renovation purposes). In rural networks, DC distribution system can be used as a replacement of the MV branch at specific transmission power. Depending on the used LVDC system, the LV network behind the branch can also be replaced with DC network [4]. The LVDC system also suitable for cases where the MV line is too expensive or LV transmission capacity is limited (i.e. underwater lines) [4].

In the case of urban networks, the LVDC can be useful as a distribution line between electricity stations, public lighting or house electrification. Moreover, it could be a good alternative for LV renovation projects where existing distribution system has reached to its maximum power transfer limits. In such cases, transmission capacity can be increased by changing the existing AC system with the LVDC system using original distribution lines without any expensive excavation [4].

2.2.1 DC in Electric Traction System

Since the end of the 19^{th} century, the LVDC has been used for electric traction systems. The major reason is that the speed control of DC machines (simply changing the series resistance) is very easy and offers a very high torque. In addition, the direct current supply provides the great advantage of having the contact line consisting of a single conductor since the rails provide the return conductor.

In the current scenario, DC has used in all type of urban transports, e.g. trams, subways, and trains with a supply voltage of 600V or 750V, up to 1500V [43]. The DC is not limited only to the vehicle traction system but also supply auxiliary circuits such as the energy storage system (ESS). These auxiliary circuits may supply essential services such as air conditioning, electrical heating system, internal and external lighting circuits, and emergency braking systems. The DC power systems are protected by circuit breakers, controlled by relays which will trip in case of overcurrent, ground fault, and short circuits.

2.2.2 PV Plant

The massive use of DC distribution system is in PV plants. A photovoltaic plant converts the energy associated with solar radiation into electrical energy (direct type). These plants are designed by using semiconducting material modules, which can generate electrical power once exposed to the rays of the sun [44].

There are two different topologies of photovoltaic plants. It can be either grid-connected or stand-alone. In the stand-alone topology, the energy storage system shall be present to provide power supply in the case when there is no solar radiation. The main element of a photovoltaic plant is the photovoltaic cell made of semiconducting material (e.g. amorphous silicon or monocrystalline/polycrystalline silicon). The cells are exposed to solar radiation and able to supply a maximum current (I_{MPP}) at a maximum voltage (V_{MPP}), which is known as a maximum power transfer (W_P). To build a larger network and achieve a desired level of voltage, many photovoltaic cells are connected in a series configuration to form strings. If a higher level of current needed, strings are connected in a parallel configuration. A stand-alone photovoltaic plant has mentioned in figure 2.7 and the function of each component has explained below:

Photovoltaic Array: It is made of photovoltaic modules appropriately interconnected and used for the conversion of sunlight energy into electrical energy.

Charge Regulator: It is an electronic device that is able to regulate charging and discharging of accumulators.

Energy Storage System (ESS): It stores energy when solar radiation is available and supply energy when solar radiation is missing.

DC/AC inverter: It converts direct current into alternating current by controlling the frequency and waveform.

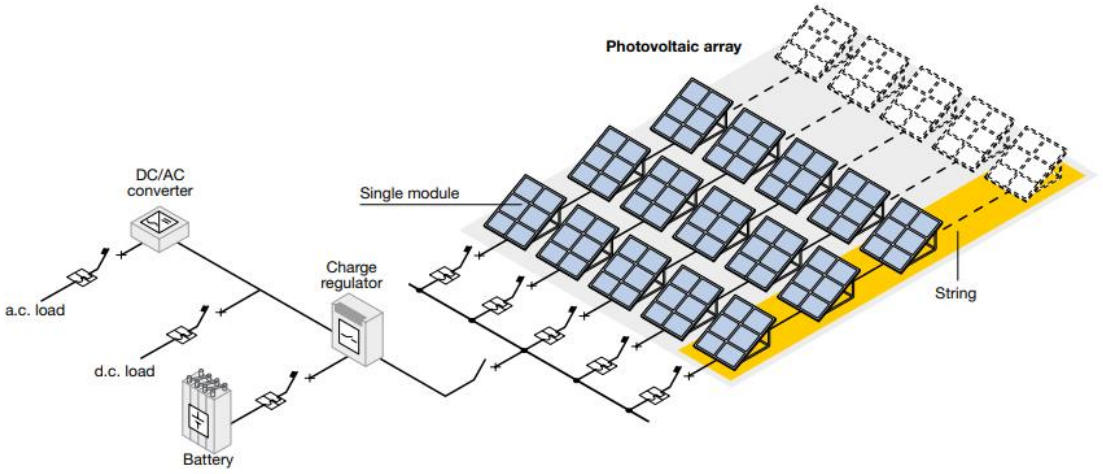

Figure 2.7 - Schematic diagram of the stand-alone PV plant [44]

2.2.3 Battery Energy Storage System (BESS)

As mentioned in section 2.2.2, It is now possible to connect the small-scale distributed generation (DG) systems with the LVDC distribution network. The battery energy storage system (BESS) become feasible for the utility-scale application, where an excess amount of electricity (e.g. renewable generation available at the time when no-load is available (off-peak load time)) can be stored and released at any time, it will provide time-critical services to the energy market. Furthermore, BESS has the potential to improve the hosting capacity of grids. In addition, the integration of BESS with power electronics can provide grid ancillary services such as peak shaving, congestion management, power oscillation damping, inertia emulation, and fast frequency support.

The three-phase BESS using a VSC for both the DC/AC grid side inverter and the DC/DC buck-boost converter, as shown in figure 2.8. In this picture, the battery management system (BMS) continuously monitor the BESS by measuring the DC current output (i_{bess}), the internal DC voltage (v_{bess}), the cell temperature (T_{bess}), and the state of charge ($\mathrm{SOC_{bess}}$). The DC/DC converter is used to charged or discharged the BESS with the help of BMS. In the latter, the DC/AC inverter injects the active power to the power grid.

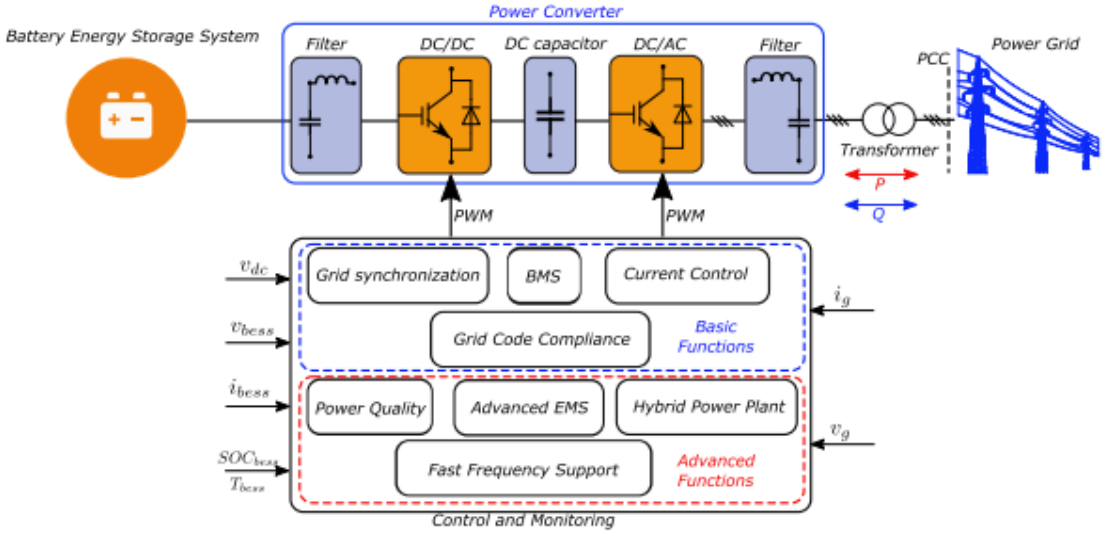

Figure 2.8 - Single line diagram of battery energy storage system [45]

Here, the voltage (v_g) and current (i_g) are related to the grid voltage synchronization and inner current control measurements [45].

2.2.4 Electric Vehicle Charging Station

With the popularization of plug-in electric vehicles (PEVs), the charging of PEV is huge and varies over time when PEV penetration becomes significant, which increases the electric demand and consequently changes the demand curve. To cope with the fast-growing demand of electricity, a technique multi-terminal low voltage direct current (MT-LVDC) has introduced into the distribution network to share the charging demand of PEVs, rather than reducing the charging load or expanding the medium voltage distribution system [46].

Typically, the electric vehicle (EV) charging system can be categorized into; on-board and off-board system. In the on-board charging system, the less energy (kW) transfer from the traditional grid into DC power to slowly charge the on-board battery pack. However, the off-board charging system uses for fast or ultra-fast charging and capable to transfer higher energy (kW). In addition, it provides a vehicle to grid services to support frequency control.

2.2.5 DC in Data Center

The commercial data center have traditionally AC distribution in their facilities. Apart from that, all the information technology (IT) equipment operates on DC supply. Therefore, a typical data center power distribution system incorporates multiple power conversion stages from AC to DC and from higher to lower voltages [47]. All the servers and IT devices are powered with AC and then convert into DC power inside their power supply module. The DC voltage is then converted into lower DC voltages as required by the IT equipment. The typical AC power distribution system results in five to seven conversion steps, with each step resulting in power losses, heat generation, and reductions in the end-to-end system reliability. The advantage of a DC architecture is evident in the reduced number of critical system components. Fewer components result directly in a lower installation cost, a smaller footprint, and higher system reliability. The efficiency gains result from fewer energy conversions and enabling the use of DC server power supplies that are more efficient at lower load levels. These efficiency gains also drive reduced cooling demand and resulting in additional energy savings [47]. A date center layout has shown in figure 2.9.

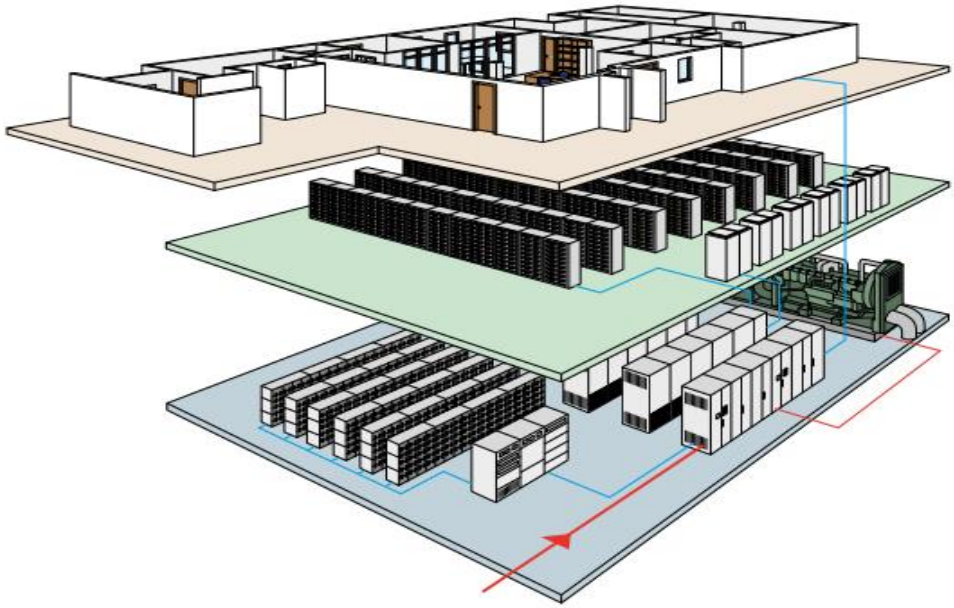

Figure 2.9 - The layout of a data center [47]

2.2.6 DC in Ships

The application of DC distribution system in ships is emerging because it facilitates fuel-saving and reduction in emission. The main advantages provided by electric propulsion systems in ship applications have created an increasing interest in all-electric ships, so hybrid power systems on-board ships have been proposed. DC distribution on-board ships provide further benefits compared to the ship AC power systems, such as space and weight savings, and flexible arrangement of equipment. The main components of a hybrid DC electric power system on-board ship include; synchronous generator, clean energy, energy storage system, inverter & converter, and ship propeller [48]. The basic function of each component is the following:

Synchronous Generator: It is the main energy source of an onboard electric ship.

DC/DC Converter: It is prominent for energy management and used to shift the DC voltage along with the DC distribution system.

Clean Energy: Fuel cells and PV modules are the clean energy sources.

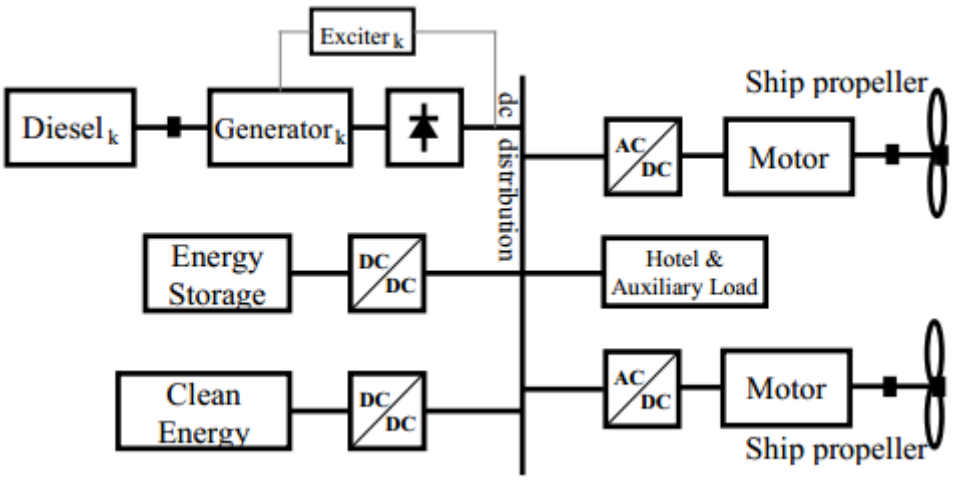

Figure 2.10 - Single-line diagram of a DC hybrid on-board ship [48]

2.2.7 Industrial Applications

The application of direct current is also well known for industries; electric welding plants, graphite manufacturing plant, metal & refining plants [49]. Furthermore, it is used for emergency or auxiliary services in all those plants where continuity of service is essential for some key processes, further applications are [47]:

- safety and emergency installations (lighting, alarms)
- industrial applications (process control systems)

In the above-mentioned installations, continuity of service is important, therefore, it is necessary to provide all the plants with an additional system able to store energy during the presence of conventional supply and provide it back when the main source of energy fails.

CHAPTER 3

LVDC Modelling, Operation, and Control

The growing rating and improved performance of self-commutated semiconductor devices have made possible Low Voltage DC (LVDC) distribution based on voltage sourced converter (VSC). This chapter describes the modeling, control, and operation of a forced-commutated voltage sourced converter low-voltage direct current (VSC-LVDC) distribution link. The model of an LVDC distribution link based on three-level neutral point clamped (NPC) VSC converters with single-phase carrier-based sinusoidal pulse width modulation (SPWM) switching. The interconnected loops (outer active & reactive power, voltage, inner current control, phase-locked loop (PLL), AC/DC voltage override, and DC voltage balance control) allow the VSC to operate as a controllable voltage source. There are different perturbations (Pref, Qref, Udref) are applied to examine the system dynamic performance. In the end, the control strategy of a two-terminal VSC-LVDC distribution system has demonstrated.

3.1 Introduction to the VSC-LVDC System

The figure 3.1 shows, the configuration of a two-terminal voltage source converter (VSC)-LVDC distribution system. This system has inter-connected with the help of two VSC stations (1&2) and DC distribution link. The station 1 works as a rectifier and station 2 as an inverter. Two different AC systems can be operated as independent networks or mutually connected nodes where a flexible power transmission link needed. The interconnection point between a station and its adjacent system is called the point of common coupling (PCC).

The main function of a VSC station is the ability of the VSC to operate as a controllable voltage source that can create voltage (AC & DC) of nominated magnitude and allow the exchange of a predetermined amount of power (active & reactive). It has achieved by operating both stations as active rectifiers that can create a voltage waveform. In order to ensure that, the dc side of the converters must maintain a rigid direct voltage. For this purpose, one of the VSC stations designated to control the voltage in the dc side at a nominal value while the other station controls the active power flow exchanged between the two ac nodes. In parallel, each of the stations can regulate the reactive power with its interconnected ac system, independently from the active power handling.

The main principle of a VSC-LVDC distribution system is its ability to independently control the active and reactive power flow at each of the AC systems to which it is connected, at the Point of Common Coupling (PCC). In contrast to the typical line-commutated distribution system, the polarity of the DC link voltage remains the same with the DC current being reversed to change the direction of power flow. The desired power exchange in a VSC station has imposed at the connection point of the phase reactor which connects the VSC station with the transformer, as shown in figure 3.1.

The DC distribution link may consist of overhead or cable type conductors, it entirely based on the operational characteristics of the distribution system. A common arrangement of the LVDC distribution is the asymmetric monopole, with or without metallic return. In this topology, only one pole is energized while the other poles are either grounded or isolated ground connections at each station. For these provisioning, the transformer must be designed

for dc stresses and there is no redundancy if the single energized pole lost. However, the bipolar connection resolves the redundancy issue by connecting two identical asymmetric monopole systems in parallel, in such a way that the grounded parts of the stations are connected to each other and there is a positive and negative pole completing the system. This arrangement is costly but if an energized pole has lost, the VSC-LVDC can keep operating with the remaining pole at a reduced power rating. The third type of VSC connection is the symmetric monopole, as shown in figure 3.1, constituted by two conductors connecting the VSC stations and operated at opposite voltages. This is achieved by splitting the dc-side capacitor into two identical parts with a grounded midpoint. In this way, the transformer does not suffer from dc stresses and redundancy is still offered at 50% of the rated power.

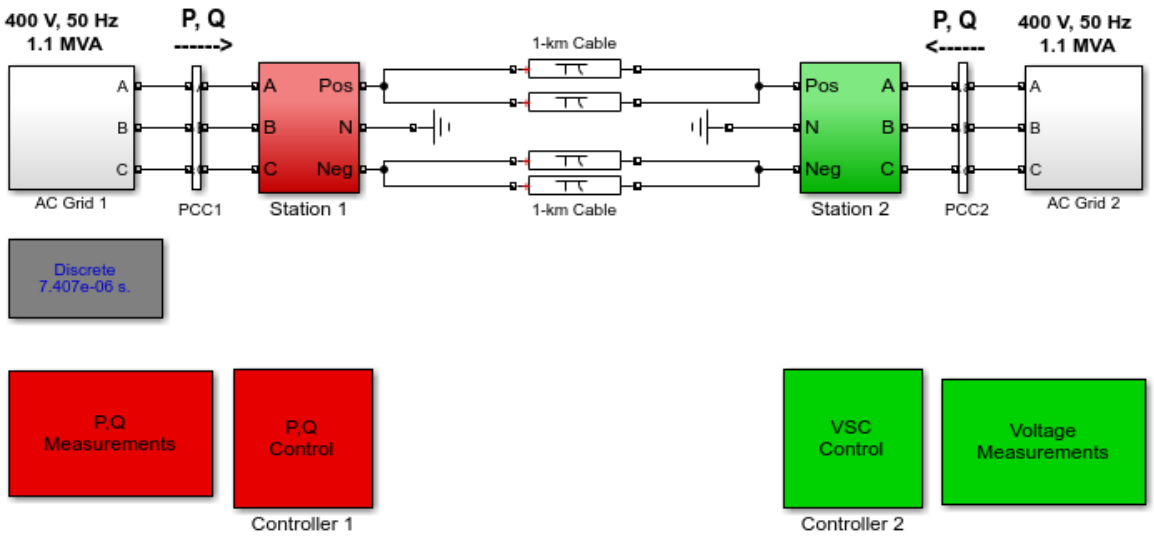

Figure 3.1 - Two-terminal VSC-LVDC distribution link

3.2 System Basic Components

The 400 Vac, 1.1 MVA AC systems (AC grid#1 and AC grid#2) are modeled at the fundamental frequency (50 Hz). The VSC converters are three-level bridge blocks using IGBT/diodes. The relative ease with which IGBT can control and its suitability for high-

frequency switching has made this device a better choice over GTO and thyristors. The component description of a VSC-LVDC distribution system has presented in figure 3.2(b). The main components are; AC grid, transformer, three-phase harmonic filters, phase reactor, converter/inverter, DC side capacitor, and DC distribution cable.

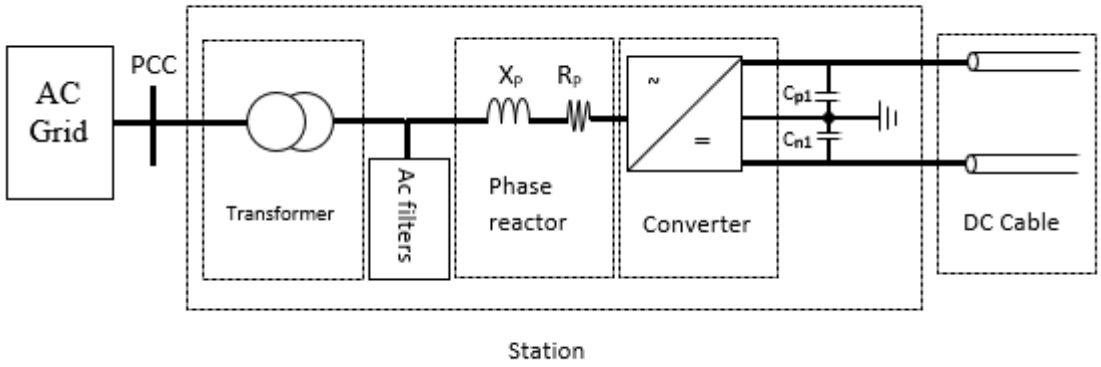

(a)

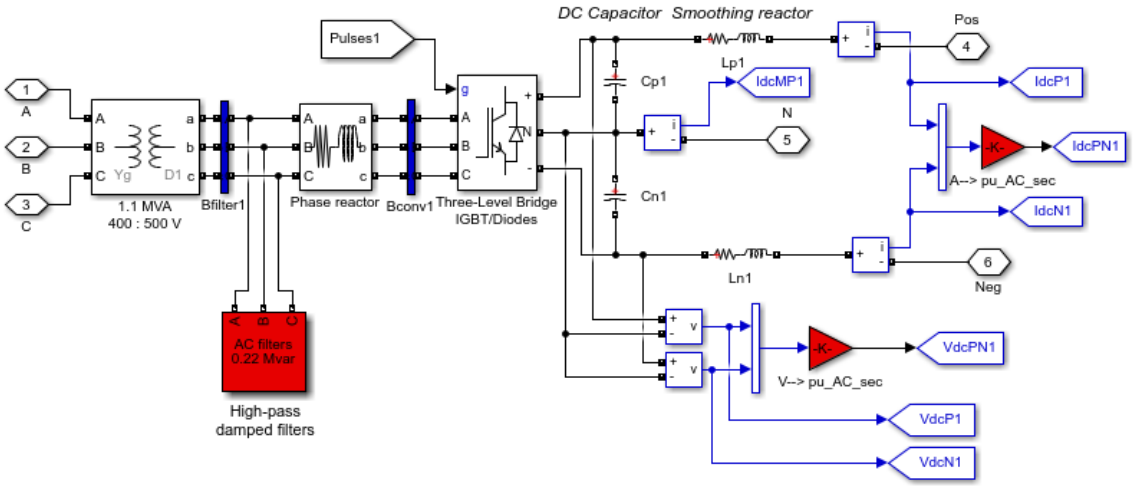

(b)

Figure 3.2 - (a) Main components of the LVDC system (b) Actual model with different measurement points

3.2.1 AC Grid

In this model, the LVDC distribution system is connected to an AC grid, 400 Vac, $Fnom = 50$ Hz. A three-phase programmable voltage source uses to apply voltage sags.

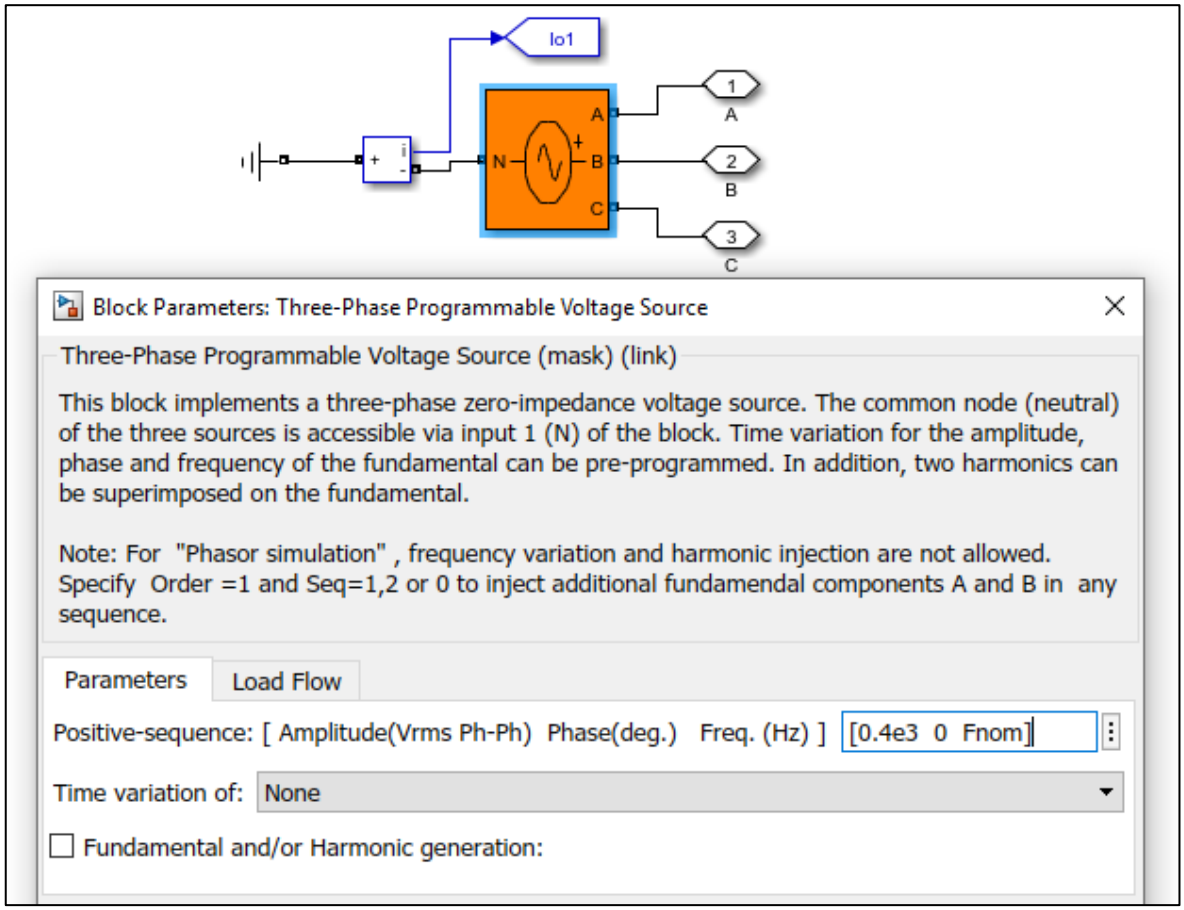

Figure - (a) Details of AC grid block

3.2.2 AC Side Transformer

A station is usually connected at the point of common coupling (PCC) to an AC grid via a transformer. The main function of the transformer is to enable the connection of the converter with an AC system whose voltage has a different rated value. A three-phase converter transformer (Wye grounded /Delta) is used to permit the optimal voltage transformation. The transformer winding selection blocks the propagation of third-order harmonics produced by the converter, and at the same time provides galvanic isolation

between the AC grid and the DC distribution system. Here, the transformer tap changer or saturations are not simulated.

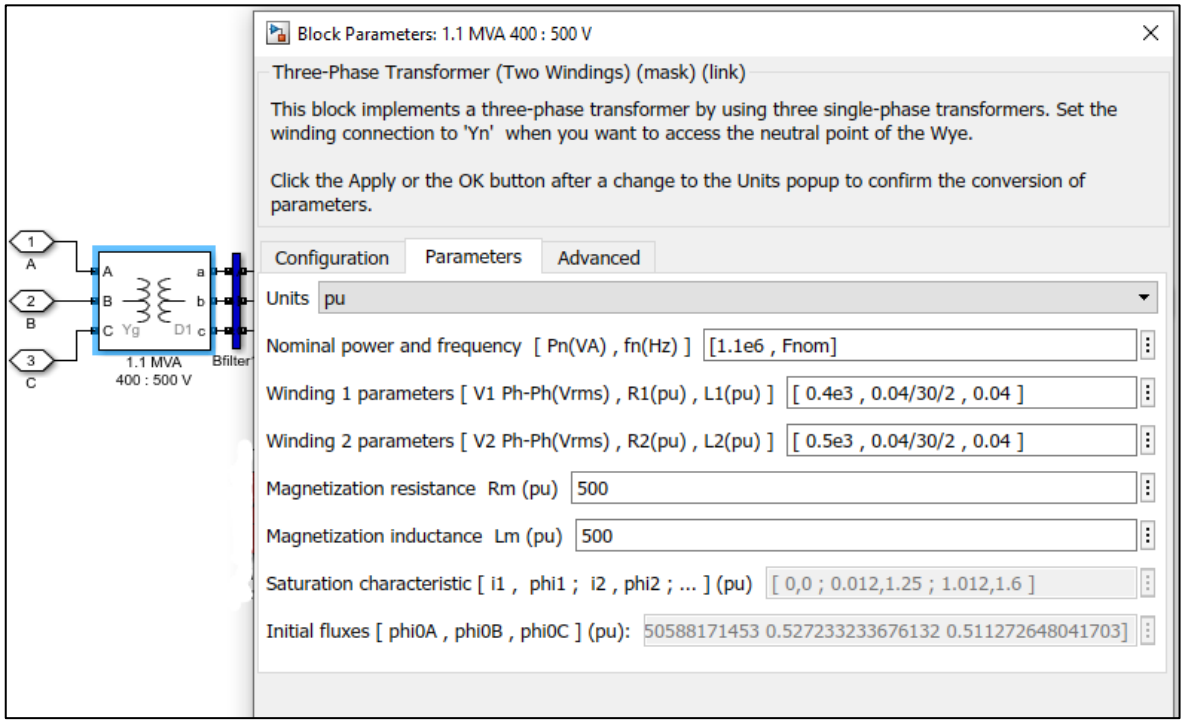

Figure - (b) Details of three-phase transformer block

3.2.3 Three-Phase Harmonic Filters

In LVDC installations, AC harmonic shunt filters are used for the following reasons:

- to reduce harmonic voltages and currents in the power system
- to supply the reactive power consumed by the converter

In this model, to cope with the AC system harmonic specifications, AC filters form an essential part of the scheme. They can be connected as shunt elements on the AC system side or converter side of the converter transformer. Here, two high pass filters are tuned for the 27^{th} and 54^{th} harmonics. The filter has built-up from passive RLC components. The values are computed using the specified nominal reactive power, tuning frequency, and quality factor.

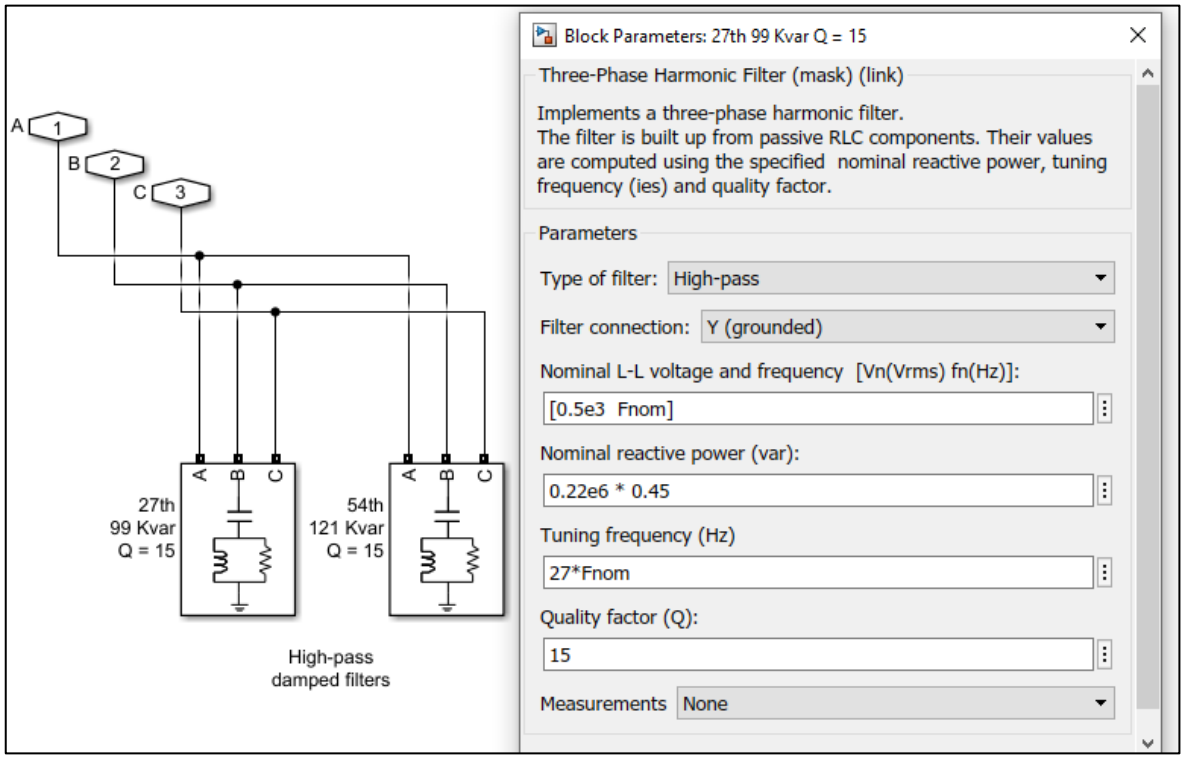

Figure - (c) Details of three-phase harmonic (high-pass damped) filter

3.2.4 Phase Reactor

The phase reactor is one of the key components of a station. Its main function is to enable the active and reactive power transfer between the station and the rest of the ac system. In a typical connection scheme, the incoming side of the reactor connected to the AC system and outgoing side connected with the VSC in order to apply a fully controlled voltage. The magnitude and phase difference of the latter system compared to the AC system voltage will induce a controlled amount of active and reactive power transfer over the reactor.

Its secondary function is to filter higher harmonic components from the converter output current and limit short-circuit currents through the IGBT. The impedance of the phase reactor, in combination with the transformer impedance, defines the short circuit current for the IGBT and diodes [50].

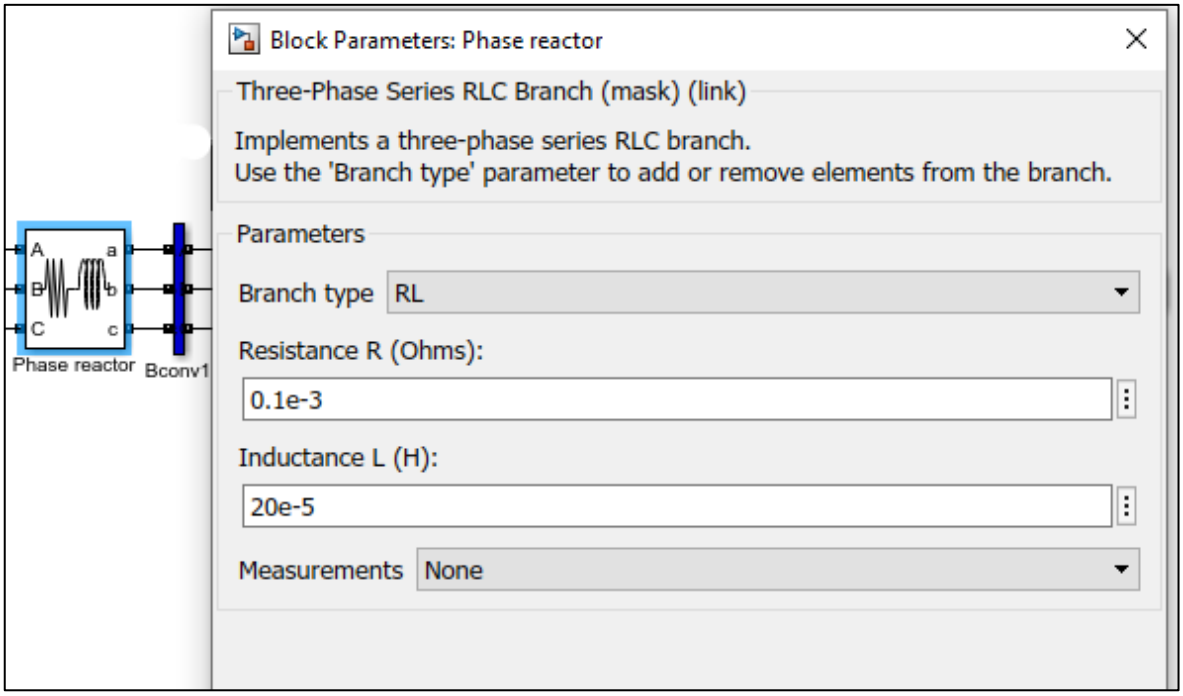

Figure - (d) Details of phase reactor block

According to [51], the typical short-circuit impedance of this type of phase reactor is 0.15 p.u. The phase reactor is modeled as an inductor in series with small resistance, which considers the reactor losses.

3.2.5 DC Side Capacitor

The main function of the DC side capacitor is to acts as a temporary energy storage device where the converter can momentarily store or absorb energy while keeping the power balance during the transients. In addition, it reduces the voltage ripple on the DC side and provides a sufficiently stable direct voltage from which alternating voltage will be generated on the AC side of the converter. Moreover, the capacitor acts as a sink for undesired high-frequency current components that are generated by the switching action of the converter and injected to the DC side. Thus, these currents prevented from propagating to the rest of the DC distribution link, being filtered by the inductance and resistance of the DC cables.

The capacitor sizing is usually performed considering the DC voltage and amount of power to be stored. Consequently, the capacitor is characterized by the capacitor time constant (τ), defined as:

$$\tau = \frac{\frac{1}{2} \times (C_{DC,N}) \times V_{DC,N}^2}{P_N} \tag{3.1}$$

where, $C_{DC,N}$ is the capacitance, $V_{DC,N}^2$ is the rated pole-to-pole direct voltage and P_N is the rated active power of the VSC. The time constant is equal to the time needed to charge the capacitor of capacitance $C_{DC,N}$ from zero to $V_{DC,N}^2$, by providing it with a constant amount of power P_N [52].

3.2.6 DC Cable

The VSC station 1 and station 2 has connected with the help of DC cable (1 pi section). The power transmission between VSC-LVDC stations is performed using DC cable: XPLE insulated single-core aluminum (1x630mm2). The existing system using two cables in parallel, as the nominal current of DC side, is twice than the cable current carrying capacity. Each DC pole can be modeled as a Π-model, with resistance R_{pole}, inductance L_{pole} and two identical capacitors with capacitance $C_{pole/2}$.

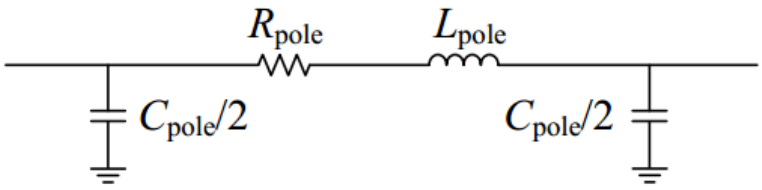

Figure 3.3 - Pi-model of DC cable

The distribution cables/lines are normally described in terms of resistance per unit length (Ω/km) $[r]$, inductance per unit length (H/km) $[l]$, and capacitance per unit length (F/km) $[c]$, along with the length of the DC distribution system being provided in kilo-meter;

Parameters	Details
Cable type	Single Core Aluminium
Cross-section [A]	630 mm^2
Length (m)	1000
Resistance per unit length (Ω/km) $[r]$	0.025
Inductance per unit length (H/km) $[l]$	0.07e-3
Capacitance per unit length (F/km) $[c]$	0.8e-6

Table 3.1 - DC bus cable details

3.3 Voltage Sourced Converter Operation

In comparison with the line-commutated converters, the voltage source converters (VSC) belong to the self-commutated converter category, being able to switch its power electronic IGBT at any value of desired current flowing through them. This feature permits the VSC to generate a constant level of direct voltage at its DC side and produce a bi-directional power flow. This section describes the operation of VSC and provides a brief introduction about the application of the pulse-width modulation (PWM) method. The author also observed that other modulation approaches can be applied in existing installations in order to reduce the system losses, but most of them share common behaviors with the PWM method. In later discussion, the operational limitations of the VSC are analyzed, and the proposed topology of VSC-LVDC has presented.

3.3.1 Converter Structure, Switching, and Modulation

The basics of VSC operation is a half-bridge converter as mentioned in figure 3.4(a), DC side is connected to DC source voltage (V_{DC}). The source voltage is divided equally between series-connected identical capacitors and each capacitor bear half of the source voltage.

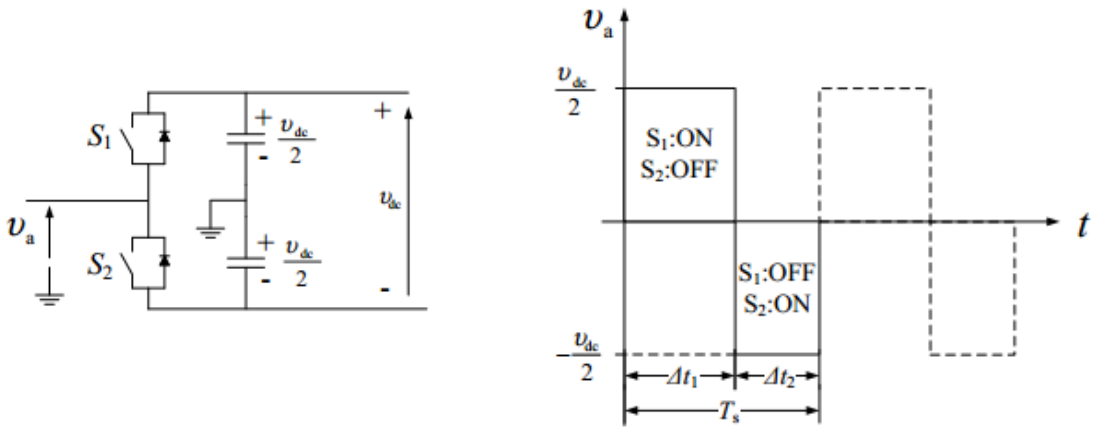

(a) (b)

Figure 3.4 - Half-bridge converter (a) Converter topology (b) Voltage output waveform [52]

The switches S_1 and S_2 are operated at a different time (Δt_1 and Δt_2) period with the following sequence of actions:

1. The switching pattern is periodic with an angular frequency ω_0 and the period T_s.
2. The switch S_1 is at ON state and switch S_2 at OFF state for a duration of Δt_1. The measured voltage at the output is equal to $+V_{DC/2}$.
3. The switch S_2 is at ON state and switch S_1 at OFF state for a duration of Δt_2 ($\Delta t_2 = T_s - \Delta t_1$). The measured voltage at the output is equal to $-V_{DC/2}$.

As shown in figure 3.4(b), the resulting periodic waveform of voltage (V_a) is fluctuating between $+V_{DC/2}$ and $-V_{DC/2}$. The waveform can be expressed in Fourier series as:

$$V_a = \frac{V_{a,0}}{2} + V_{a,1}\, sin(\omega_0 t + \phi_1) + \sum_{n=2}^{\infty} V_{a,n}\, sin(n\,.\,\omega_0 t + \phi_n) \qquad (3.2)$$

here the term $V_{a,n}$ and ϕ_n are the Fourier coefficient and angles. The DC offset term ($V_{a,0}/2$) becomes equal to zero during a duty cycle of 0.5 ($\Delta t_1 = T_s/2$). Hence, equation (3.2) becomes:

$$V_a = V_{a,1}\, sin(\omega_0 t + \phi_1) + \sum_{n=2}^{\infty} V_{a,n}\, sin(n\,.\,\omega_0 t + \phi_n) \tag{3.3}$$

it is implying from the equation (3.3) that there is a fundamental sinusoidal harmonic with an amplitude ($V_{a,1}$) at a frequency (ω_0) along with higher harmonics. The nth-order harmonic will have amplitude ($V_{a,n}$) and frequency ($n\,.\,\omega_0$). So, for this type of square waveform, the amplitude of the sinusoidal component is defined as:

$$V_{a,n} = \frac{2\,.\,V_{DC}}{\pi\,.\,n}, \qquad n = 1,3,5,\ldots(odd) \tag{3.4}$$

$$V_{a,n} = \frac{2\,.\,V_{DC}}{\pi\,.\,n}, \qquad n = 1,3,5,\ldots(odd) \tag{3.5}$$

The fundamental component has the largest amplitude, when $V_{a,n} < V_{a,n-1}$ for every odd value of n. Thus, under the adopted switching pattern, the half-bridge leg behaves as a voltage source, generating an alternating voltage output that contains a fundamental sinusoidal component of fixed amplitude and varying phase (achieved by delaying the whole switching pattern over time), together with higher-order harmonics of smaller magnitude.

The fundamental component has the largest amplitude, when $V_{a,n} < V_{a,n-1}$ for every odd value of n. Thus, under the adopted switching pattern, the half-bridge leg behaves as a voltage source, generating an alternating voltage output that contains a fundamental sinusoidal component of fixed amplitude and varying phase (achieved by delaying the whole switching pattern over time), together with higher-order harmonics of smaller magnitude.

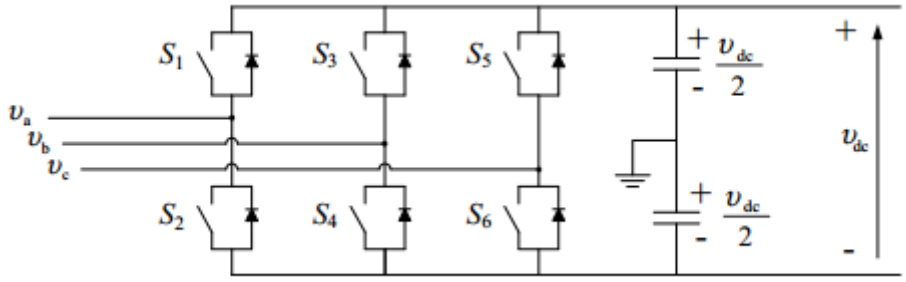

Figure 3.5 - Three-phase six bridge VSC converter [52]

When three half-bridge legs are connected to a voltage source and DC side capacitor in a configuration mentioned in figure 3.5, as a result, a three-phase voltage sourced converter can be created. In this arrangement, each leg being able to produce an independently alternating voltage ($V_a, V_b, or\ V_c$). In this case, if all the three legs are provided the same square wave with a switching pattern of 0.5 duty cycle and frequency (ω_0), but consecutively phase-shifted by 2π/3 radians between one leg to the next. Consequently, the VSC acts as a three-phase voltage source with same voltage magnitudes and phase-shifted by 2π/3 radians.

Figure 3.5 shows a three-phase two-level VSC and its output phase voltage ($V_a, V_b, or\ V_c$) relative to the supply mid-point. This type of converter is known as two-level converter because it can generate only two voltage levels ($+V_{DC/2}$ and $-V_{DC/2}$) at the output phases (a, b, and c) relative to the supply mid-point (0). VSC uses composite self-commutated switching devices such as the insulated gate bipolar transistor (IGBT) and anti-parallel diodes to enable bi-directional current flow in each phase-leg, hence bidirectional power flow between AC and DC sides, as seen in figure 3.6.

There are numerous designs for potential VSC converters exist, however only a few of them are implemented due to the commercial reasons. The great majority of all VSC-based transmission system having been built to date [53] are based on the two-level converter, as mentioned in figure 3.5. Though, the produced two-level AC side voltage has higher harmonic content and so the use of filters is necessary. The main reasons for the losses being high, due to the high switching frequency at which the IGBTs are operated [54].

So, the author has proposed three-level diode clamped converter also known as neutral-point clamped (NPC) converter, as shown in figure 3.6(a).

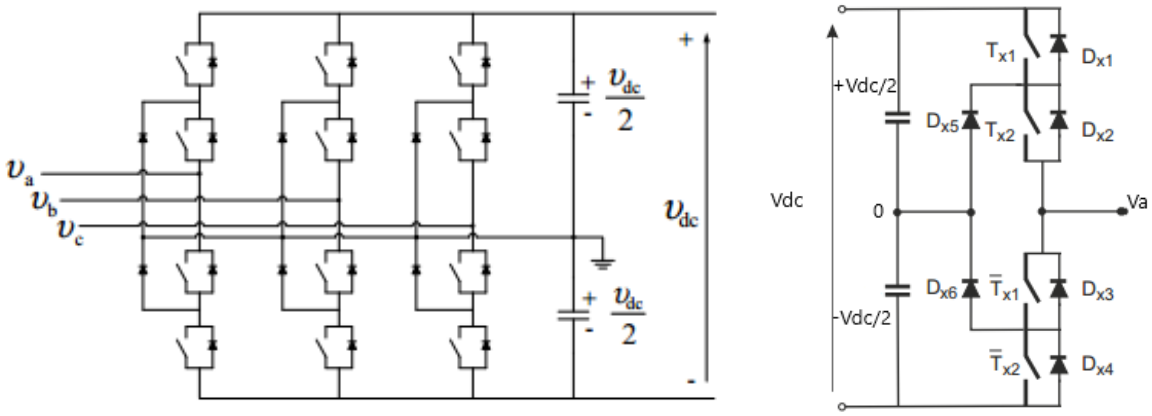

(a) (b)

Figure 3.6 - (a) Neutral point clamped three-level VSC (b) Single leg of a three-level converter [52]

Three-level configuration can generate three voltage levels ($+V_{DC/2}$, 0, $-V_{DC/2}$), at the output of each phase ($V_a, V_b, or\ V_c$) relative to supply mid-point or neutral-point '0', as shown in figure 3.6(b). Its proper operation requires the DC voltage across the DC side capacitors to be maintained at a value of $V_{DC/2}$.

For the sake of simplicity, the author considers only one phase with four switches, as mentioned in figure 3.6(b). The switching of two complementary switches pairs (T_{x1} & T_{x2}) and ($\overline{T}_{x1}$ & $\overline{T}_{x2}$), respectively.

1. When switches (T_{x1} & T_{x2}) are at on-state, the three-level converter generates voltage level ($+V_{DC/2}$) at output relative to neutral-point '0'.
2. When switches (T_{x2} & $\overline{T}_{x1}$) are at on-state, the three-level converter generates voltage level (0) at the output.
3. When switches ($\bar{T}_{x1}$ & $\bar{T}_{x2}$) are at on-state, the three-level converter generates voltage level ($-V_{DC/2}$) at output relative to neutral-point '0'.

When three legs are connected to a voltage source and DC side capacitor in a configuration mentioned in figure 3.6(a), as a result, a three-phase three-level voltage sourced converter can be created. In this arrangement, each leg being able to produce an independently alternating voltage ($V_a, V_b, or\ V_c$).

The first effort towards multilevel AC voltage is performed by adapting the neutral point clamped (NPC) converter to LVDC standards. This type of converter leading to lower total harmonic distortion, losses and filter requirements but at the cost of high mechanical complexity. The complexity increased converter size, challenges in balancing the DC side capacitors and uneven loss distribution among the IGBTs [53],[55],[56].

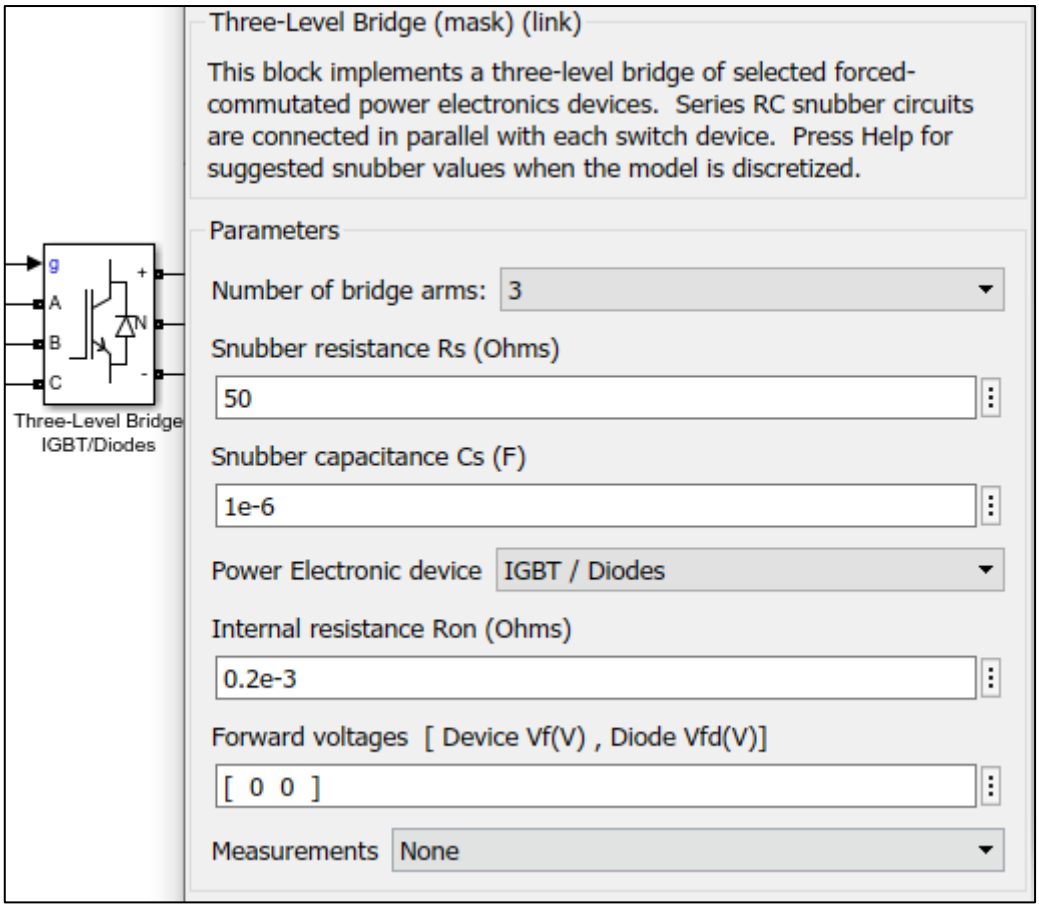

Figure - (e) Details of three-level neutral point clamped bridge block

Here, the terminals (A, B, C) are three-phase output voltage connected with the phase reactor, the terminals $(+, N, -)$ are connected with DC distribution system, and the terminal (g) is a firing pulses signal fed by the sinusoidal pulse width modulation.

3.3.2 Sinusoidal Pulse Width Modulation

Several pulse width modulation (PWM) techniques have been developed to control the output voltage magnitude of fundamental component and to reduce the harmonic content in voltage and current waveforms. In the previous section 3.3.1, square waveform modulation has applied on a half-bridge converter. The disadvantage of this type of modulation, it cannot modulate the amplitude of the sinusoidal components if V_{DC} is fixed with the fundamental component (i.e. being the object of interest). However, it is possible to control the phase of the resulting voltage waveform. In addition, the equations (3.4 & 3.5) indicate that there are many low-frequency range harmonics with significant amplitude, as a result, large filters would be needed to ensure that the out voltage is mainly represented by the fundamental component. There are some well-known modulation strategies in use today, these are selective harmonic elimination (SHE), sinusoidal pulse width modulation (SPWM) and space vector modulation (SVM) [57],[58].

The author is using the half-bridge converter as mentioned in figure 3.4(a), according to the PWM method, the switches S_1 and S_2 do not necessarily have to be switched with a fixed duty cycle. A selected sequence of alternating switching with different time durations can create an output voltage whose fundamental component can have controllable amplitude, while the amplitude of higher harmonics can be significantly reduced [52]. The concept of sinusoidal pulse width modulation (SPWM) is presented in figure 3.7 and applied on the half-bridge converter figure 3.4(a).

The main concept of SPWM in VSC, the sampling of the desired reference signal in order to regenerate it as an output voltage. Here, a periodic triangular wave carrier signal has used for the sampling with an amplitude (A_C) and frequency (F_C). The amplitude (A_C) value has considered equal to $V_{DC/2}$. Let's assume that the desired reference output voltage of VSC as following:

$$V_{a,ref} = A_r \,.\, sin\,(2\pi f_r t + \phi) \tag{3.6}$$

here, A_r is the amplitude of the reference and f_r is its frequency. The modulation index (m_a) and the frequency ratio (m_f) are defined below:

$$m_a = \frac{A_r}{A_c} \tag{3.7}$$

$$m_f = \frac{f_r}{f_c} \tag{3.8}$$

when this approach applied to the half-bridge converter 3.4(a), both amplitudes, carrier, and reference (A_c&A_r) are normalized by the value ($V_{DC/2}$). The normal value of the carrier is equal to 1 ($A_{c,norm} = 1$), however the reference signal in equation (3.6) becomes:

$$(V_{a,ref})_{norm} = A_{r,norm}\, sin\,(\omega_0 t + \phi) = \frac{A_r}{V_{DC}/2}\, sin\,(\omega_0 t + \phi) \tag{3.9}$$

now, the modulation index will become:

$$m_a = \frac{A_r}{V_{DC}/2} \tag{3.10}$$

There are four graphs being presented in figure 3.7, the first graph shows the superposition of a normalized referenced signal at a reference frequency ($f_r = 50$Hz), and corresponding to a reference voltage amplitude (A_r) slightly smaller than $V_{DC/2}$ at a carrier signal 1.5 kHz ($f_c = 1.5\ kHz$). The basic SPWM method rules are the following:

- When the reference signal has a higher value than the carrier signal, S_1 is set at on-state and S_2 is kept at off-state.
- When the reference signal has a lower value than the carrier signal, then S_1 is kept at off-state and S_2 is set at on-state.

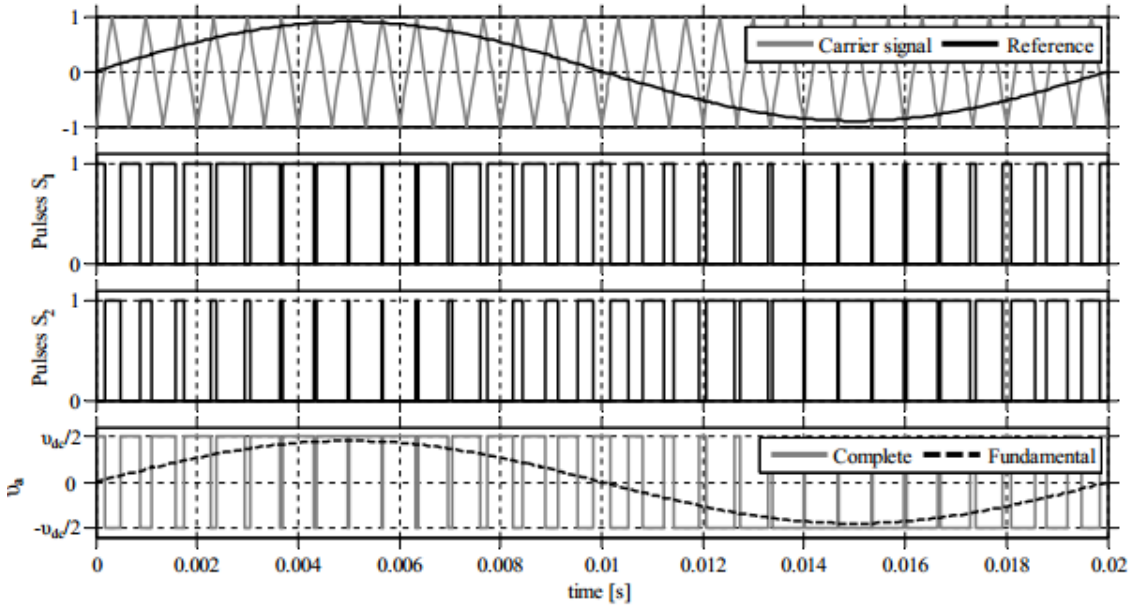

Figure 3.7 - Application of SPWM to a half-bridge converter [52]

The graphs in figure 3.7 show the carrier and reference waves, the pulses to the active switches and the output voltage waveforms. The behavior of S_1 and S_2 switching pulses are shown in the second & third graph of figure 3.7, with values 1 and 0 correspondings to on-state and off-state. According to these switching patterns, the resulting waveform of the half-bridge converter varies between $+V_{DC/2}$ & $-V_{DC/2}$, and the amplitude ($V_{a,1}$) of the fundamental is:

$$V_{a,1} = m_a . \frac{V_{DC}}{2} = \frac{A_r}{V_{DC}/2} . \frac{V_{DC}}{2} = A_r \qquad (3.11)$$

Consequently, the resulting waveform has a fundamental component which is identical to the reference voltage ($V_{a,ref}$), as seen in equation (3.6). Hence, the converter can reproduce a reference with varying amplitude while keeping V_{DC} constant. The same principle applies to three-phase VSC, as mentioned in figure 3.7.

The operating region of the VSC verifies w.r.t the modulation index. When $m_a \leq 1$, the VSC operates in its linear region and relation (3.11) applies. If $m_a > 1$ (the reference signal has higher amplitude than the carrier signal), the VSC operates in overmodulation region, here relation (3.11) does not apply. In this case, the amplitude of the fundamental is no longer equal to the amplitude of the reference, so it can reach a maximum value of $2V_{DC}/\pi$, as defined by equations (3.4&3.5), and it corresponds to a fully square waveform of the VSC output voltage.

Furthermore, when VSC operated in its linear region, the high-order harmonics of voltage output primarily appears at the close vicinity of frequencies that are integer multiples of the carrier frequency (f_c). As the frequency ratio (m_f) increases, the harmonics are also shifted toward higher frequencies level, where associated passive filters can have a smaller size and low-cost. However, the higher carrier frequency (f_c) implies higher switching per reference period, which directs higher switching losses. Therefore, it is important to find a reasonable point between switching losses and the cost of filters.

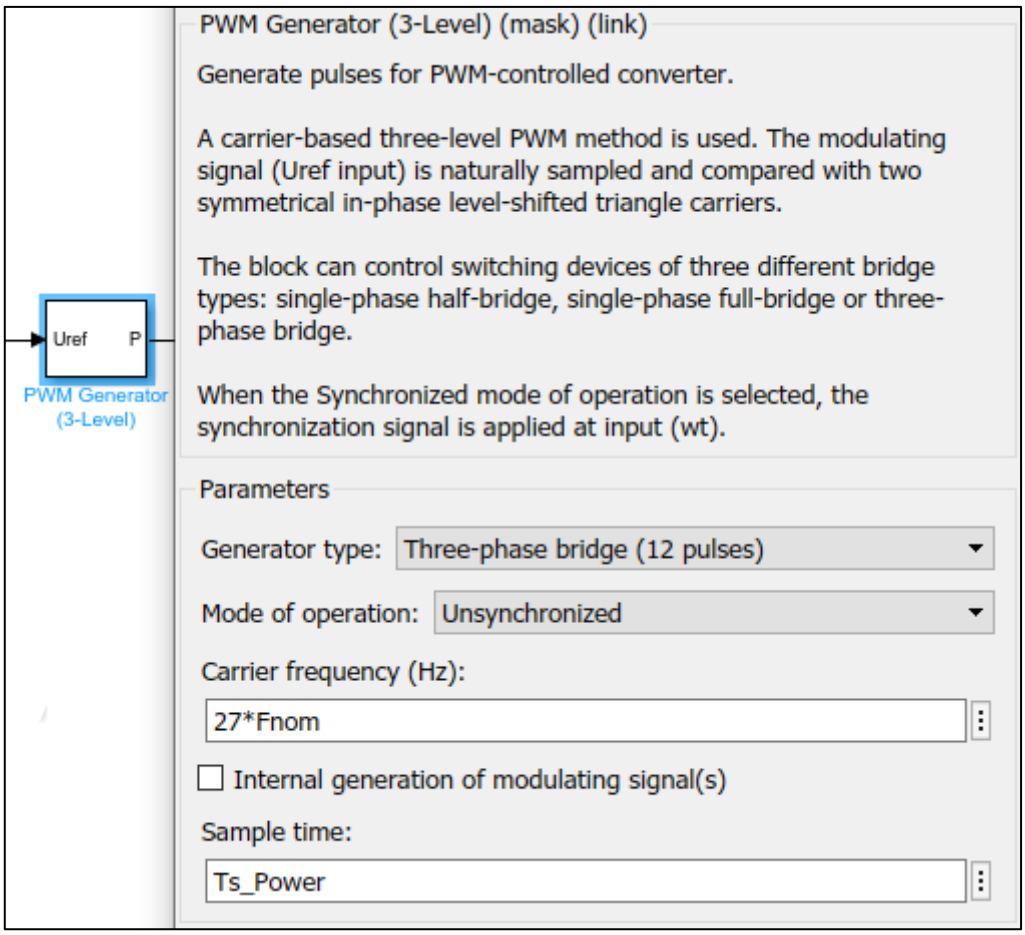

Figure - (f) Details of sinusoidal pulse width modulation block

3.3.3 PQ Capability

As discussed in section 3.3.2, the VSC can produce a fully controllable output alternating voltage, now it is possible to examine the power-transfer capabilities of a VSC-LVDC station. In the below figure 3.8, shows a proportion of LVDC distribution link with a VSC station and the phase reactor. The associated AC system; transformer and AC side filters are considered by an equivalent Thevenin model which connected to the phase reactor, the connection point having a voltage phasor $\overline{U}_f$ ($\overline{U}_f = U_f\angle 0$). The phase reactor and the IGBT of the station are supposed to be lossless for the sake of simplicity.

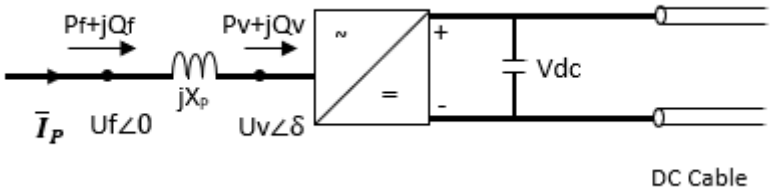

Figure 3.8 - Power transfer on the AC side of VSC-LVDC converter

The output voltage of the converter $\overline{U}_v$ ($\overline{U}_v = U_v\angle\delta$) with the desired magnitude ($\overline{U}_v$) and an angle (δ). In this system, the steady-state per-unit complex power absorbed by the VSC at the connection point of the phase reactor is equal to:

$$S_f = \overline{U_f}\,.\,[\bar{I}_p]' = U_f\left[\frac{U_f - U_v\angle\delta}{jX_p}\right] \tag{3.12}$$

$$S_f = -\frac{U_f.U_v}{X_p}.sin(\delta) + j\frac{U_f^2}{X_p} - j\frac{U_f.U_v}{X_p}.cos(\delta) \tag{3.13}$$

here active and reactive power are:

$$P_f = -\frac{U_f U_v}{X_p}.sin(\delta) \tag{3.14}$$

$$Q_f = \frac{U_f^2}{X_p} - \frac{U_f U_v}{X_p}.cos(\delta) \tag{3.15}$$

now, considers that the phase shift (δ) is usually very small, the Taylor approximation of sin (δ) and cos (δ) equals to δ and 1, respectively. So, the equations (3.14) and (3.15) can be written as:

$$P_f = -\frac{U_f U_v}{X_p}.(\delta) \tag{3.16}$$

$$Q_f = \frac{U_f - U_v}{X_p}.U_f \tag{3.17}$$

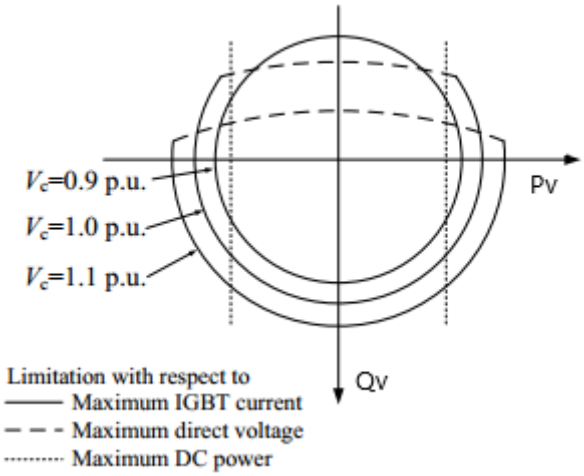

Figure 3.9 - PQ capability curve of VSC transmission system [59]

According to [59], now considering that U_f is quite rigid and the voltage variation range of converter voltage (U_v) is normally small (0.9-1.1 p.u.). We can see in the equations (3.16 & 3.17), the active power (P_f) is control by phase shift (δ), and the reactive power (Q_f) is control by the voltage magnitude differences ($U_f - U_v$). Hence, it can be claimed that the active power is controlled by the angle difference of the voltages across the phase reactor, and the reactive power is controlled by the magnitude difference of the voltage phasors. As mentioned in equations (3.16 & 3.17), the VSC can independently control the magnitude and phase of its output voltage, so it can be claimed that the VSC is able to control independently the active and reactive power transfer.

Nevertheless, the PQ capabilities of a VSC station are not limitless and one should consider it so that the certain limits are not exceeded. There are mainly three factors that limit the power capability seen from a power system stability perspective [59].

The first limit is the maximum current passing through the IGBTs of the converter. Here, the maximum apparent power $|S_{max}|$ that the VSC can output at its AC side is:

$$|S_{max}| = |P_v + jQ_v|_{max} = \sqrt{(P_v^2 + Q_v^2)_{max}} = U_v . I_{p,max} \qquad (3.18)$$

where $I_{p,max}$ is the maximum allowed current passing through the IGBTs, the equation (3.18) defines a circle of maximum apparent power $|S_{max}|$ with a radius $U_v . I_{p,max}$. Consequently, for a given $I_{p,max}$ and changing U_v, the maximum allowed apparent power (MVA) limit of the VSC changes, accordingly, as mentioned in figure 3.9.

The second limit is the maximum direct voltage level $U_{dc,max}$ at steady state. The reactive power is mainly dependent on the voltage difference, between the alternating voltage that the VSC can generate from the direct voltage on its dc side and the grid AC voltage. In case, If the grid AC voltage is high, the difference between the $U_{dc,max}$ and the AC voltage will be low, then reactive power capability increases with decreasing ac voltage.

The third limit is associated with the maximum direct current through the cable, which has an effect only on the active power. The enclosed area between the previous limits defines the allowed operational area of the VSC.

Consequently, If all these limits are to be considered for active and reactive powers (P_f & Q_f), the small adjustments have to be made, due to the presence of phase reactor which accounts for the active power losses and reactive power absorption.

3.4 VSC Control Scheme

The vector control is a dominant method uses for VSC control. As mentioned in [60], the vector control has been widely applied in high-performance motor drive applications for the control of VSC-driven electrical machines. It is also pragmatic in AC to DC grids tied with converters. The main idea of the vector control is the representation of a three-phase alternating quantity of the AC system as a vector with DC type of properties, positioned on a dq-rotating frame. The resulting vectors can be controlled in a similar manner as the voltage and current of a DC system, and finally restored to its three-phase alternating representation applied to the AC system. This control technique permits independent control of active and reactive powers with a fast-dynamic response [61].

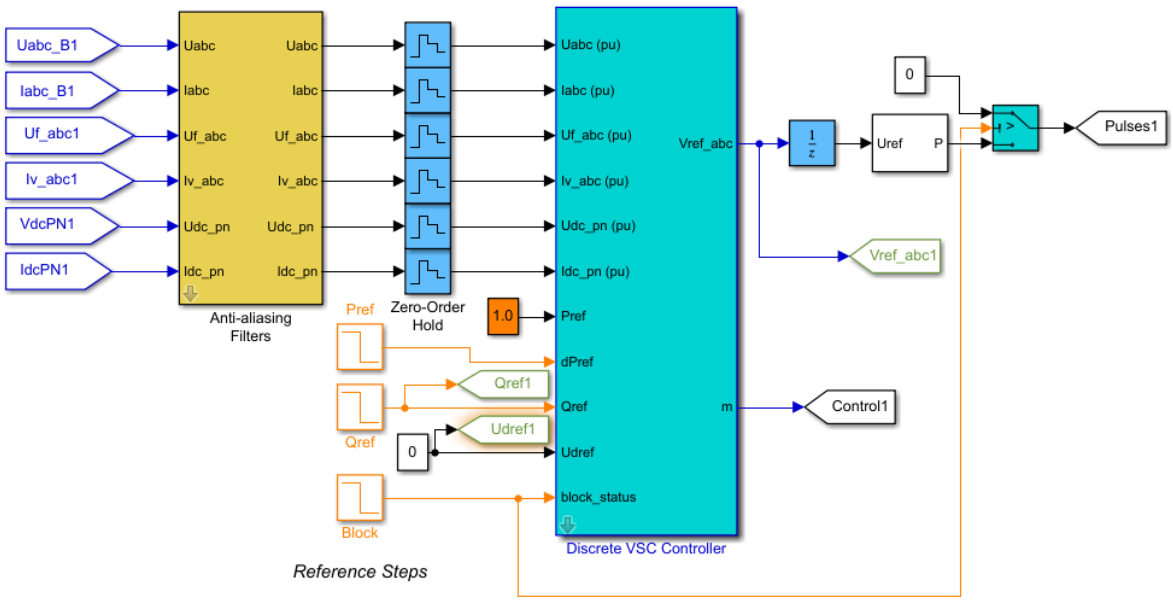

(a)

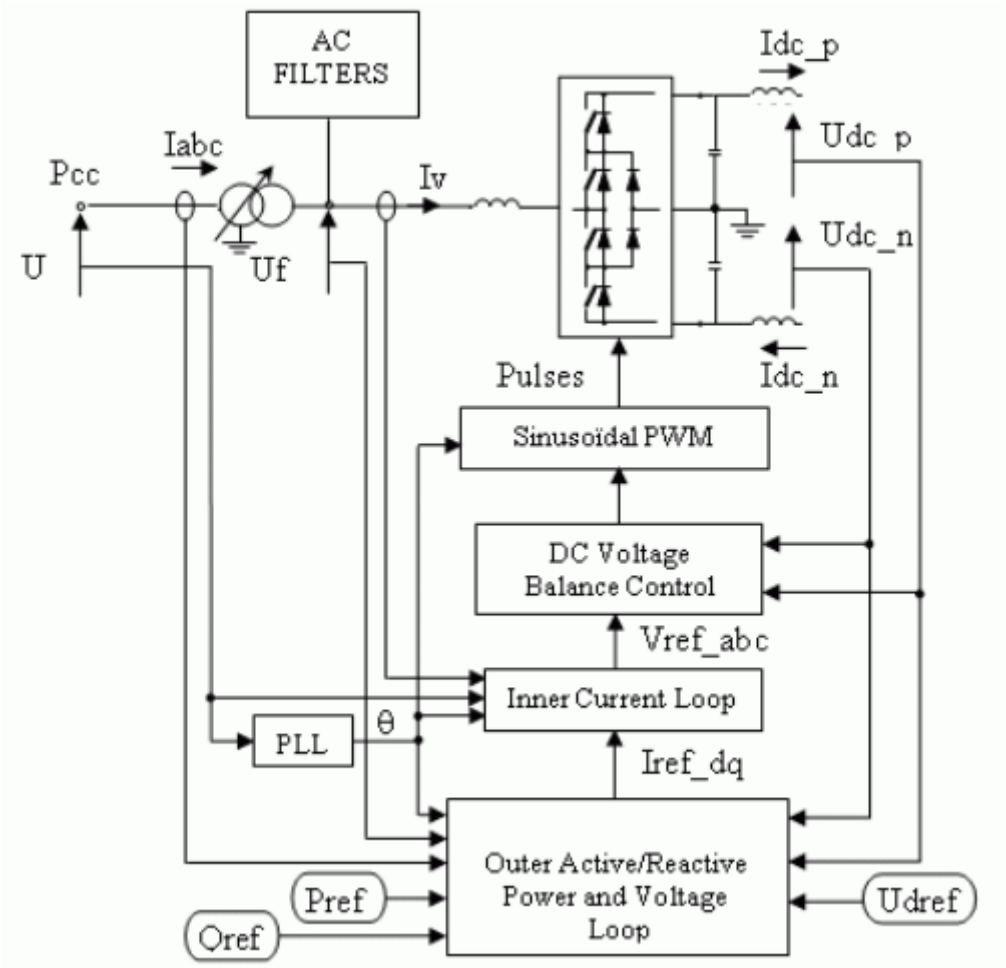

(b)

The typical structure of a VSC-LVDC control system is illustrated in figure 3.10. The active power, reactive power, and voltage loop contains the outer loop regulators that calculate the reference value of the converter current vector (I_{ref_dq}) which is the input to the inner current loop. The control scheme of the inner current loop receives the currents references I_{ref_dq} as inputs and provide an output voltage references U_d^* and U_q^*. The direct axis deals with active power flow at PCC or the pole-to-pole DC voltage depending on the control mode selection (active & reactive power or DC voltage & reactive power) and quadratic axis deal with the reactive power flow at PCC in both control modes. Then, these rotating frames are transformed into three-phase quantities (V_{ref_abc}) and provided as modulating signals to the sinusoidal pulse width modulation (SPWM) block, which will generate appropriate firing signals (pulses) for the VSC IGBT.

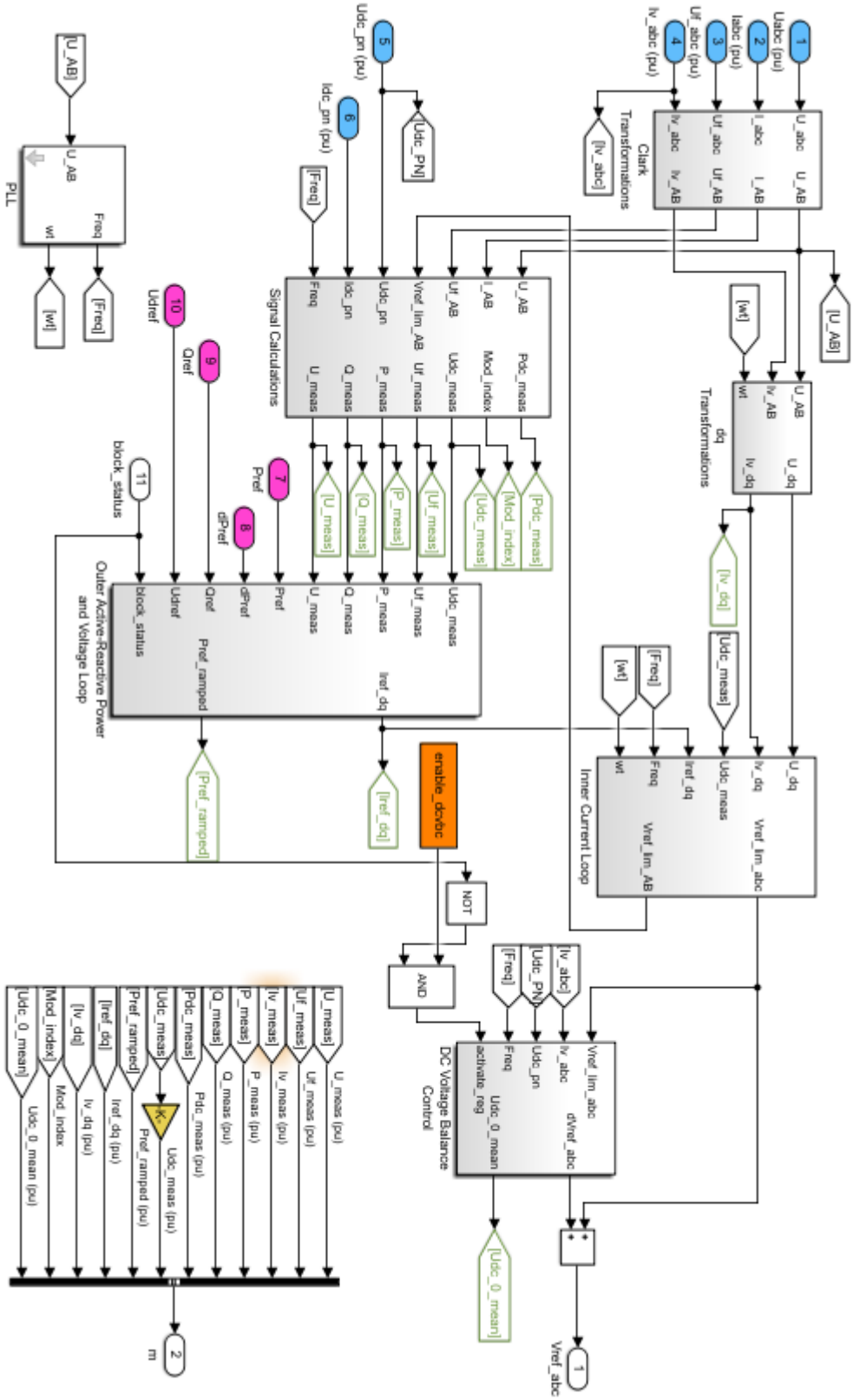

Figure 3.10 - (a) Actual model of VSC control system (b) & (c) Control system overview

3.4.1 Phase-Locked Loop (PPL)

The duty of PLL in the VSC control system is to estimate the phase synchronous angle θ of the measured voltage at PCC (U_{abc}). A Phase-Locked Loop (PLL) is based on Clarke and park transformation. It used to synchronize the dq-rotating frame of the converter with the rotating vector ($U_{\alpha\beta}$) in αβ-coordinates, providing a reliable reference frame for any abc-to-dq and dq-to-abc transformations.

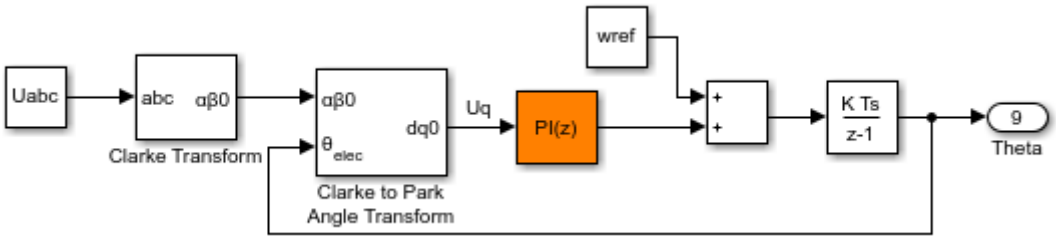

Figure 3.11 - Block diagram of PLL

The structure of the adopted PLL is depicted in figure 3.11, the voltage (U_{abc}) is transformed into $U_{\alpha\beta}$ and by using the PLL's estimation theta (θ), it calculates U_{dq}. Based on the error U_q, the output of the PI controller is a correction signal Δω which is added into a constant pre-estimation of the vector's angular speed ω_{ref}. This provides the converter angular speed ω and then integrated to produce the updated version of angle θ (Theta), which is feedback (θ_{elec}) to the αβ-to-dq (Clarke to Park angle transform) block and produces the new U_q. If we sum-up, it measures system frequency and provides angle θ for dq transformation block. In steady-state, the phase synchronous angle θ is in phase with the fundamental (positive sequence) of the α component and phase A of the PCC voltage (U_{abc}).

3.4.2 Outer Active, Reactive Power, and Voltage Loop

There are two main control modes of a VSC-LVDC system: Active & Reactive Power, DC Voltage & Reactive Power. In this thesis, station 1 is working as an active & reactive

power controller, while the station 2 is working as a DC voltage & reactive power controller. The outer loop block consists of different control loops such as active power, reactive power, DC voltage override, AC voltage override, and DC voltage loop. The author has explained below the function of each loop along with their inputs, outputs, and limitations.

Active Power Loop: The main function of active power loop is to introduce the flow of active power equal to a certain reference. The VSC circuit measured the active power at the PCC. If the considered station is in power control mode, the controller power corresponds to the power that enters the phase reactor towards the IGBT of VSC.

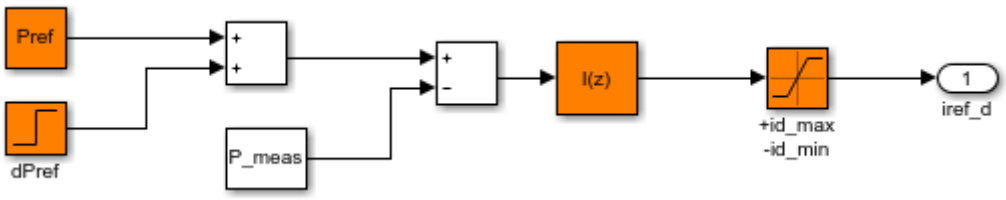

Figure 3.12 - Active power controller

As mentioned in figure 3.12, active power solely depends on the current (I_d) and the voltage (U_{abc}). The active power control loop has two input blocks P_{ref} and dP_{ref}. The amount of active power to be injected into the station via P_{ref} block while the extra ramping block (dP_{ref}) ramps the power order towards the desired value with an adjusted rate when the control is de-blocked. The ramped value is reset to zero when the converter is blocked.

The latter experience, where an Integral controller is used to generate the current reference (I_{ref_d}) that will be fed to the inner current loop. The controller has an anti-windup function where the reference (I_{ref_d}) is limited to a maximum value (I_{d_max}) equal to a rated property (I_{abc_base}). It can be the rated AC current of the converter or a value close to the maximum allowed IGBT current, both turned into an appropriate *dq*-current quantity.

DC Voltage Override Control: The DC voltage override control block based on two PI regulators. This type of controller will override the active power regulator to maintain the

DC voltage within a secure range, especially during a perturbation period (e.g. during active power injection) in the AC system of the station controlling the DC voltage.

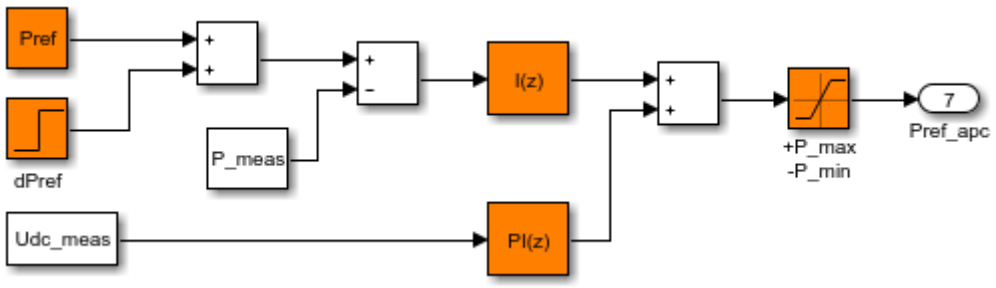

Figure 3.13 - Direct voltage override controller

Reactive Power Loop: The reactive power is measured at the PCC that enters the phase reactor, with a direction towards the VSC IGBT. The selected measurement point is proportional to the voltage value (U_{abc}) and the current (I_q). As a result, reactive power (Q) can be considered only a function of current (I_q). The Integral based reactive power controller can regulate (Q) to follow a reference (Q_{ref}) by creating an appropriate current reference (I_{ref_q}), which will provide to the inner current controller.

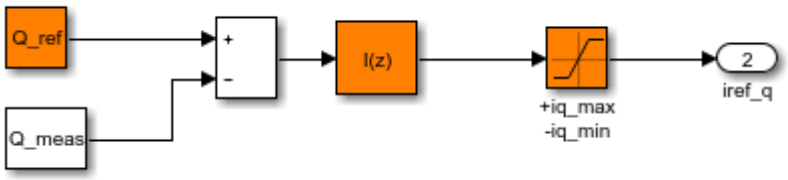

Figure 3.14 - Reactive power controller

As like active power controller, it also has an anti-windup function where the reference (I_{ref_q}) is limited to a maximum value (I_{q_max}), to avoid the saturation issues, the anti-windup function takes the following actions:

- Error is reset to zero when the measured voltage at PCC is less than a constant value (i.e. during an AC perturbation).
- When the regulator output is limited, the limitation error is fed back with the right sign, to the integrator input.

AC Voltage Override Control: The AC voltage override control block based on two regulators (PI). This controller will override the reactive power regulator to maintain the AC voltage at PCC within a secure range especially during the steady-state condition.

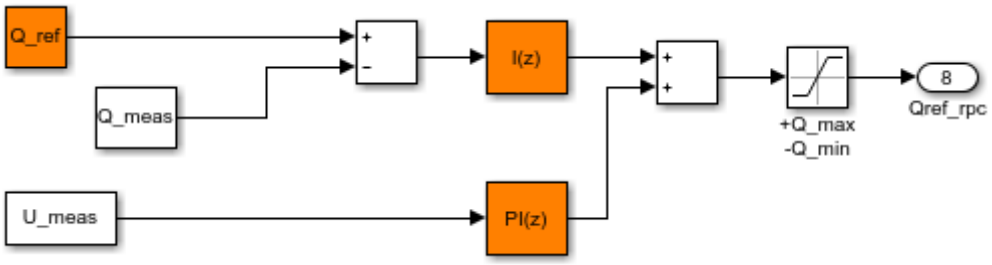

Figure 3.15 - Alternating voltage override controller

DC Voltage Loop: The DC voltage regulator uses a PI controller. The controller has a reference block (U_{dref}) to receive an anticipated level of DC voltage at converter output with a step change. This block is only enabled if the DC voltage & reactive power control block is selected at the main control mode. The block output is a current reference value ($I_{ref\_d\_dcvc}$) for the d-component of converter current vector, which will be fed to the current reference limitation block and finally injected into the inner current loop.

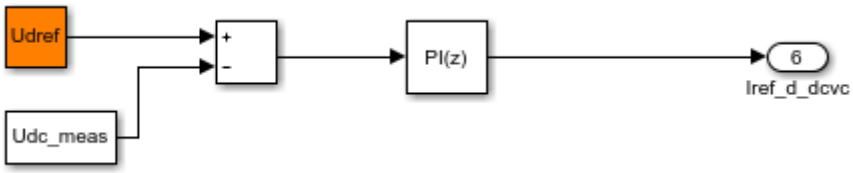

Figure 3.16 - DC voltage regulation

In the power control mode, the equal scaling is applied to the active and reactive power reference when a limit is imposed. However, in the DC voltage control mode, the higher priority is given to the active power when a limit is imposed for efficient control of the voltage.

3.4.3 Inner Current Loop

The inner (vector) current controller is the main part of the voltage sourced converter control scheme. Considering the equivalent process representing the VSC in figure 3.17, if we apply Kirchhoff's voltage law (KVL) across the phase reactor, the following differential equations can be obtained for the three phases.

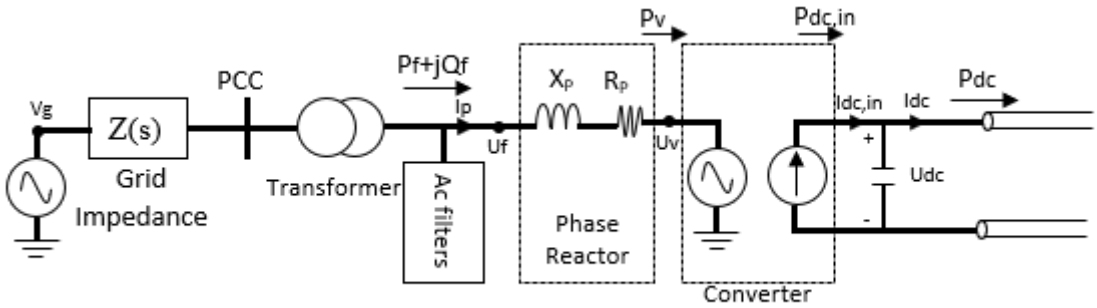

Figure 3.17 - VSC equivalent model

here

$$U_{f\_abc} - U_{v\_abc} = L_p \frac{dI_{p\_abc}}{dt} + R_p I_{p\_abc} \tag{3.19}$$

by applying Clarke transformation, the equation (3.19) transformed into $\alpha\beta$-coordinates:

$$\underline{U}_{f\_\alpha\beta} - \underline{U}_{v\_\alpha\beta} = L_p \frac{d\underline{I}_{p\_\alpha\beta}}{dt} + R_p \underline{I}_{p\_\alpha\beta} \tag{3.20}$$

now apply park transformation, the PLL of VSC is synchronized with the voltage vector ($\underline{U}_{f\_dq}$). The considered voltage and current vectors can express as:

$$\underline{U}_{f\_\alpha\beta} = \underline{U}_{f\_dq}.e^{j\theta_f} \tag{3.21}$$

$$\underline{U}_{v\_\alpha\beta} = \underline{U}_{v\_dq}.e^{j\theta_f} \tag{3.22}$$

$$\underline{I}_{p\_\alpha\beta} = \underline{I}_{p\_dq}.e^{j\theta_f} \tag{3.23}$$

by applying dq-coordinates (3.21,3.22, & 3.23) into equation (3.20):

$$\underline{U}_{f\_dq}.e^{j\theta_f} - \underline{U}_{v\_dq}.e^{j\theta_f} = L_p \frac{d(\underline{I}_{p\_dq}.e^{j\theta_f})}{dt} + R_p \underline{I}_{p\_dq}.e^{j\theta_f}$$

$$\underline{U}_{f\_dq}.e^{j\theta_f} - \underline{U}_{v\_dq}.e^{j\theta_f} = j.\frac{d\theta_f}{dt} L_p.\underline{I}_{p\_dq}.e^{j\theta_f} + L_f.e^{j\theta_f} \frac{d(\underline{I}_{p\_dq})}{dt} + R_p \underline{I}_{p\_dq}.e^{j\theta_f}$$

$$\underline{U}_{f\_dq}.e^{j\theta_f} - \underline{U}_{v\_dq}.e^{j\theta_f} = j\omega_f L_p.\underline{I}_{p\_dq}.e^{j\theta_f} + L_p.e^{j\theta_f} \frac{d(\underline{I}_{p\_dq})}{dt} + R_p \underline{I}_{p\_dq}.e^{j\theta_f} \tag{3.24}$$

here ω_f is the angular frequency of the dq-rotating frame. Typically, the variation in $\omega_f(t)$ are very small over time and it can be considered as a constant. So, eliminate the term ($e^{j\theta_f}$) and the equation (3.24) can be written as:

$$\underline{U}_{f\_dq} - \underline{U}_{v\_dq} = j\omega_f L_p.\underline{I}_{p\_dq} + L_p \frac{d(\underline{I}_{p\_dq})}{dt} + R_p \underline{I}_{p\_dq} \tag{3.25}$$

$$L_p \frac{d(\underline{I}_{p\_dq})}{dt} = \underline{U}_{f\_dq} - \underline{U}_{v\_dq} - j\omega_f L_p.\underline{I}_{p\_dq} - R_p \underline{I}_{p\_dq} \tag{3.26}$$

the real and imaginary parts are segregated:

$$L_p \frac{d(\underline{I}_{p\_d})}{dt} = \underline{U}_{f\_d} - \underline{U}_{v\_d} - \omega_f L_p.\underline{I}_{p\_d} - R_p \underline{I}_{p\_d} \tag{3.27}$$

$$L_p \frac{d(\underline{I}_{p\_q})}{dt} = \underline{U}_{f\_q} - \underline{U}_{v\_q} - \omega_f L_p.\underline{I}_{p\_q} - R_p \underline{I}_{p\_q} \tag{3.28}$$

here the equations (3.27 & 3.28) represents cross-coupled first-order subsystem, with the cross-coupling being initiated by the terms $\omega_f L_p.\underline{I}_{p\_d}$ *and* $\omega_f L_p.\underline{I}_{p\_q}$.

So, the complex power in the system is:

$$S_f = \underline{U}_{f\_dq} \cdot [\underline{I}_{p\_dq}]'$$

$$S_f = (U_{f\_d} + jU_{f\_q})(I_{p\_d} - jI_{p\_q})$$

$$S_f = U_{f\_d}(I_{p\_d} - jI_{p\_q}) + jU_{f\_q}(I_{p\_d} - jI_{p\_q})$$

$$S_f = U_{f\_d}I_{p\_d} - jU_{f\_d}I_{p\_q} + jU_{f\_q}I_{p\_d} + U_{f\_q}I_{p\_q}$$

$$S_f = (U_{f\_d}I_{p\_d} + U_{f\_q}I_{p\_q}) + j(U_{f\_q}I_{p\_d} - U_{f\_d}I_{p\_q}) \quad (3.29)$$

here, the active and reactive powers are:

$$P_f = (U_{f\_d}I_{p\_d} + U_{f\_q}I_{p\_q}) \quad (3.30)$$

$$Q_f = (U_{f\_q}I_{p\_d} - U_{f\_d}I_{p\_q}) \quad (3.31)$$

now consider that the PLL performs synchronization by aligning the d-axis of dq-rotating frames to the voltage vector ($\underline{U}_{f\_dq}$), the q-component of the latter will be zero at steady-state, thus:

$$\underline{U}_{f\_dq} = U_{f\_d} \quad (3.32)$$

by applying the equation (3.32) into equation (3.30 & 3.31):

$$P_f = U_{f\_d}I_{p\_d} \quad (3.33)$$

$$Q_f = -U_{f\_d}I_{p\_q} \quad (3.34)$$

It is verified by the mathematical model that the active power can be controlled via the d-component of the current (I_{p_d}), however, the reactive power can be controlled via the q-component of the current (I_{p_q}). If the two currents (I_{p_d} & I_{p_q}) can be controlled independently, the VSC could have an independent and decoupled control of the active and reactive power.

Regarding the active-power balance at both sides of the VSC (as reactive power does not propagate to the DC side) and for the simplicity, the losses on the IGBT are assumed negligible, then:

$$P_v = P_{dc,in} \Rightarrow Real.(\underline{U}_{v\_dq}(\underline{I}_{p\_dq})') = U_{dc}I_{dc,in} \Rightarrow U_{v\_d}I_{p\_d} + U_{v\_q}I_{p\_q} = U_{dc}I_{dc} \Rightarrow$$

$$I_{dc,in} = \frac{U_{v\_d} I_{p\_d} + U_{v\_q} I_{p\_q}}{U_{dc}} \tag{3.35}$$

it is the direct current that propagates to the DC side of the VSC, as shown in figure 3.18. During steady-state, the current ($I_{dc,in}$) becomes equal to the (I_{dc}), neglecting the harmonics due to the switching and the assuming a lossless DC capacitor.

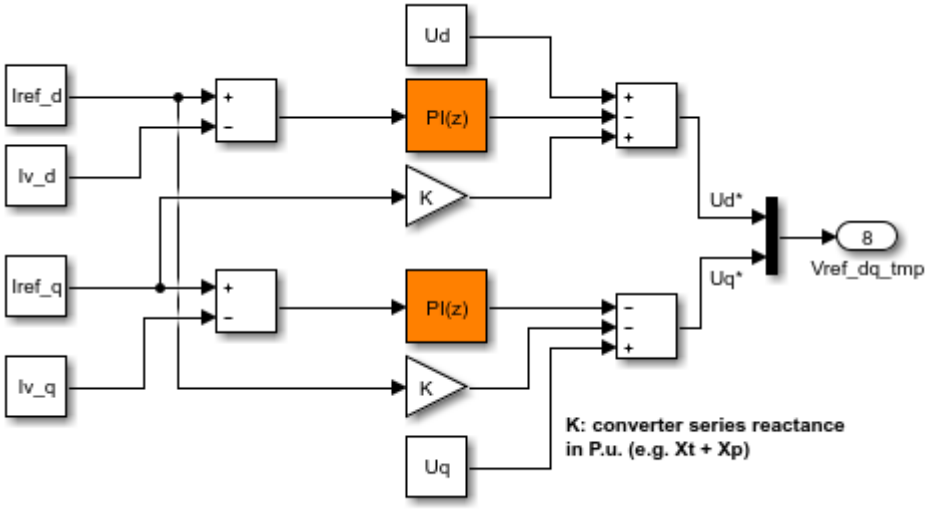

Figure 3.18 - Inner current controller

The main functions of the inner current loop (ICL) are to collect current reference (I_{ref_dq}) fed by outer active, reactive power and voltage loop, compared with current reference vector (I_{v_dq}) and generates voltage reference (V_{ref_abc}) accordingly, which used by sinusoidal pulse width modulation (SPWM) to generate firing pulses for the converter.

The inner current loop comprises of three different blocks AC current control, reference voltage conditioning, and reference voltage limitation block. The main role of the AC current control block is to track the current reference vector (dq-components) with a feed-forward scheme to achieve a fast control of the current during load changes and disturbances. It also has the information of the voltage vectors (U_{dq}) and compute the converter voltages (U_d^* & U_q^*) by adding the voltage drops due to the currents across the impedance (transformer & phase reactor) between the U_{abc} and the PWM-VSC voltages.

The state equations are used which represent the dynamics of the VSC-currents (an approximation is made by neglecting the AC filters). The d and q components are decoupled to obtain two independent first-order plant models. A proportional-integral (PI) feedback controller of the converter current has used to reduce the error at zero in steady-state. The output of the AC current control block is the unlimited reference voltage vector ($V_{ref\_dq\_tmp}$).

The unlimited reference voltage vector ($V_{ref\_dq\_tmp}$) had fed to reference voltage conditioning block. This block contemplates the actual DC voltage ($U_{dc-meas}$) and the theoretical maximum peak value of the fundamental bridge phase voltages in relation to the voltage for generating the new optimized reference voltage vector (V_{ref_dq}). These optimized references are limited in reference voltage block to an amplitude of 1.0 since over modulation is not needed. Normally, the modulation index is lower than 1 (ma < 1) so the VSC operates in a linear region, as mentioned in the section (3.3.2). In latter, the Inverse park (dq) and Inverse Clarke transformation blocks are required to generate the three-phase voltage references (V_{ref_abc}) for the PWM.

3.4.4 DC Voltage Balance Control

The DC voltage balance control can be enabled or disabled based on a selection made in the control modes. The author is using balance control only in station 2, based on DC Voltage & Reactive Power control mode. Typically, there are three main reasons for the small deviations between the pole voltages; the change in active/reactive converter current, lack of precision in the execution of the pulse width modulated bridge voltage, and unbalance in the circuit components impedance. Hence, this kind of control maintains the balance in DC side voltages (positive and negative pole) of the converter at a steady state.

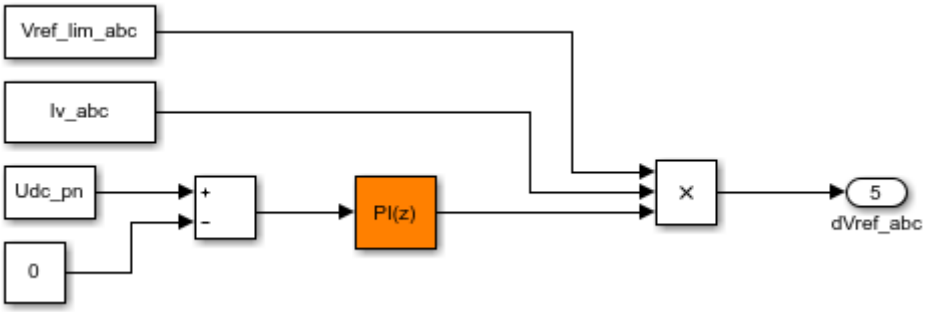

Figure 3.19 - DC side voltage balance controller

3.5 Control Strategy

The configuration of a two-terminal VSC-LVDC distribution link as mentioned in figure 3.20&3.21, station 1 is working as an active power controller and station 2 as DC voltage controller. The basic function of station 1 is as a rectifier (for utility interface, etc.) and station 2 as an inverter (to supply AC loads). The power flow between two systems can be controlled bidirectionally. In case of power flow reversal, the previous control duties are swapped between the stations. The main purpose of the control strategy is to allow the DC voltage-controlled station to control the voltage in the dc-distribution link. As soon as there is power flow through the DC cables, a voltage drop will occur across the resistance of the cables. The station that injects power to the DC link will have a higher DC voltage output. Therefore, for safety concerns, the station 1 has enabled with direct voltage override control in case of power injected into the LVDC link.

The structure of VSC-LVDC model in figure. 3.1, having a distribution link comprised of 1 km long cable, whose physical characteristics are provided in table 3.2. The AC grids connected with the VSC stations are considered enormously strong and therefore represented by nominal source voltage 400 V. However, the Ac grid # 1 contains a three-phase programmable voltage source to apply voltage sags.

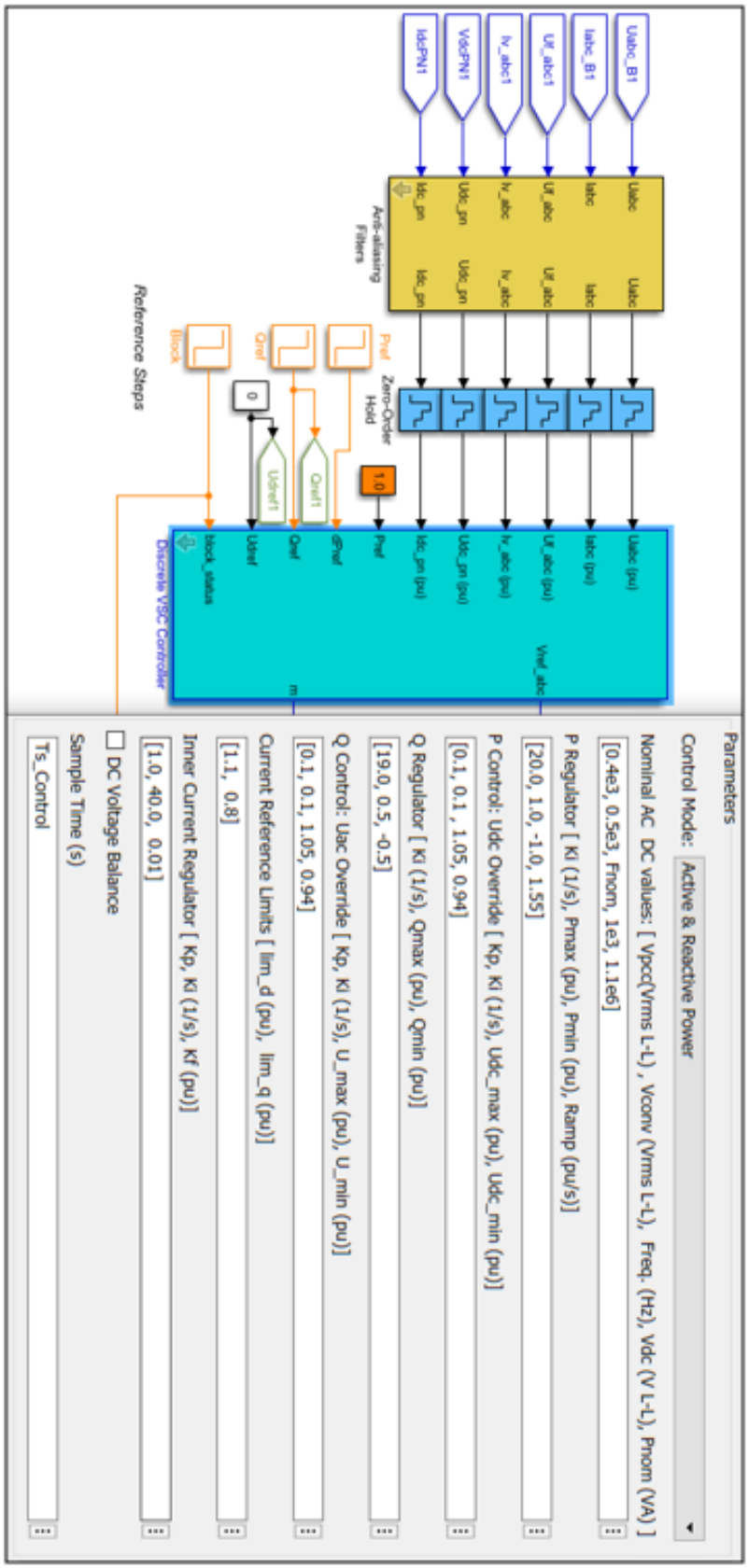

Figure 3.20 - Station 1 Controller (Active & Reactive Power)

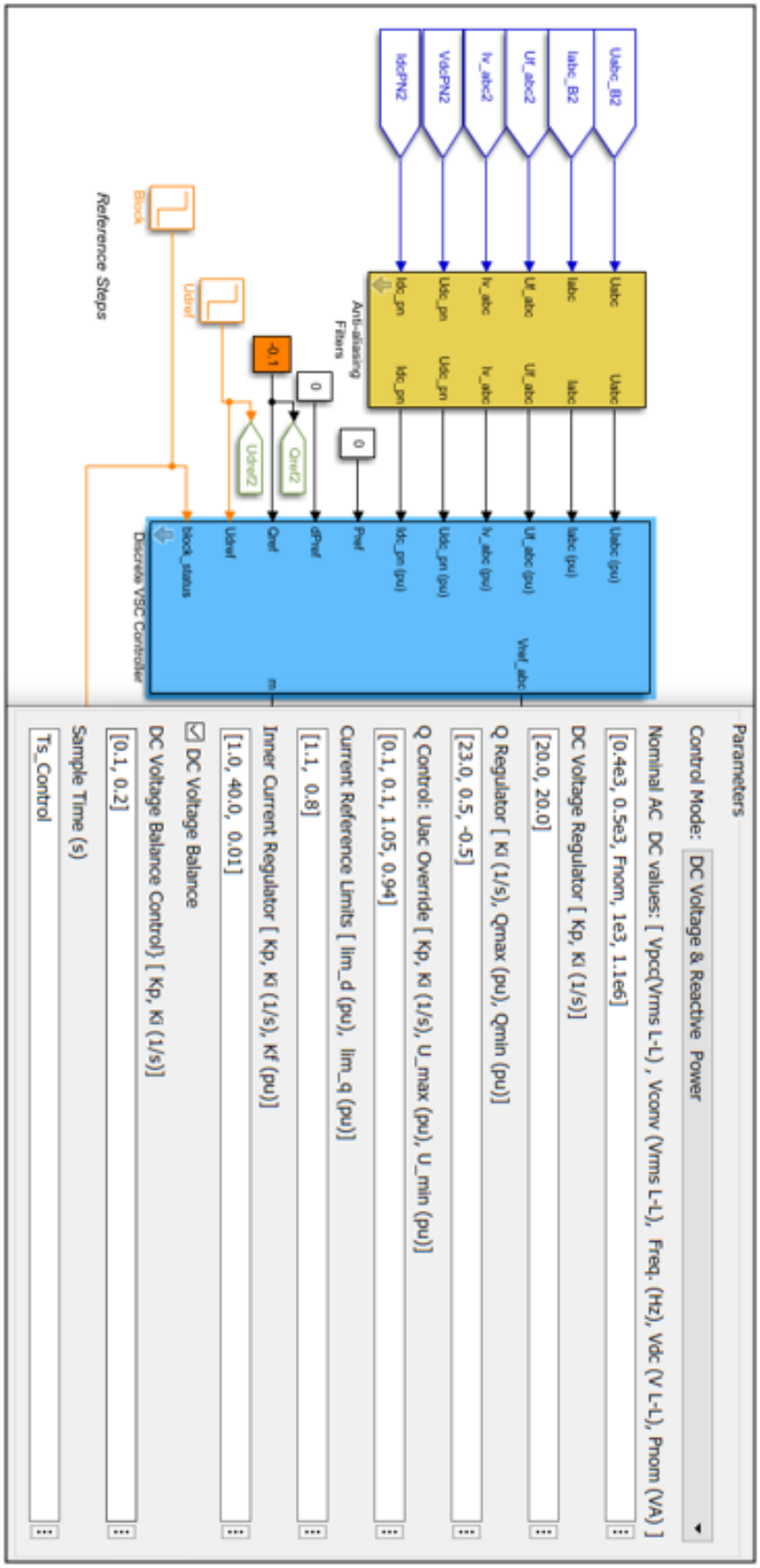

Figure 3.21 – Station 2 Controller (DC Voltage & Reactive Power)

The characteristics of the VSC stations are provided in table 3.2, the control strategy of the stations is the following:

- Both stations receive the same DC voltage reference (U_{dref}) but each of them receives an individual power reference ($Pref$ & $Qref$).
- Each station is initially set to direct-voltage control mode.
- If a station is provided with a negative power reference (power being injected to the AC side of the VSC), the station is set to active-power control mode.
- If a station receives a positive power reference and used to be in active-power control mode, it will remain in this mode until its measured transferred power drops to zero. After this event, it will switch to the direct-voltage control mode.

Parameters	**Value**	**Unit**
Rated power at AC side (S_N)	1.1	[MVA]
Rated voltage at transformer primary side ($U_{P,\,N}$)	400	[V_{AC}]
The rated voltage at the transformer secondary side ($U_{S,\,N}$)	500	[V_{AC}]
Transformer leakage inductance (X_T)	5	[%]
Phase reactor inductance (X_P)	0.2	[mH]
Phase reactor resistance (R_P)	0.1	[mΩ]
Rated voltage at DC side ($U_{DC,\,N}$)	1	[kV]
Capacitor at DC side (C_P, C_N)	0.2	[F]
Nominal frequency (F_{NOM})	50	[Hz]
Carrier frequency (F_C)	1350	[Hz]
Sample time of the controller model ($T_{S\_Control}$)	74.07	[µsec]
Fundamental sample time (T_{S_Power})	7.407	[µsec]

Table 3.2 - Rated values of the VSC-LVDC stations

CHAPTER 4

Control Investigations of Network

The control investigation of the LVDC network allows a variety of analysis. This work concentrates on the following key issues: system control, power quality, and transient behavior. These aspects are analyzed by applying customized model implementations of the LVDC network and its components. The issues addressed in the simulations comprise of customer-end power quality and harmonic transfer, the system transient behavior and the voltage stability of the DC network. The output of the model is measured and compared with reference values of the LVDC network.

In section 4.1, the LVDC network transient and dynamic state stability is studied in the time-domain by applying the model of the LVDC network in the Simulink environment.

In section 4.2, the power quality of the LVDC network is analyzed by applying the model of the LVDC network in the Simulink environment with the help of Fast Fourier Transformation (FFT) analysis.

In section 4.3, the start-up behavior of the LVDC network is analyzed in the Simulink environment.

4.1 Network Transient and Dynamic State Stability

To understand the behavior of the network, the author performed a dynamic and transient state stability analysis. With the help of this analysis, it is possible to describe the impact of system set points on the DC bus voltages of station1 & station2. Hence, a time-domain simulation is performed in the Simulink program to support the analysis.

4.1.1 Test Bench Analysis

A test bench analysis of the LVDC distribution system has modeled in Simulink environment with two stations, as mentioned in figure 4.1. The station 1 is working on Active & Reactive Power control mode with a capability to inject 1.1 MVA power into the DC distribution system, while the station 2 is working at DC Voltage control mode to maintain ± 500 DC voltage. Both stations are connected along with 1 km long cables to distribute the voltage across the network.

To simulate the network behaviour in the simulation environment, as mentioned in figure 4.1, setpoint changes have made in the active power reference ($Pref$), reactive power reference ($Qref$), and DC voltage reference ($Udref$) during a time window of 3.5 seconds. The first step-change occurs at time 0.3 seconds, the station 1 rectifier varied the power range 0-1.1 MVA (0-1.0 p.u.) in a period of 0.65 sec (starting from 0.30 sec to 0.95 sec) with a power ramp 1.55 (p.u./sec). However, the active power in station 2 decreases in order to maintain the DC bus voltage at a nominal value ± 500 volts (1 p.u.). Therefore, the DC voltage of station 1 and station 2 reaches to 1.09 (p.u.) & 1.028 (p.u), respectively.

At time 1.5 sec, the active power setpoint reduces to 0.7 (p.u.), as a result, the voltage of DC bus is also reduced accordingly. Another change occurs in reactive power setpoint at time 2 sec and reaches -0.1(p.u.). The reactive power does not propagate into the DC side of the network, as mentioned in section 3.4.3, thus, the DC bus voltage does not change.

Finally, the step change of 0.04 p.u. occurs in the DC reference voltage at time 2.3 sec. As a result, the LVDC network voltages decreases, as shown in figure 4.1, accordingly.

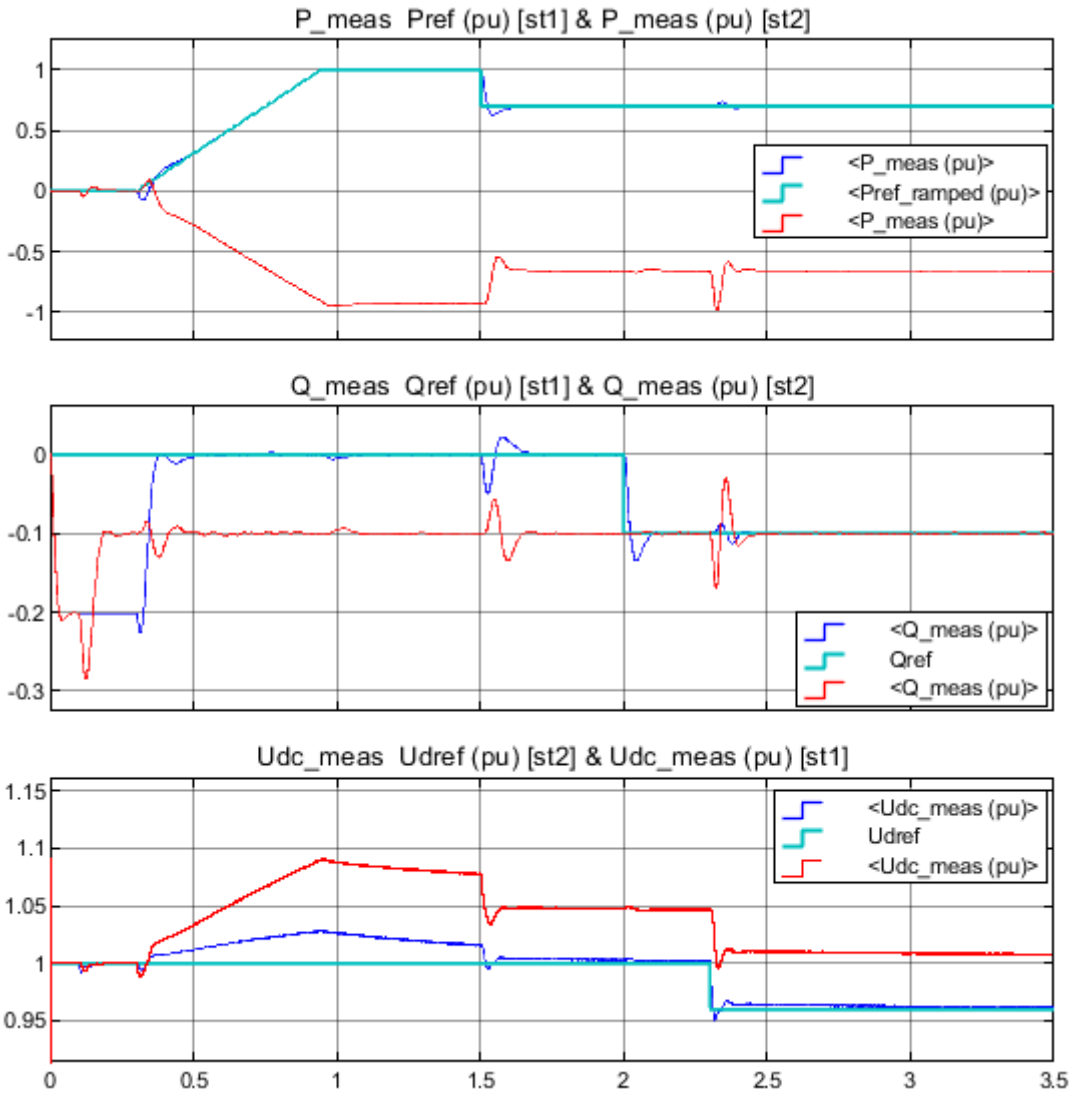

Figure 4.1 - LVDC network voltage changes during the reference changes

The adequate amount of DC capacitance, inside the operating area, no divergent oscillatory behavior has observed, and hence instabilities will not arise. Therefore, the transient and dynamic state of the system is stable. However, with an insufficient DC capacitance size, overshoots were detected in the step changes, but they were well damped. Depending on the

the protection device settings, those overshoots could result in tripping of the protection devices and possible loss of the network dynamic state stability resulting in the power-off. The simulation scenario changes are mentioned in table 4.1:

Time	**Station 1**		**Station 2**	
T [sec]	**Pref [p.u.]**	**Qref [p.u.]**	**Qref [p.u.]**	**Udref [p.u.]**
0	0	0	0	1
0.1	0	0	-0.1	1
0.3	1.0	0	-0.1	1
1.5	-0.3	0	-0.1	1
2.0	0	-0.1	-0.1	1
2.3	0	-0.1	-0.1	0.96
3.0	0	-0.1	-0.1	0.96

Table 4.1 - Step changes for active, reactive power and voltage reference

4.2 Power Quality Analysis

According to [62], the electricity network disturbances such as transients, voltage sags, swells, harmonics, and momentary interruptions are related to power quality issues. Furthermore, electronic loads are susceptible to power quality issues, which have a huge economic impact [63]. Therefore, the quality of electricity service for sensitive loads has become as important as its reliability. In the case of an LVDC power distribution network, the customer-end loads are powered by an inverter (CEI), which differs from the traditional LVAC network solution. As a result, the analysis on the power quality of the LVDC power distribution network is an essential part of a power system reliability study, which is a key aspect of the power system design and planning. Therefore, the harmonic content and the harmonic transfer through the LVDC network should be investigated.

This section provides an analysis of harmonic content in the LVDC distribution system. The analysis is based on the Powergui Fast Fourier Transform (FFT) analysis tool available in the simulation model.

4.2.1 LVAC Power Quality Issues

The power quality in a customer-end LVAC network depends on the inverter control algorithms. The supply voltage quality in the power electronics-based LVDC fed LVAC network was found to outperform the voltage quality standards (EN 50160/EN 61000-2-2) [64].

The IEEE standard 519- 1993 [65] introduces limits for harmonic pollution at the point of common coupling (PCC). For the LVDC network, the PCC is located on the 400 low-voltage lines, which is powering the primary windings of the LVDC network front-end transformer rectifier. Taking this into consideration, the harmonic transfer from rectifier through the LVDC network and at customer-end inverter has examined in this work. Further, the system's compliance with the power quality standards on the PCC is verified. It is pointed out that harmonics can be dangerous to the network equipment, and therefore, the harmonic content of the currents and voltages in the network must be examined.

In the LVDC network, the DC voltage is produced by a passive rectifier, which generates a ripple voltage about the DC level. If the PWM rectifier is used to produce DC voltage, a high-frequency waveform produced by the PWM switching is superimposed on the DC side. The standard IEEE 1709-2010 limits the RMS value of the ripple and the high-frequency noise to 5 % per unit.

In the simulated case, the model consists of the grid-connected rectifier and customer-end inverter. The maximum power injected from the grid is 1.1 MVA. As seen in figure 4.2, the voltage output (Uv_abc2) of the three-level bridge IGBT/Diodes is not purely sinusoidal and contains a certain harmonic. Furthermore, it causes issues in the current flowing through the phase reactor at the same frequencies, apart from the desired sinusoidal component at the grid frequency. These distorted currents are not desired to flow into the rest of the AC grid as they could cause additional losses.

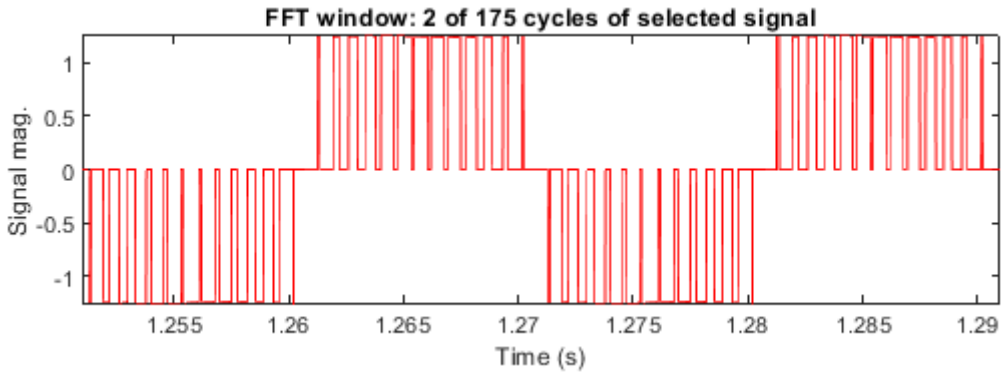

Figure 4.2 - Customer-end inverter phase-1 voltage waveform during maximum power injection from the grid

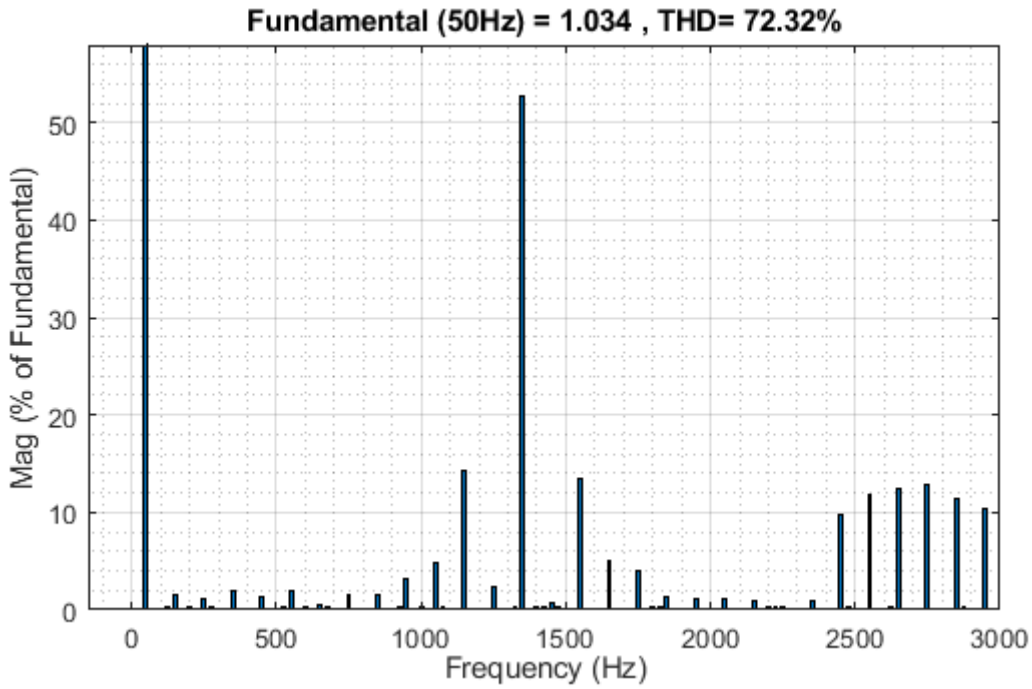

Figure 4.3 - FFT analysis of customer-end inverter phase-1 voltage

The principal harmonic voltages are generated, mainly due to the switching process (type of PWM, frequency index p (e.g. $p = 1350/50 = 27$), and modulation index), as mentioned in chapter 3. As seen in figure 4.4, the principal harmonic voltages are generated at around and multiples of frequency index p. Hence, 27th and 54th harmonics must be limited.

To cope with the customer-end AC system harmonics, three-phase harmonic filters uses to form an essential scheme. They can be connected as shunt elements with AC system side or the converter side of the converter transformer. As there are only high-frequency harmonics, therefore shunt filtering is relatively small compared to the converter rating. Thus, it is adequate to have two high pass-filter for two different frequencies. The later arrangement uses phase reactor which separates the fundamental frequency (filter bus) from the raw PWM waveform (converter bus), as seen in figure 4.4. Furthermore, depending on the converter topology and its switching levels, the harmonic content of the converter output can be reduced to a level where the necessary AC side filters can be reduced in number and size or even neglected.

In the reference case, the total harmonic distortion (THD) reaches at 73% (27^{th} = 54% and 54^{th} = 13%). Later, the total harmonics distortion (THD) decreases to a value of 4.74%. There are no strict limits for the harmonic current in PCC for distribution network installations, however, the IEEE standard 519-1993 provides limits for individual harmonic components at the point of common coupling (PCC).

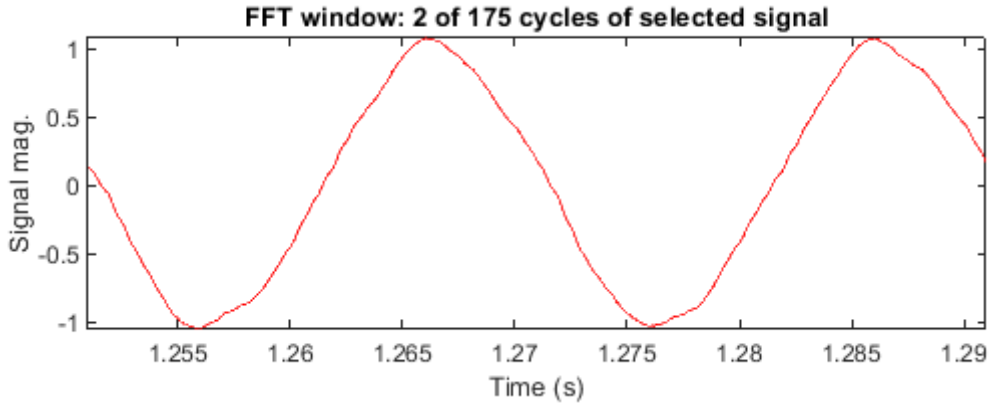

(a)

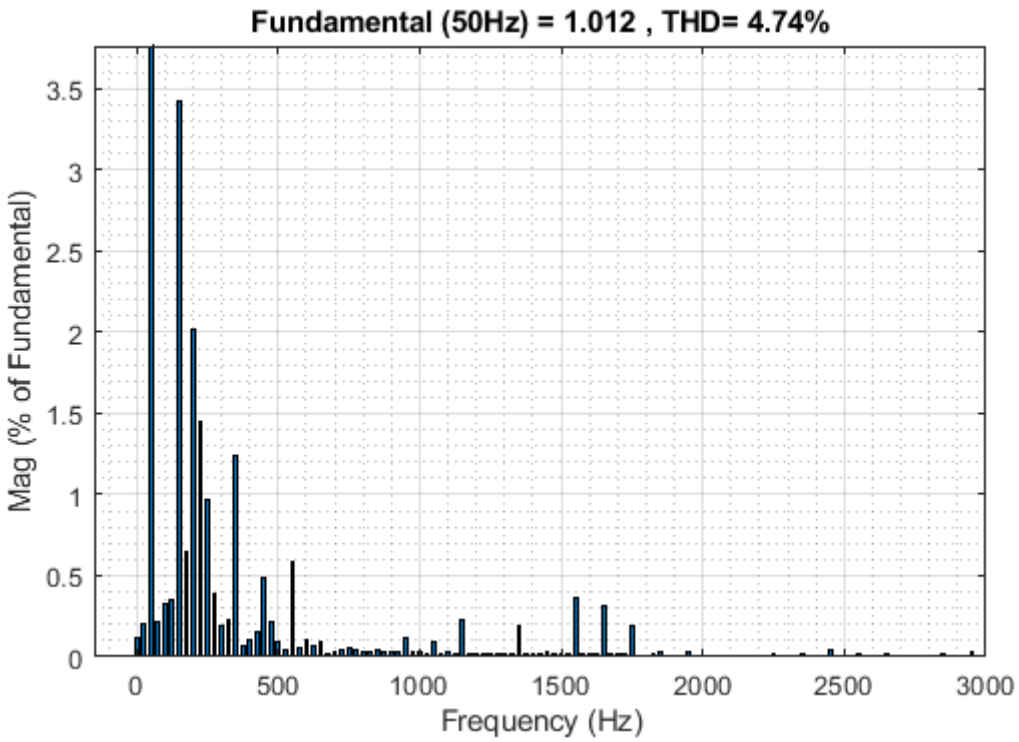

(b)

Figure 4.4 - (a) Filter bus phase-1 voltage waveform during maximum power injection from grid (b) FFT analysis of filter bus phase-1 voltage

4.3 Star-up of LVDC Network

The start-up of the LVDC network was analyzed and found that three-level bridge rectifier is a better choice for the LVDC network applications to control the network inrush current. In this section, the transient behavior of the network analyzed during start-up, DC voltage & active power controllers on-state, and changes in power and voltage references (Pref, Qref, and Udref).

Point of Common Coupling Voltage: The voltage measured at the point of common couplings of rectifier and inverter, when maximum power was injected (1.1 MVA) into the network, as shown in figure 4.5:

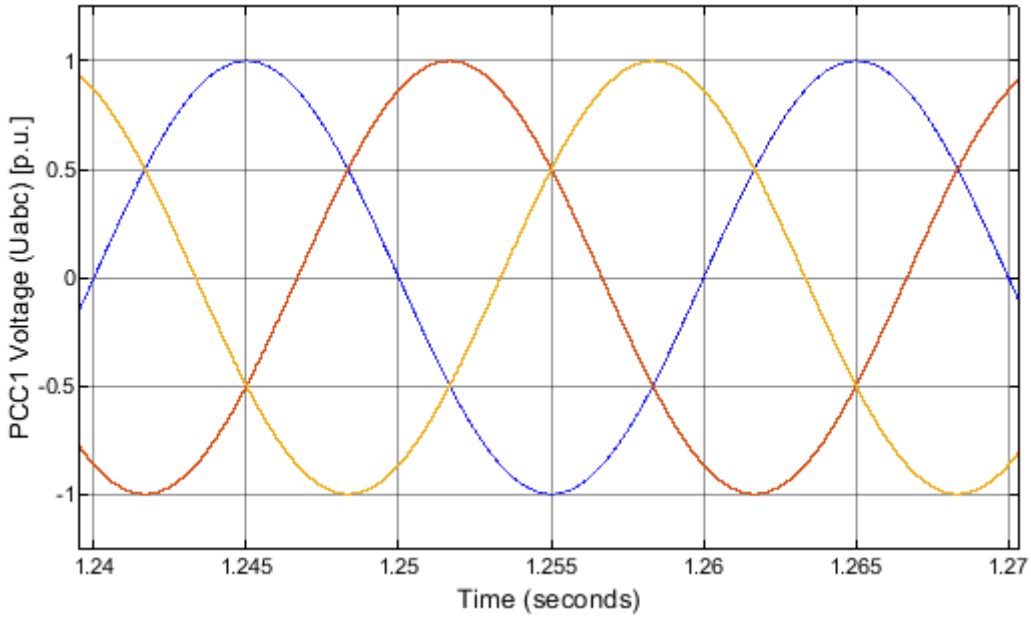

(a)

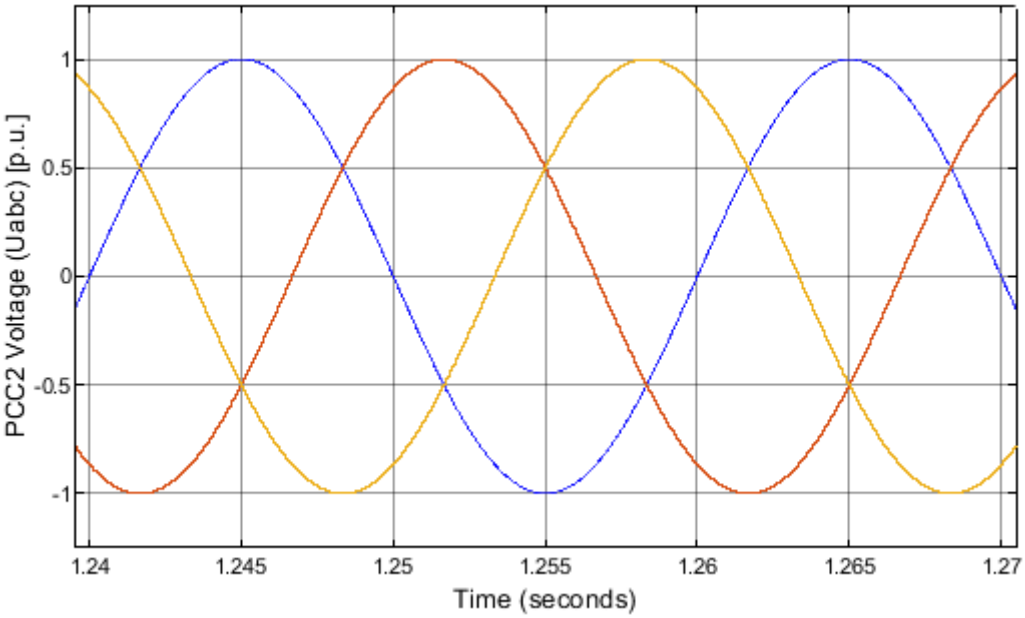

(b)

Figure 4.5 - Point of common coupling voltage (a) Rectifier side (b) Inverter side

Point of Common Coupling Current: The current measured at the point of common couplings of rectifier and inverter, when maximum power was injected (1.1 MVA) into the network, as shown in figure 4.6:

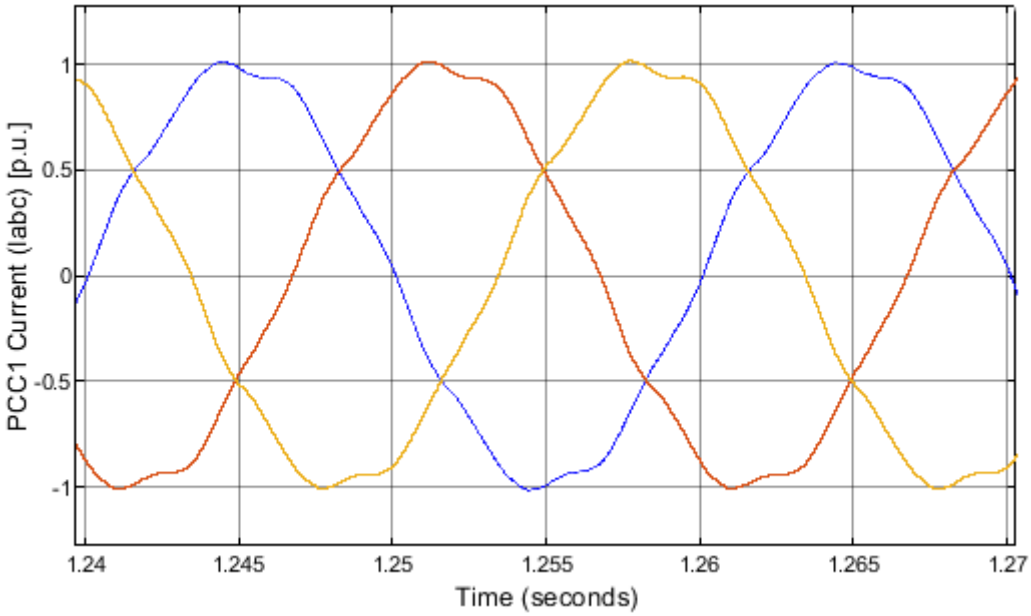

(a)

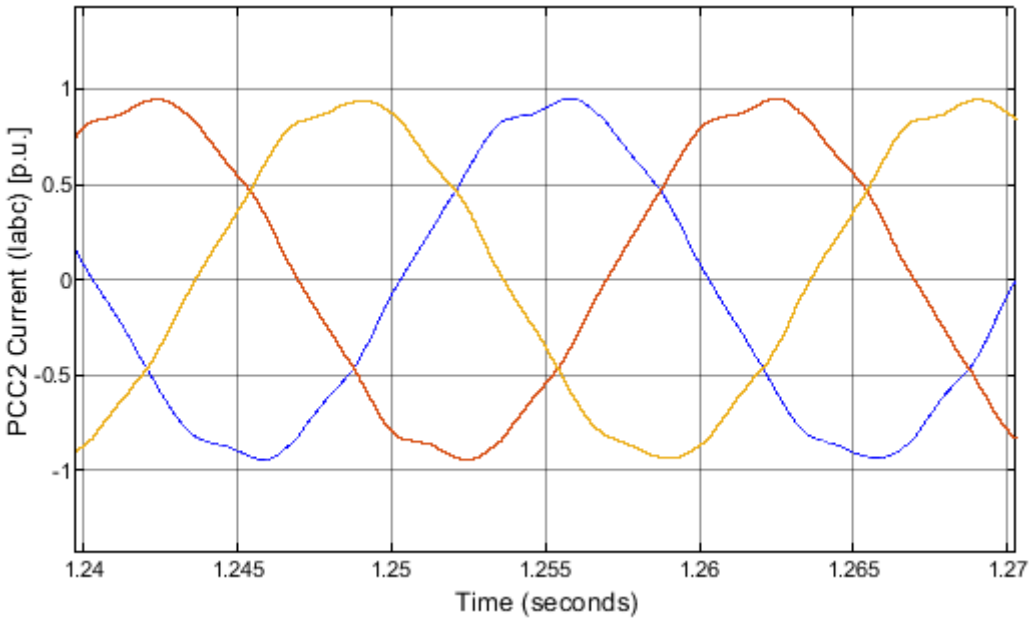

(b)

Figure 4.6 - Point of common coupling current (a) Rectifier side (b) Inverter side

Voltage References: The voltage reference from VSC controllers fed to sinusoidal pulse width modulation which creates pulses for both rectifier and inverter unit, when the maximum power was injected (1.1 MVA) into the network, as shown in figure 4.7:

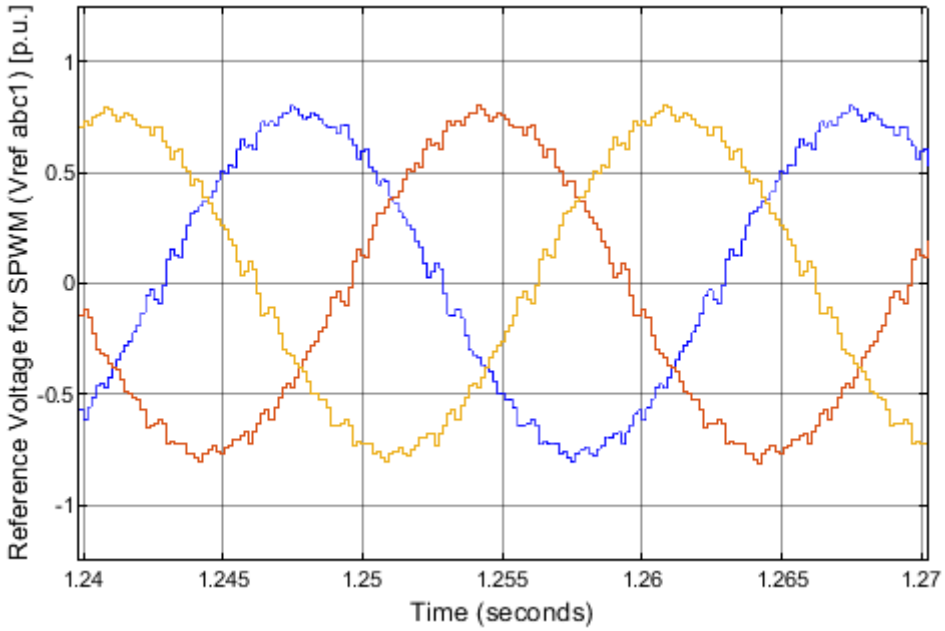

(a)

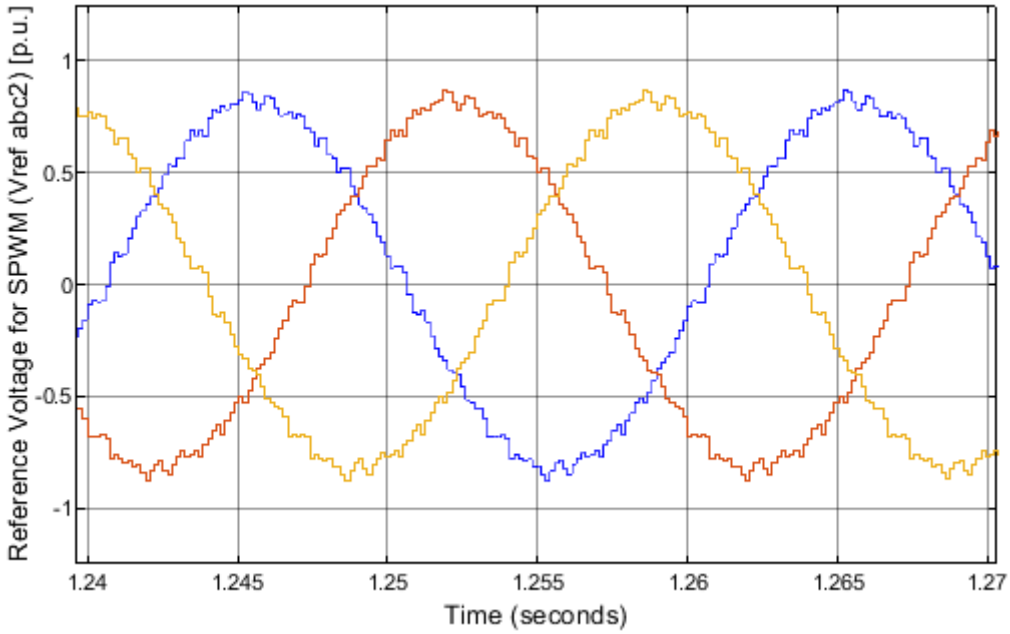

(b)

Figure 4.7 - Voltage reference (a) Rectifier unit (b) Inverter unit

Filter Bus Voltage: The voltage measured at the filtering bus (transformer secondary side) of rectifier and inverter, when maximum power was injected (1.1 MVA) into the network, as shown in figure 4.8:

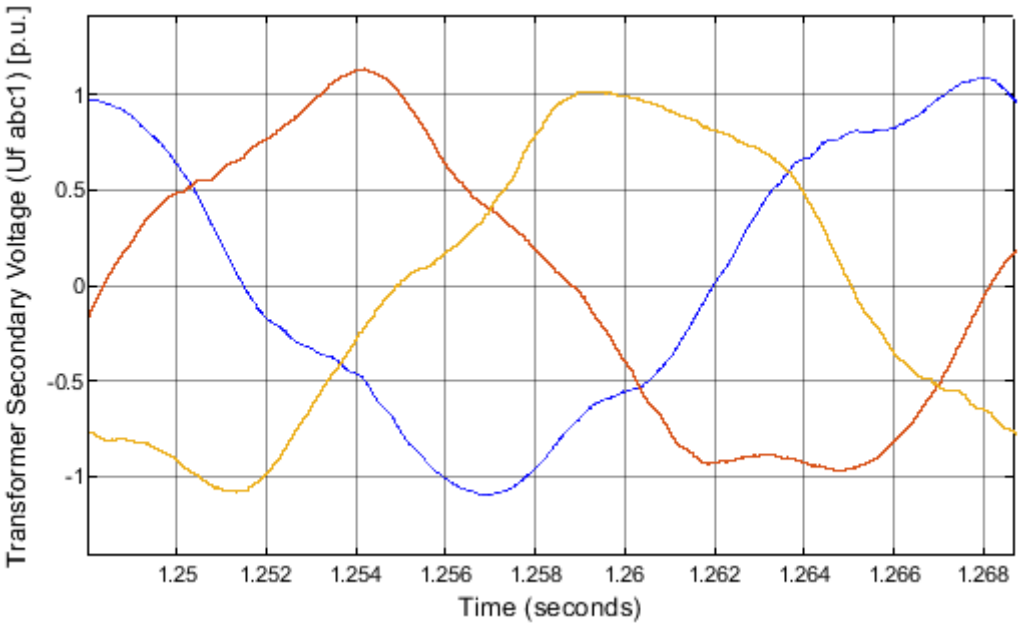

(a)

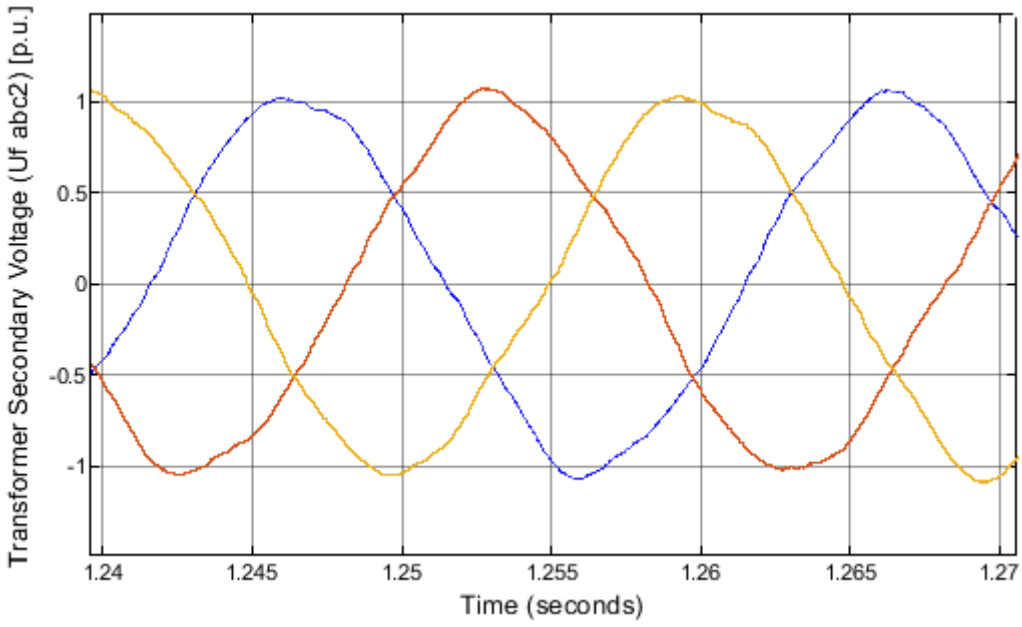

(b)

Figure 4.8 - Filter bus voltage (a) Rectifier unit (b) Inverter unit

Filter Bus Current: The current measured at the filtering bus (secondary side of the transformer) of rectifier and inverter, when maximum power was injected (1.1 MVA) into the network, as shown in figure 4.9:

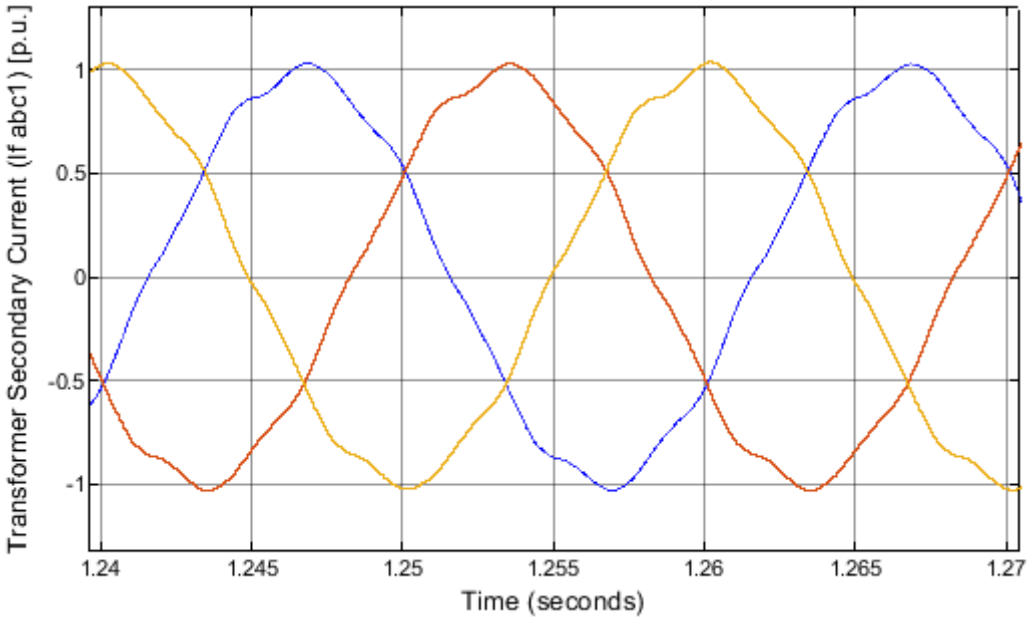

(a)

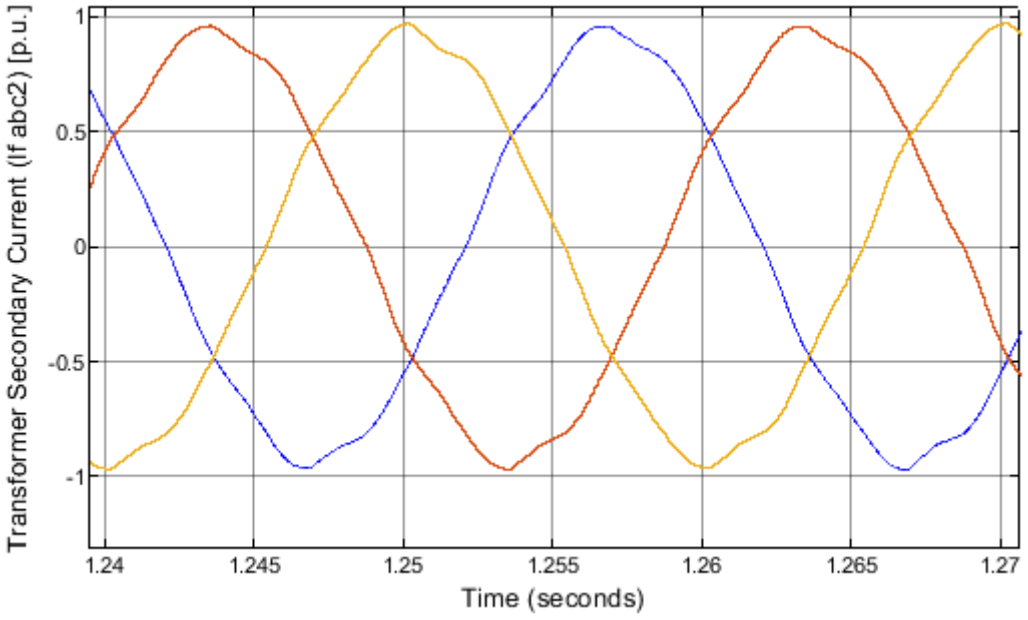

(b)

Figure 4.9 - Filter bus current (a) Rectifier unit (b) Inverter unit

Rectifier & Inverter Bus Voltage: The voltage measured at the rectifier bus when maximum power was injected (1.1 MVA) into the network, as shown in figure 4.10:

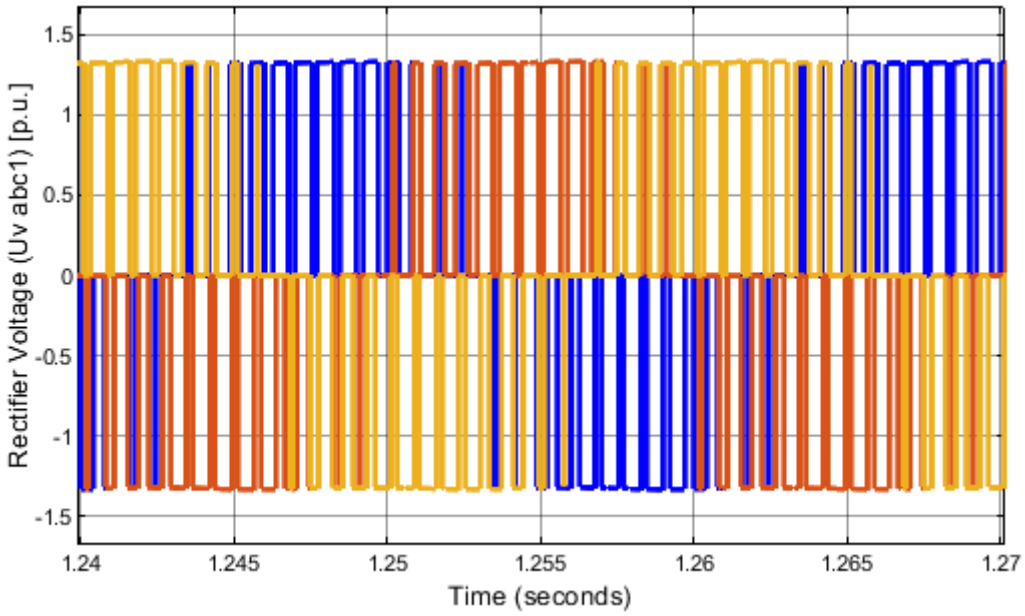

(a)

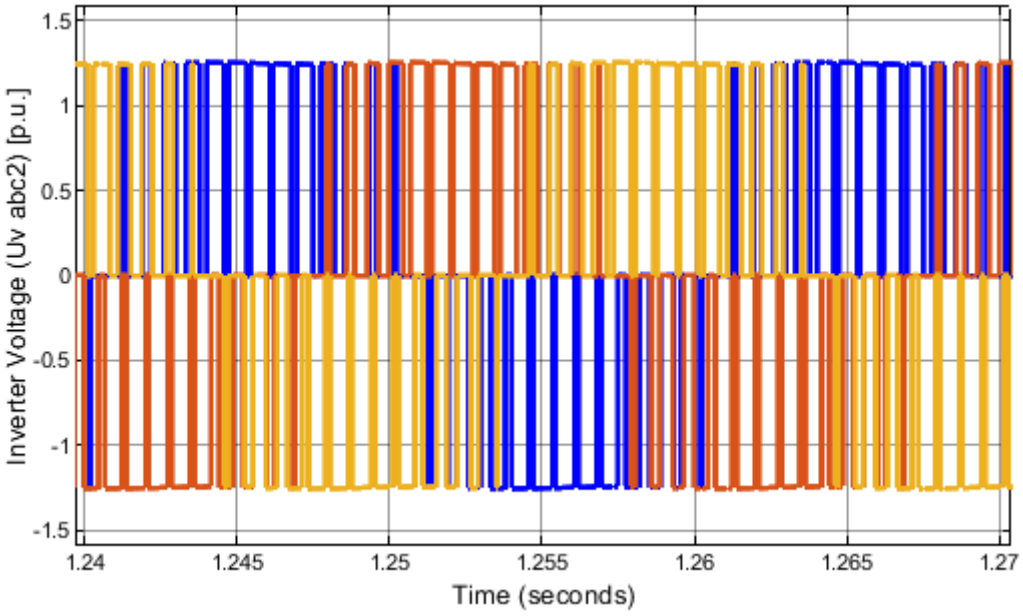

(b)

Figure 4.10 - (a) Rectifier bus voltage (b) Inverter bus voltage

Rectifier & Inverter Bus Current: The current measured at the rectifier bus when maximum power was injected (1.1 MVA) into the network, as shown in figure 4.11:

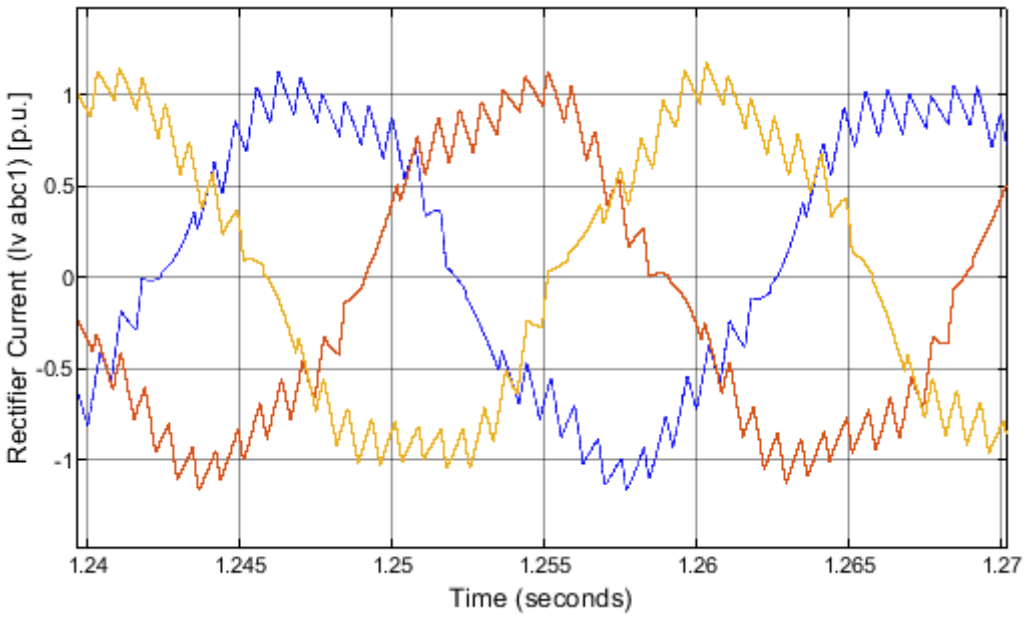

(a)

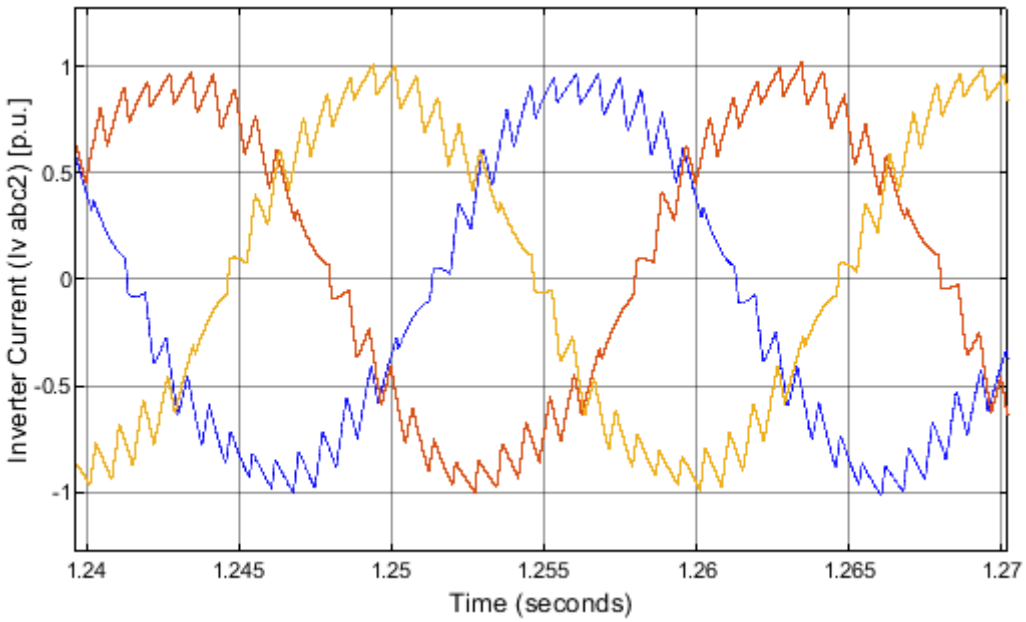

(b)

Figure 4.11 - (a) Rectifier bus current (b) Inverter bus current

DC Bus Voltage: The DC bus voltage measured at both sides of rectifier and inverter end. The behavior of the DC voltage is analyzed during the time period of 3.5 seconds, mentioned in figure 4.12. The step changes in DC bus voltage is the following:

- At t = 0.3 sec, the active and reactive power controller started to inject active power into the network at ramp 1.55 p.u./sec, the power injection process completed at t = 0.95 sec. At time (t = 0.95 sec), the DC bus voltage measured from rectifier side is 1.09 p.u. (545 Vdc) and 1.028 p.u. (514 Vdc) at the inverter side, respectively.
- At t = 1.5 sec, the active power controller reduced the active power reference (Pref) to 0.7 p.u., as seen in picture 4.1. At the time (t = 1.58 sec), the DC bus voltage measured from the rectifier side is 1.048 p.u. (524 Vdc) and 1.005 p.u. (503 Vdc) at the inverter side, as seen in figure 4.12, respectively.
- Later, at t = 2.3 sec, the DC voltage controller reduced the DC voltage reference (Udref) to 0.96 p.u., as seen in picture 4.1. Hence, the DC voltage at time (t = 2.4 sec) from rectifier side is 1.009 p.u. (505 Vdc) and 0.9636 p.u. (482 Vdc) at the inverter side, as seen in figure 4.12, respectively.

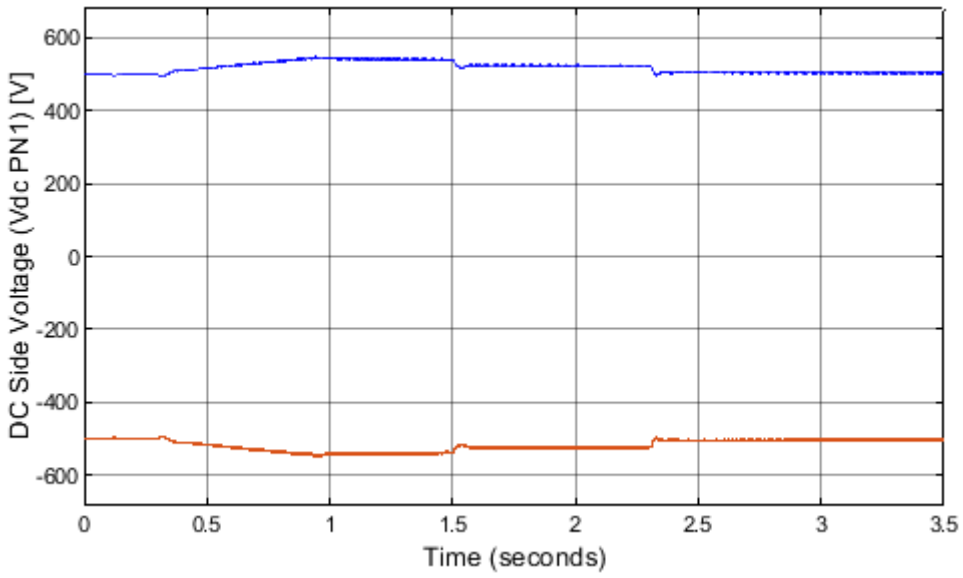

(a)

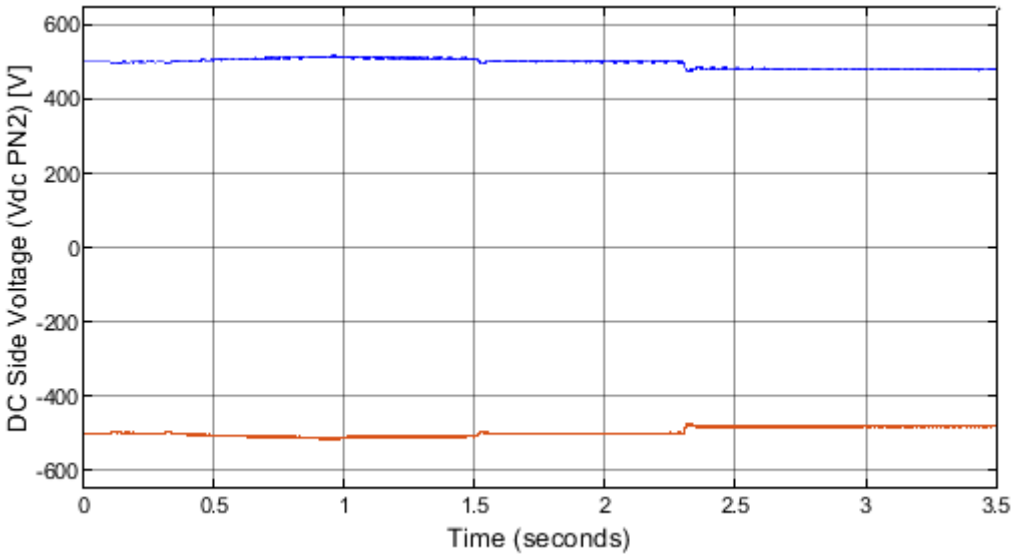

(b)

Figure 4.12 - DC bus voltage (a) Rectifier side (b) Inverter side

DC Bus Current: The current measured at both sides of DC bus, rectifier and inverter. The behavior of the DC current is analyzed during the time period of 3.5 seconds, mentioned in figure 4.13.

The simulation results shows, during the start-up, the inrush current is measured in DC network, which is mainly due the capacitance takes charging current. According to [66], the total capacitance of the DC network is always significantly higher if compared with the traditional AC network. When the LVDC network is started-up, the capacitances take charging current. If the current is not properly controlled, the outcome can be (1) a rectifier failure or (2) a protection device trip, and if the rectifier and the protection devices can withstand the high charging current, (3) over-voltages in the DC network. The step changes in DC bus current is following:

- At t = 0.1 sec, the dc voltage and reactive power controller started to inject reactive power. Therefore, a small change in DC current has been observed due to the change in the reactive power of the DC network.
- At t = 0.3 sec, the active and reactive power controller started to inject active power into the network at ramp 1.55 p.u./sec, the power injection process completed at t =

0.95 sec. At the time (t = 0.95 sec), the DC bus current measured from rectifier side is 1025 amps and 994 amps at the inverter side, respectively.

- At t = 1.5 sec, the active power controller reduced the active power reference (Pref) to 0.7 p.u., as seen in picture 4.1. At the time (t = 1.6 sec), the DC bus current measured from the rectifier side is 709 amps and 730 amps at the inverter side, as seen in figure 4.13, respectively.
- Later, at t = 2.3 sec, the DC voltage controller reduced the DC voltage reference (Udref) to 0.96 p.u., as seen in picture 4.1. Hence, the DC voltage at the time (t = 2.4 sec) from the rectifier side is 729 amps and 755 amps at the inverter side, as seen in figure 4.13, respectively.

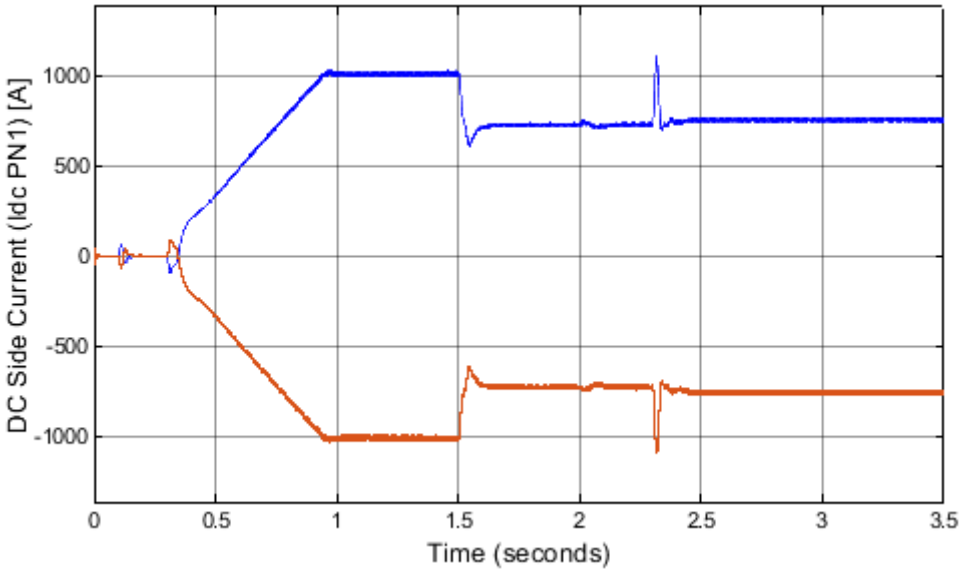

(a)

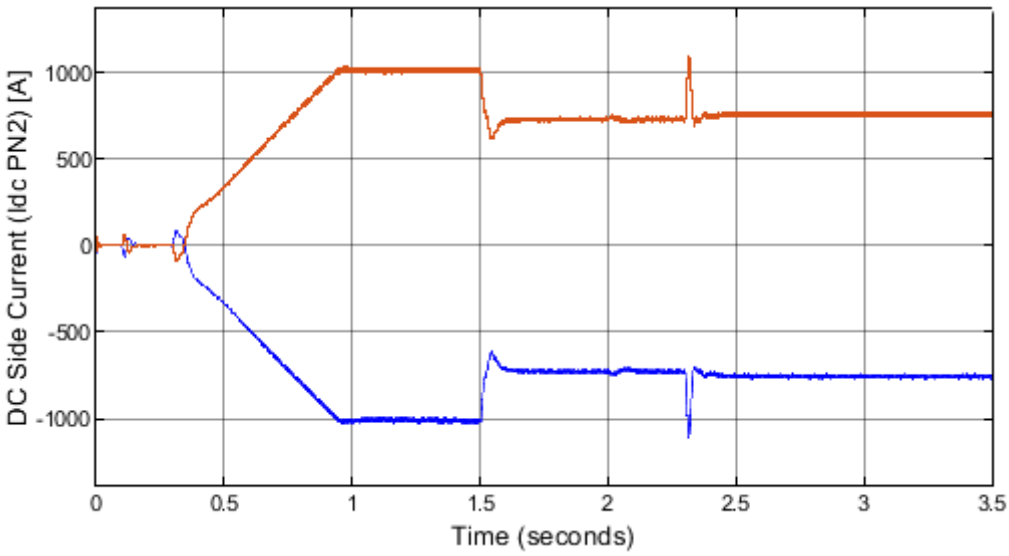

(b)

Figure 4.13 - DC bus current (a) Rectifier side (b) Inverter side

CHAPTER 5

DC Protections and CASE Studies Assessment

The proliferation of RES, electronics loads, electric vehicles (EV), building applications, traction system, data center, ships, and many industrial applications demand modern power systems such as the LVDC distribution system. As a result, developing a DC electrical system architecture depends on the essential power electronics and protection devices. The development of an effective and economical protection scheme for a DC system with bidirectional power flow is still a bottleneck for DC microgrids implementations.

In section 5.1, the types of DC faults (pole to pole and pole to ground faults), different types of earthing schemes for DC network, and the available circuit breakers technology for DC systems are discussed.

In section 5.2, different types of faults in the LVDC distribution network are studies and the impact of these faults on AC side transformer, DC bus voltage, active and reactive power controllers are observed. Later, the DC voltage override control has studied and implemented in the proposed model.

5.1 DC Protections

In this section, an overview and comparison of LVDC distribution systems have made based on DC protections. The time constant of DC protections and control is usually very close, the post fault behavior of converters within a DC network becomes a new issue that involves both active converter control and passive circuit elements. Therefore, an analysis of DC fault types, earthing schemes, available circuit breakers technologies under different fault conditions is required to develop standard protection criteria for the DC network.

5.1.1 Types of DC Faults

The network faults in a DC system can be categorized as a positive pole to negative pole short circuit fault (pole to pole fault) and positive or negative pole to ground fault (pole to a ground fault). The post-fault voltage profile may vary significantly in these two fault types, the nature of short circuit current is largely similar for both types. Apart from the fault impedance itself, the location of the short circuit point affects the post fault behavior as the feeder impedances between the fault point and source often plays a significant role in fault current transient. As the fault originating at the main bus produces a higher transient current which usually posts the most severe threat to the network as the fault loop impedance is minimum [67]. Therefore, the fault current analysis is crucial for designing a protection system as well as maintenance and post fault restoration [68].

In pole to pole fault, as seen in figure 5.1 (b), the transient of fault current from point A to B is caused by the immediate current discharging from the converters smoothing capacitors. The contribution of this type of fault current from the capacitors can be demonstrated as [69]:

$$i_C(t) = \frac{V_{DC}}{R_C}(e^{-t/\tau_d}) \tag{5.1}$$

where, V_{DC} denotes the voltage at the DC bus when a fault occurs, R_C is the capacitor series resistance and $\tau_d = C_d R_C$ represents the time-constant of the converter and DC bus RC system.

In addition, cable impedance should be incorporated in the calculation if the cable length from the converter to the DC bus is considerable which would result in a higher-order dynamic system [69]. Therefore, the total fault current between the short-circuited conductors can be evaluated by adding all the currents contributed to the fault current as:

$$i_f(t) = \sum_{k=1}^{n} i_{s,k}(t) \tag{5.2}$$

where k is the number of sources connected to the DC bus. However, in pole to ground fault, the system fault current is the sum of the contribution of all connected sources and the path of fault currents are mainly depends on the earthing configurations.

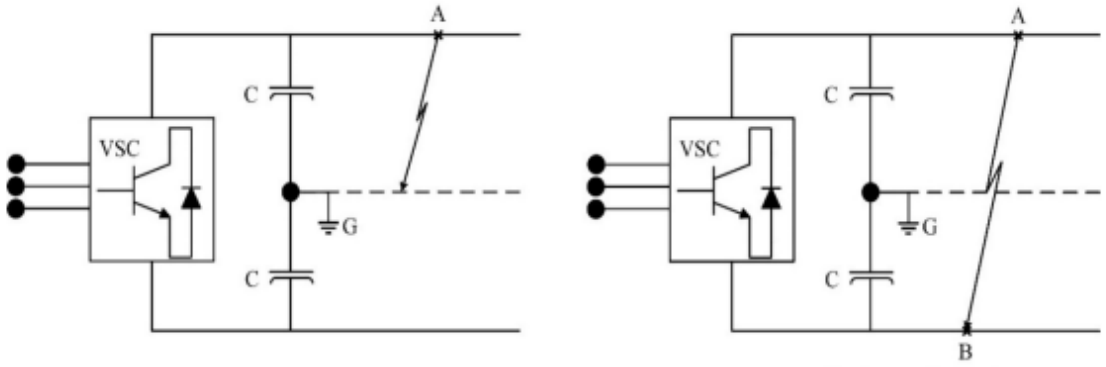

(a) (b)

Figure 5.1 - Faults types in DC system (a) Pole to ground fault (b) Pole to pole fault

Apart from capacitor discharging current during the fault, the source side contribution towards the fault is another important factor need to be considered while developing a fault locating criteria. The source-side contribution is highly dependent on the converter technology type, either isolated or non-isolated [25].

5.1.2 Earthing of DC Network

Earthing is one of the key factors in DC networks, which highly influence the transient fault current, over-voltage and the protection settings of the system. The design of earthing is crucial in detecting the ground fault, minimizes the stray currents and provide personnel & equipment safety. In LVDC networks, the earthing schemes can be categorized into the isolated (unearthed) system, resistance earthed system, and solidly earthed system.

Isolated DC System: Isolated DC system, as seen in figure 5.2(a), provides better reliability of power supply as compared to the grounded system because it can allow the system to continue its operation during a single line to ground fault occurs. The earthing current is very low, it makes difficult to detect pole to ground fault using current detection only. In addition, unpredictable DC voltage offset in the presence of small leakage current is another disadvantage of this system. Moreover, the electrical noise problem in the entire system can be encountered, which may disrupt the signal resulting in missing pulses. So, additional insulation may require to withstand the uncertain potential between conductors line and earth, which increases the cable cost [70].

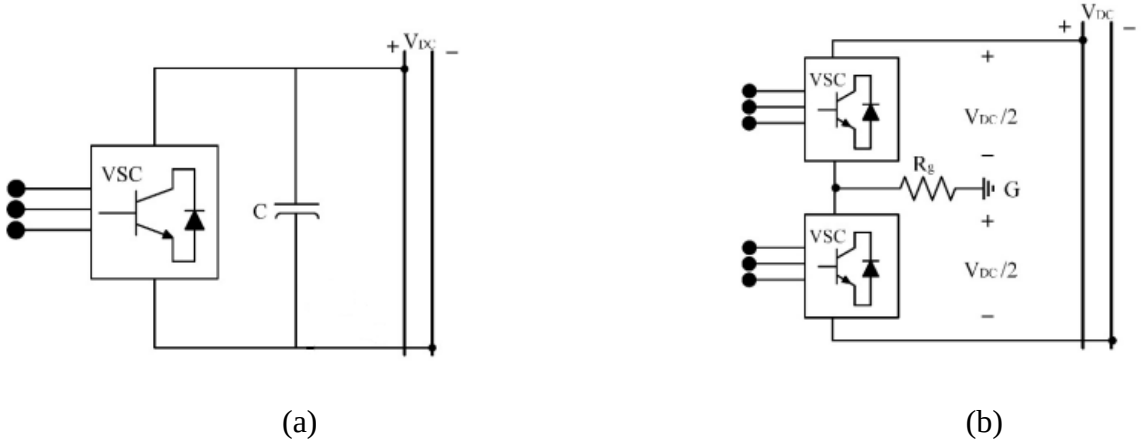

(a) (b)

Figure 5.2 – DC earthing systems (a) Isolated (b) Neutral point earthing [71]

Earthed DC System: DC earthing can be achieved either the negative pole of VSC is earthed via a certain amount of impedance or connecting the common neutral point between the converters to earth, as mentioned in figure 5.2(b).

The resistance earthing has often configured without a neutral point and is practically implemented in early VSC-HVDC systems [70]. If a DC power system is earthed at a neutral point, a bipolar system is formed, therefore, a large earthing resistance can be used to limit the power losses during normal operation. In general, neutral point earthing scheme is used for reducing ground potential against live conductors hence improve personnel safety and relieve some stress of insulation during normal operation. It can also minimize the circulating current with respect to the AC side neutral grounded system, which helps to suppress the current and voltage transient during pole to ground fault. However, fault measurement and detection become challenging for small ground fault currents which may energize metal enclosures of loads. Equipment insulation requirement becomes higher than normal condition during a pole to ground fault as it must withstand the full bipolar DC voltages before the fault is isolated [71].

Solid Earthed DC System: In a solid earth system, the middle point between the two poles is electrically connected to the ground without any (or very small) impedance, as shown in figure 5.3. This type of earthing system produces larger ground current and higher voltage transient than other earthing schemes [35], therefore, the successful detection of such fault becomes relatively easier. The insulations required for equipment and the cables is to withstand half of DC pole to pole voltage, which reduces the overall systems cost, space, and weight.

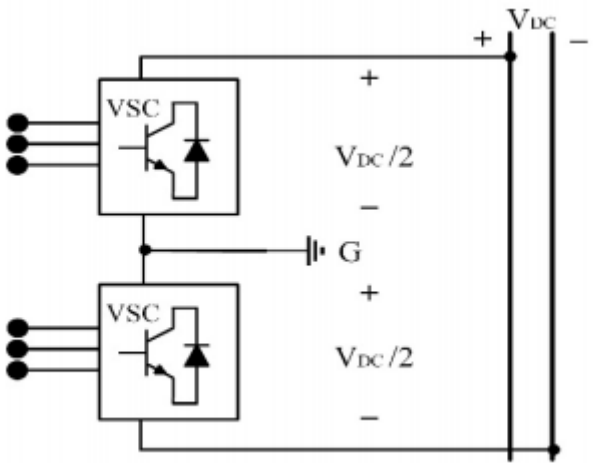

Figure 5.3 – Solid earthing of middle point system [71]

However, the solid earthing can also be implemented in monopole DC power grid by connecting the negative pole to earth, but it causes leakage current that can be 30 times greater than unearthed in traction systems[25]. Solid earthing is not suggested to be used in modern power systems due to its major drawback of corrosion and safety issues [72].

5.1.3 DC Circuit Breaker Technology

Circuit breaker uses to isolate the fault in the DC networks. As the lack of natural zero-crossing and high current changing rate (di/dt) are the major challenges to disconnect an LVDC circuit fault. This makes DC current interruption more difficult, thus, bringing consequent challenges for designing DC circuit breakers (DCCB). Appropriate design and implementation of circuit breakers is a fundamental requirement for developing the protection scheme for the DC distribution system.

Mechanical Circuit Breakers: Typical mechanical circuit breakers (Moulded Case Circuit Breaker (MCCB)) are widely used in AC systems. This type can also be used in the LVDC system with a small amendment which operates with resonance circuitry to generate zero-crossings [25], as seen in figure 5.4(a).

The basic configuration works as the MCCB switch opens after the fault current detection, the resonance circuit can generate a negative transient current to counter the fault current in the main circuit. As the negative current grows, it may eventually become higher than the fault current when a zero-crossing is created. So, the fault current can be interrupted with MCCB. It is known as a passive resonance DC circuit breaker. Based on the similar principles to create zero-crossing, however, the active MCCB configuration adds an additional switch and pre-charges the capacitor to exciter the resonant circuit[25]. This can accelerate the rise of the resonance current, eventually leading to a faster operation of MCCB, as shown in figure 5.4(b).

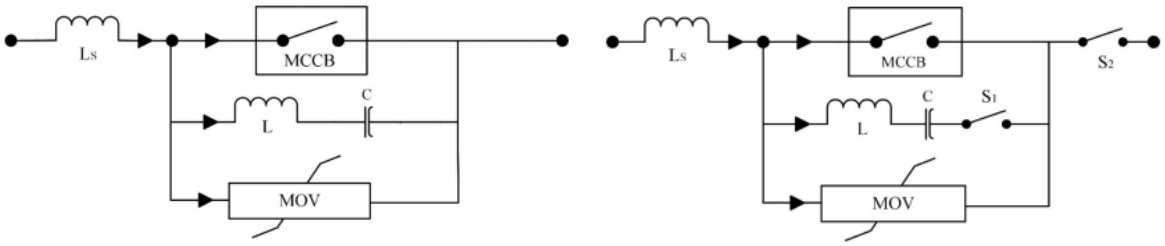

(a) (b)

Figure 5.4 – DC earthing systems (a) Passive resonance MCCB (b) Active resonance MCCB [73],[74]

The fault interruption of MCCB takes typically 30 to 100 milliseconds [25]. Such low operating speed limits their usage since a DC transient current can reach its peak value up to tens of the nominal value in a few milliseconds. However, the application of a mechanical circuit breaker requires the system to be able to withstand let-through energy (i^2t) over longer time comparing with those DC circuit breakers that can operate faster.

Solid-State Circuit Breakers: The power electronics-based protective devices have been developed for DC applications, generally known as Solid-State Circuit Breakers (SSCBs). Typical SSCBs are based on semiconductor devices, such as Insulated-Gate Commuted Thyristor (IGCT), Insulated-Gate Bipolar Transistor (IGBT) and Gate Turn-off Thyristor (GTO). These types of CBs require an energy dissipation element to be attached in the circuit to prevent the pulsing energy from damaging switching devices. Generally, those energy dissipation elements are Metal-Oxide Varistors (MOV), capacitors, switched resistors and combinations of them [75].

As seen in figure 5.5(a), a surge arrester branch (i.e., MOV) is connected in series with a free-wheeling diode which is connected in parallel to the DC bus. The semiconductor device remains on and loads current flows through it under normal conditions. However, when a fault is initiated, the semiconductor turns off and the fault current is forced to commutate through the free-wheeling diodes with the surged energy captured by the MOV [75]. This CB structure is for unidirectional only as there is only one fully controllable semiconductor device.

Two unidirectional SSCBs are connected in anti-series directions so the current flowing in both ways can be switched off, as shown in figure 5.5(b). Nevertheless, the bidirectional operation also introduces twice time conduction losses during-steady state operation as compared with unidirectional SSCB.

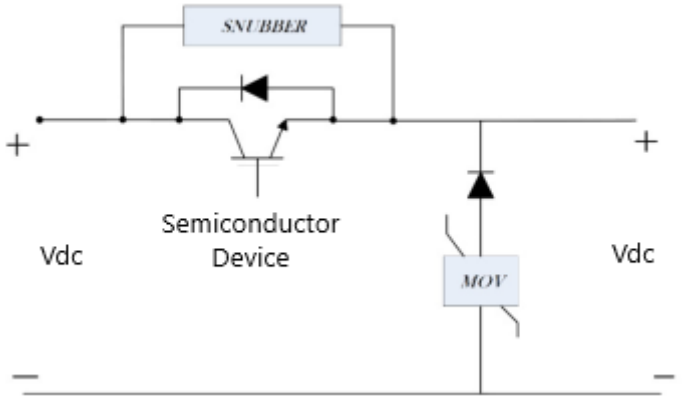

(a)

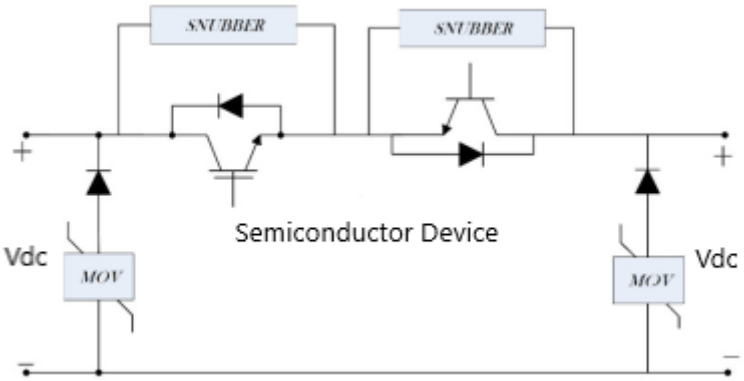

(b)

Figure 5.5 – Solid-state circuit breaker model (a) General SSCB configuration (b) Bidirectional SSCB configuration [25]

The operation time of the solid-state circuit breaker is within 100 micro-seconds, which enables the system with fast fault isolation capabilities. However, the major drawback of SSCB is considerable conduction losses at steady-state condition, which is more significant in LV systems since the conduction voltage drop of a semiconductor is more considerable with respect to the nominal voltage level.

Hybrid Solid-State Circuit Breaker: The hybrid circuit breaker (HCB) is introduced to reduce the conduction losses due to the semiconductor devices, which introduce a bypass branch (mechanical switching devices) to provide an alternate path for current at steady state, as seen in figure 5.6. All the current flows through the bypass branch whereas current remains zero in the main branch under normal conditions. When a fault occurs, fast mechanical switch (CB) opens and the fault current instantly gets commutated to the main SSCB by the load commutation switches [76]. The HCBs are not being generally used and developed for LVDC applications due to their high complexity and the inherited cost. However, Hybrid SSCBs have been modeled for 320 kV or higher HVDC systems, which claims an operational time of fewer than 5 milliseconds [76].

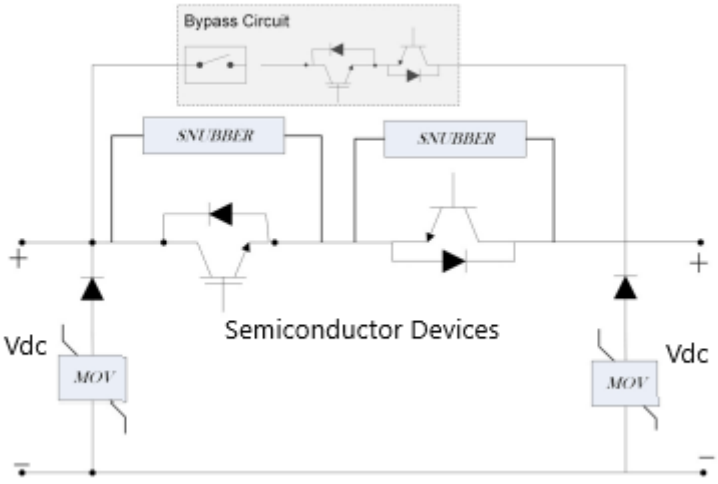

Figure 5.6 – Hybrid solid-state circuit breaker model

5.2 Case Studies Assessment

In this section, different types of cases are studies to understand the real-time behavior of the system components. All the cases are related to the LVDC side faults and their impact on the AC voltage of the LV distribution system has been observed. The simulations have been performed using the Simulink environment. The different types of case are:

- Pole to pole fault
- Pole to ground fault
- Short circuit across DC side capacitor
- Three-phase to ground fault at the customer-end AC network

The Simulink model uses for these study cases has shown in figure 5.7. In the case of pole to pole, pole to ground fault, and short circuit across DC side capacitor, a single-phase breaker is used with an internal time clocked signal. However, in the case of a customer-end three-phase ground fault, a built-in block (three-phase fault) is used to generate a fault.

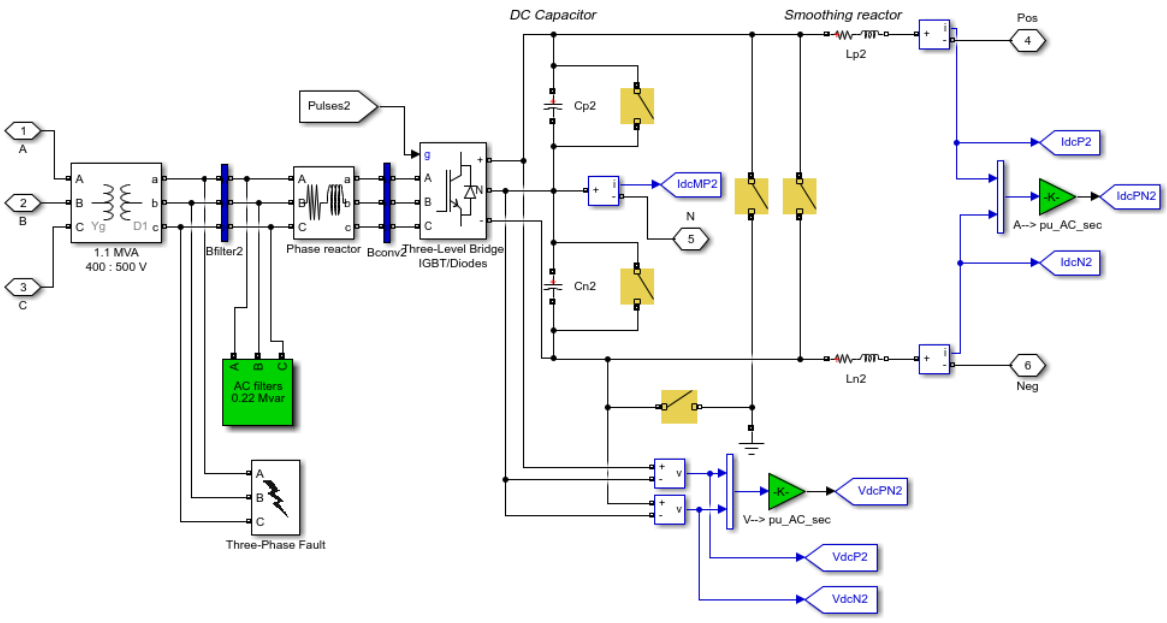

Figure 5.7 – Station 2 topology for the study cases assessment

5.2.1 LVDC Network Faults

In this section, all the faults (pole to pole & pole to the ground) are generated at DC side of the rectifier and observed their impacts on the AC side voltage (Uf_abc1), AC side current (If_abc1), DC bus voltage (VdcPN1), DC bus current (IdcPN1). Furthermore, the behavior of active and reactive power is also observed during these faults. In all the below-mentioned simulations, the faults are generated at a time (t = 1.15 sec), during this time the grid is injecting 1.1 MW (with a setpoint of 1.0 p.u.) power and the voltage at DC bus is ± 500 Vdc (with a setpoint of 1.0 p.u.), as seen in figure 5.8(c).

Pole to Pole Fault: In this case, a short circuit occurs between positive and negative pole of rectifier at a time (t = 1.15 sec). The DC bus voltage drops to zero but a huge amount of short circuit current flows in DC bus (8000 amps) for a time period of 500 msec. However, the AC side voltages decrease to 0.8 p.u. and short circuit current reaches to 5.2 p.u., respectively, as seen in figure 5.8 (a). Active and reactive power also reaches zero after the fault, as seen in figure 5.8(c).

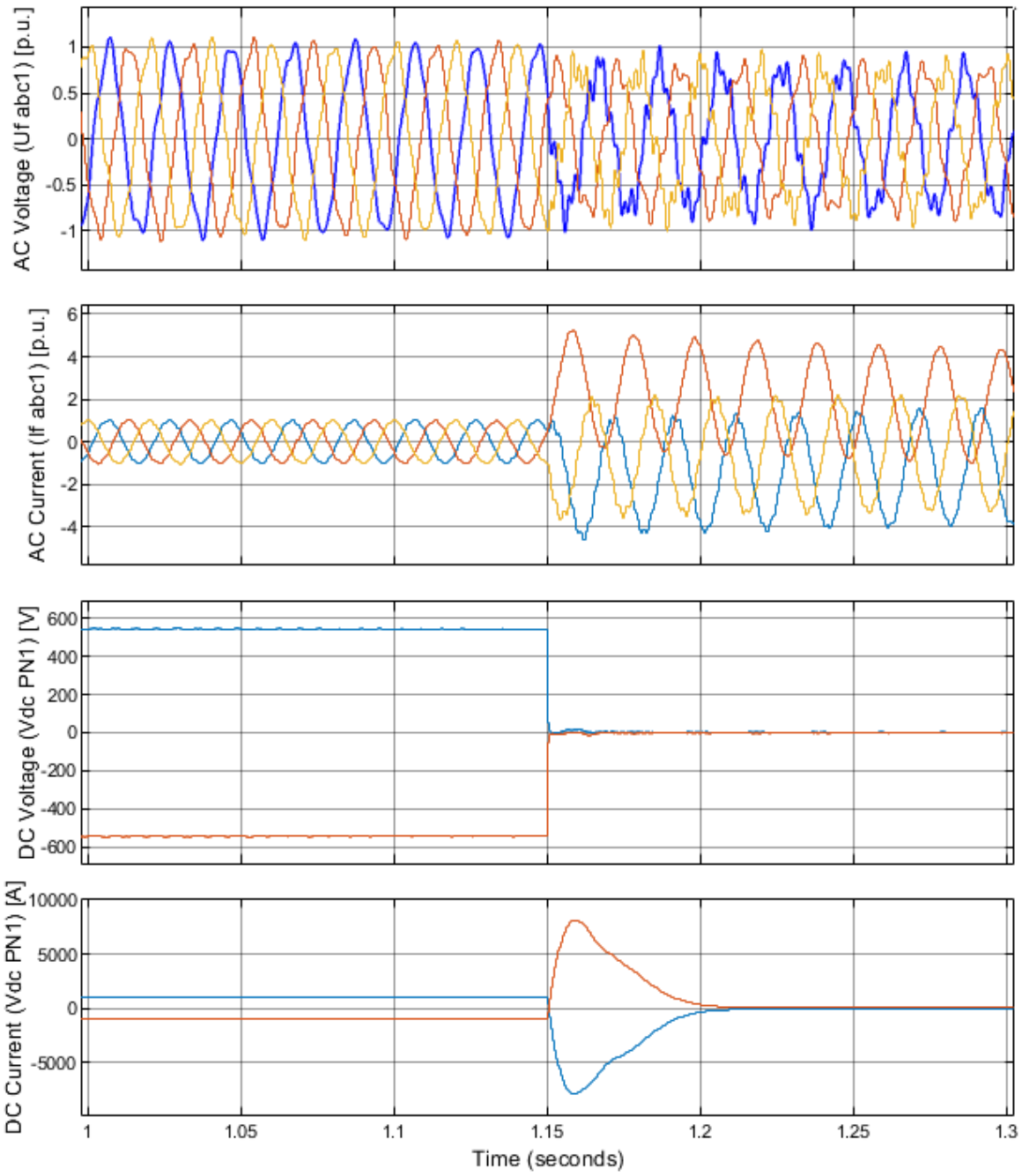
AC Voltage (Uf abc1) [p.u.]
AC Current (If abc1) [p.u.]
DC Voltage (Vdc PN1) [V]
DC Current (Vdc PN1) [A]
Time (seconds)

(a)

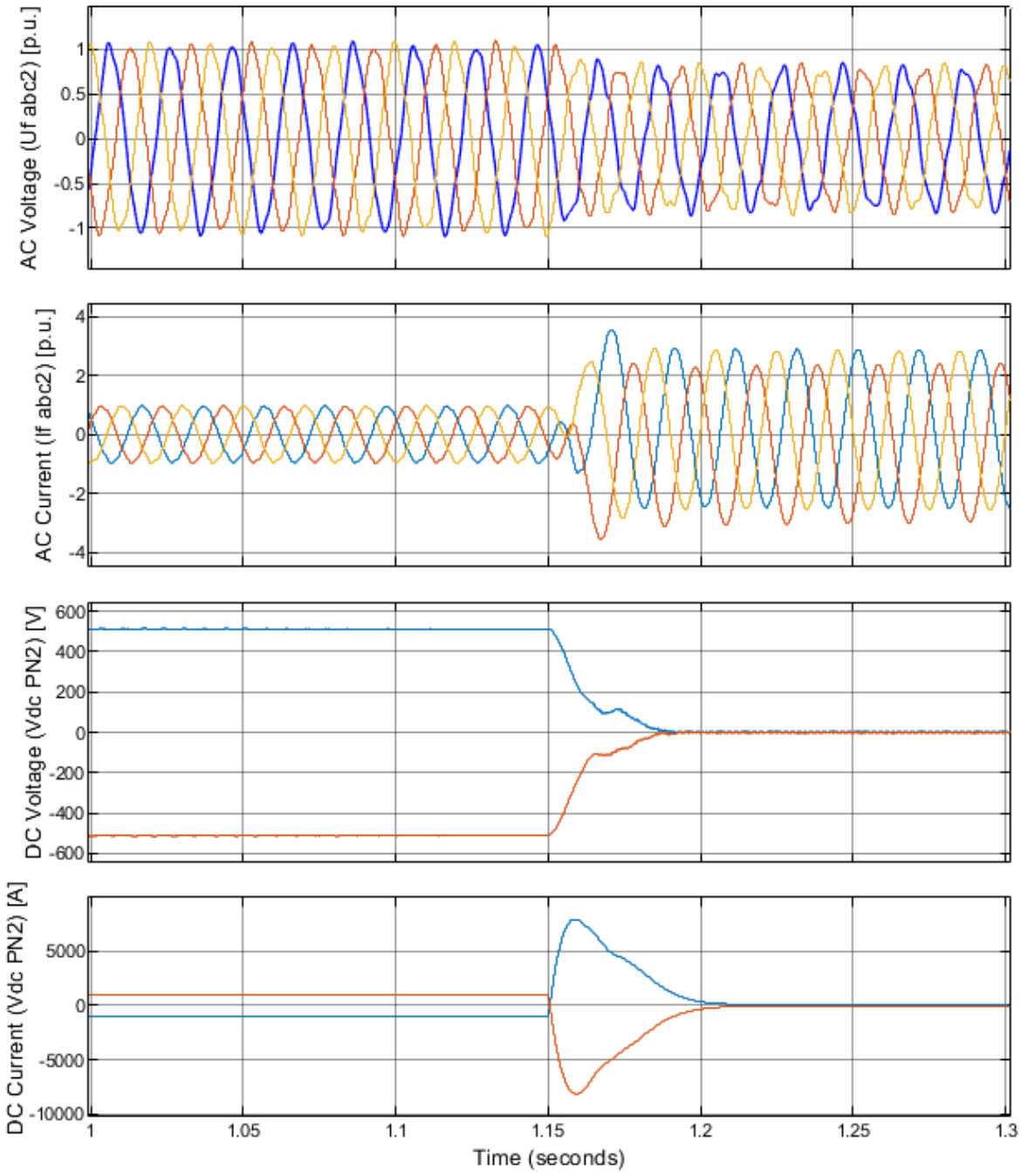
AC Voltage (Uf abc2) [p.u.]
1
0.5
0
-0.5
-1
AC Current (If abc2) [p.u.]
4
2
0
-2
-4
DC Voltage (Vdc PN2) [V]
600
400
200
0
-200
-400
-600
DC Current (Vdc PN2) [A]
5000
0
-5000
-10000
1
1.05
1.1
1.15
1.2
1.25
1.3
Time (seconds)

(b)

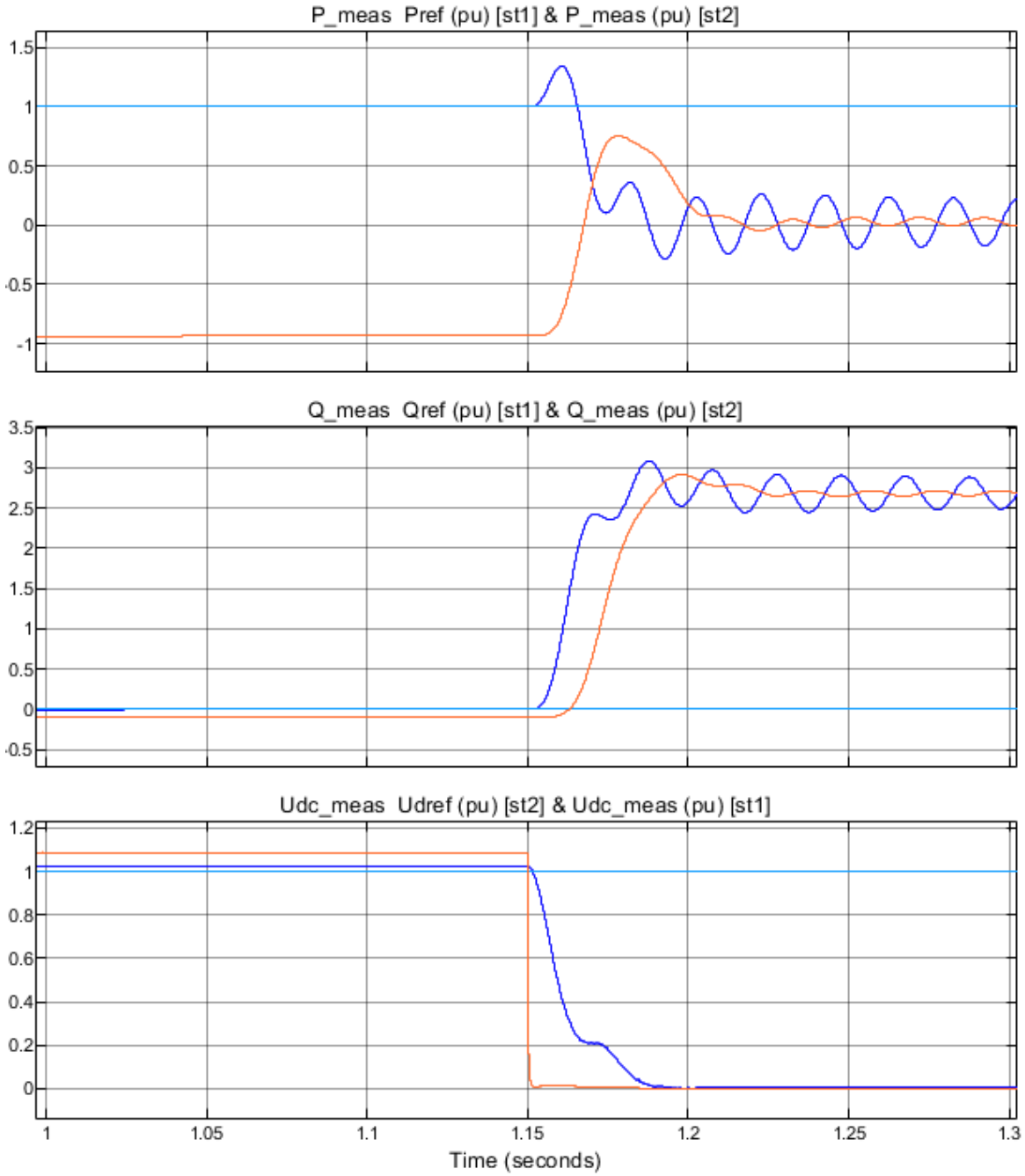

(c)

Figure 5.8 – Short circuit between positive and negative pole (a) Rectifier side (b) Inverter side (c) Power response

Positive Pole to Ground Fault: In this case, a short circuit occurs between the positive pole and ground of rectifier at a time (t = 1.15 sec). The positive pole DC voltage drops to zero but the huge amount of short circuit current flows in the positive pole (-8000 amps) for a time period of 300 milliseconds and after 700 milliseconds it reaches to zero. However, the negative pole DC voltage increases to 1000 Vdc (pole to pole voltage) but the transient occurs in the negative pole current (1000 amps) and finally reaches to -2000 amps, respectively, as seen in figure 5.9 (a).

However, the inverter side AC voltage reaches to 20 p.u. and DC side currents start increasing up to 6000 amps, as seen in figure 5.9(b). There is approximately 4000 amps difference between positive and negative poles.

On the other hand, active power reaches twice its nominal value and reactive power also increases to 0.45 p.u., as seen in figure 5.9(c).

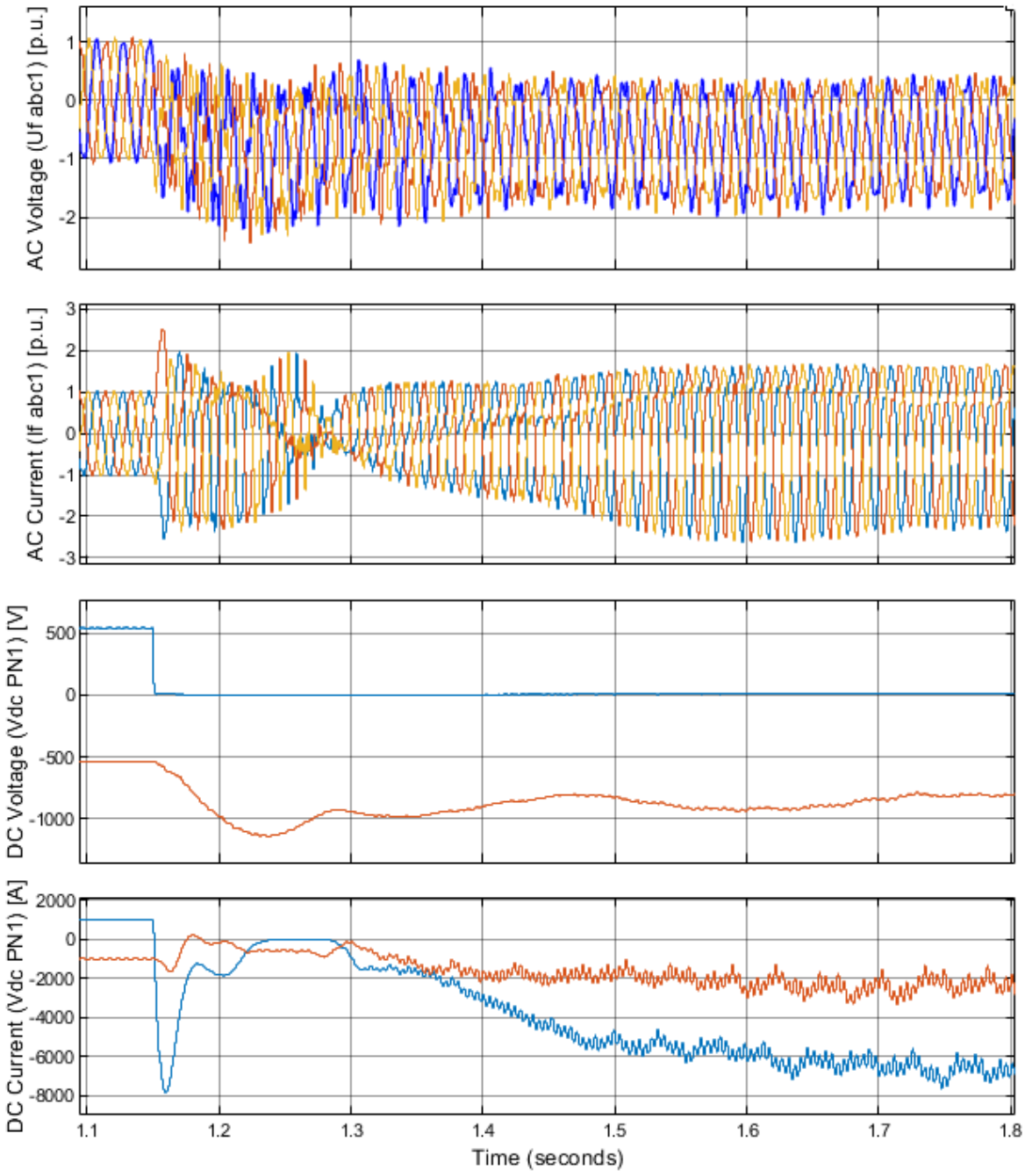
AC Voltage (Uf abc1) [p.u.]
AC Current (If abc1) [p.u.]
DC Voltage (Vdc PN1) [V]
DC Current (Vdc PN1) [A]
Time (seconds)

(a)

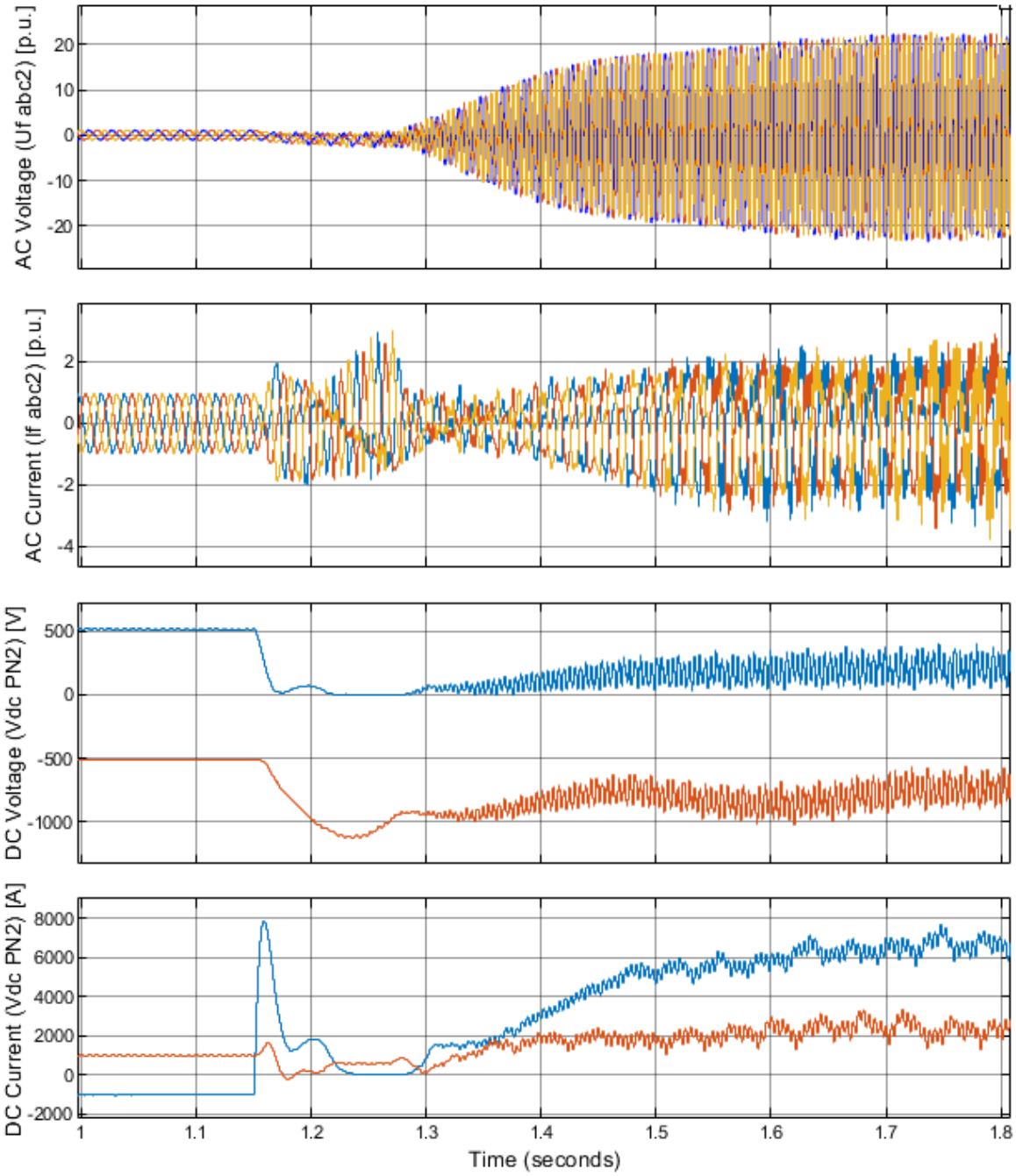
AC Voltage (Uf abc2) [p.u.]
20
10
0
-10
-20
AC Current (If abc2) [p.u.]
2
0
-2
-4
DC Voltage (Vdc PN2) [V]
500
0
-500
-1000
DC Current (Vdc PN2) [A]
8000
6000
4000
2000
0
-2000
1
1.1
1.2
1.3
1.4
1.5
1.6
1.7
1.8
Time (seconds)

(b)

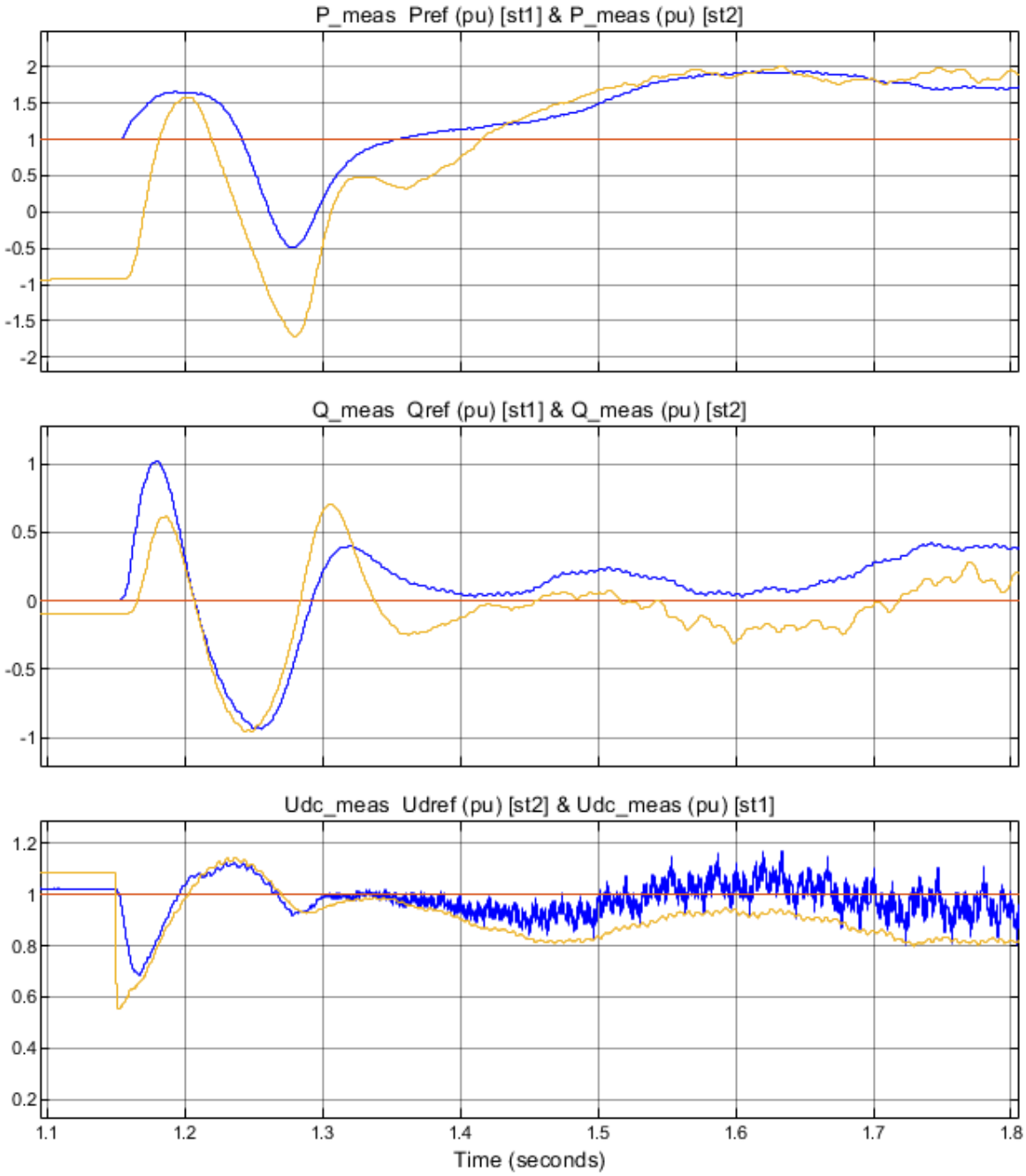

(c)

Figure 5.9 – Short circuit between positive pole and ground (a) Rectifier side (b) Inverter side (c) Power response

Negative Pole to Ground Fault: In this case, a short circuit occurs between negative pole and ground of rectifier at a time (t = 1.15 sec). The negative pole DC voltage drops to zero but the huge amount of short circuit current flows in the negative pole (8000 amps) for a time period of 300 milliseconds and after 700 milliseconds it reaches to zero. However, the positive pole DC voltage increases to 1000 Vdc (pole to pole voltage) but the transient occurs in the positive pole current (0 amps) and finally reaches to 2000 amps, respectively, as seen in figure 5.10 (a).

However, the inverter side AC voltage reaches to 20 p.u. and negative pole currents start increasing up to -6000 amps, as seen in figure 5.10(b). There is approximately 4000 amps difference between positive and negative poles current.

On the other hand, active power reaches to twice its nominal value and reactive power also increases to 0.45 p.u., as seen in figure 5.10(c).

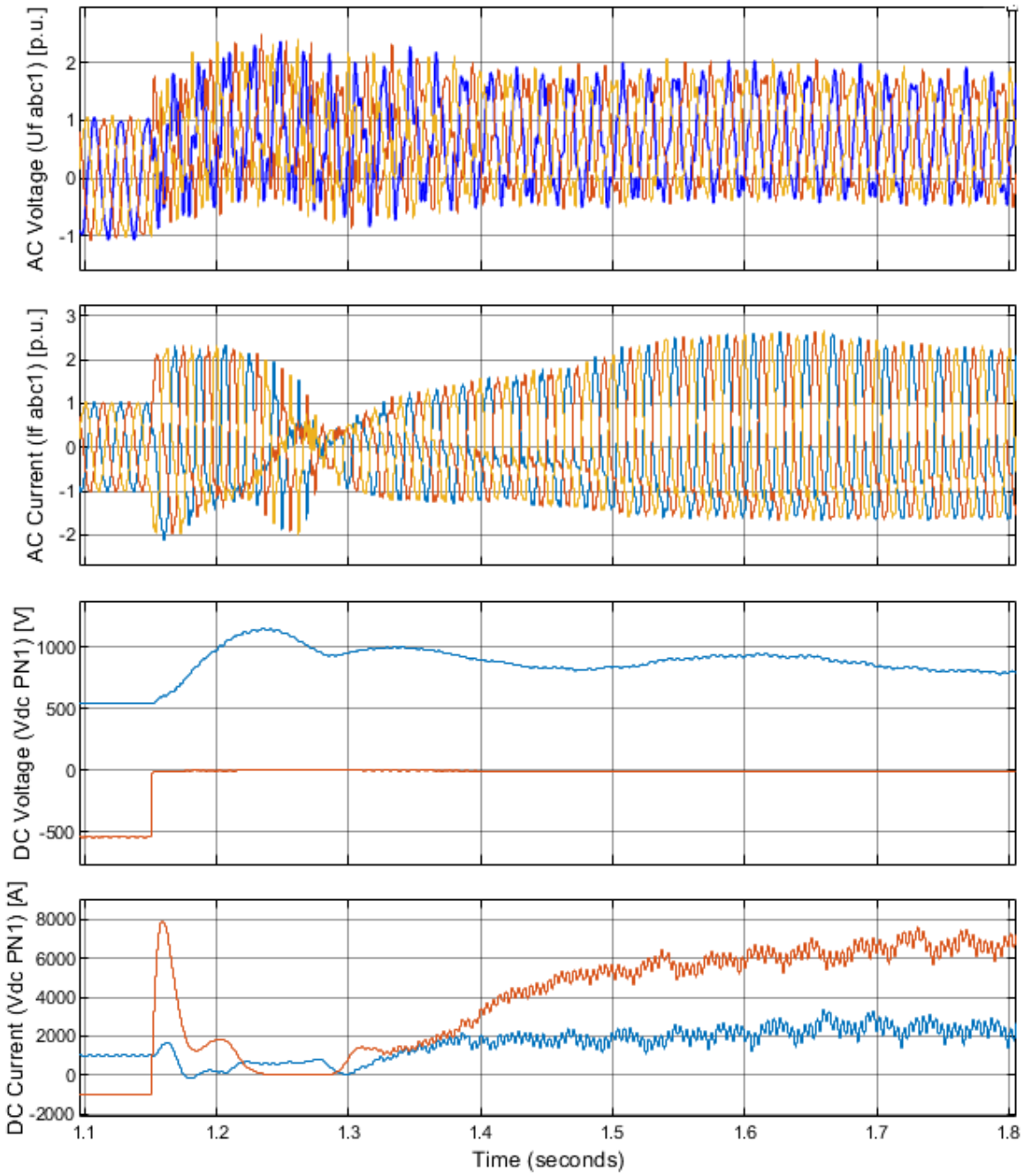
AC Voltage (Uf abc1) [p.u.]
AC Current (If abc1) [p.u.]
DC Voltage (Vdc PN1) [V]
DC Current (Vdc PN1) [A]
Time (seconds)

(a)

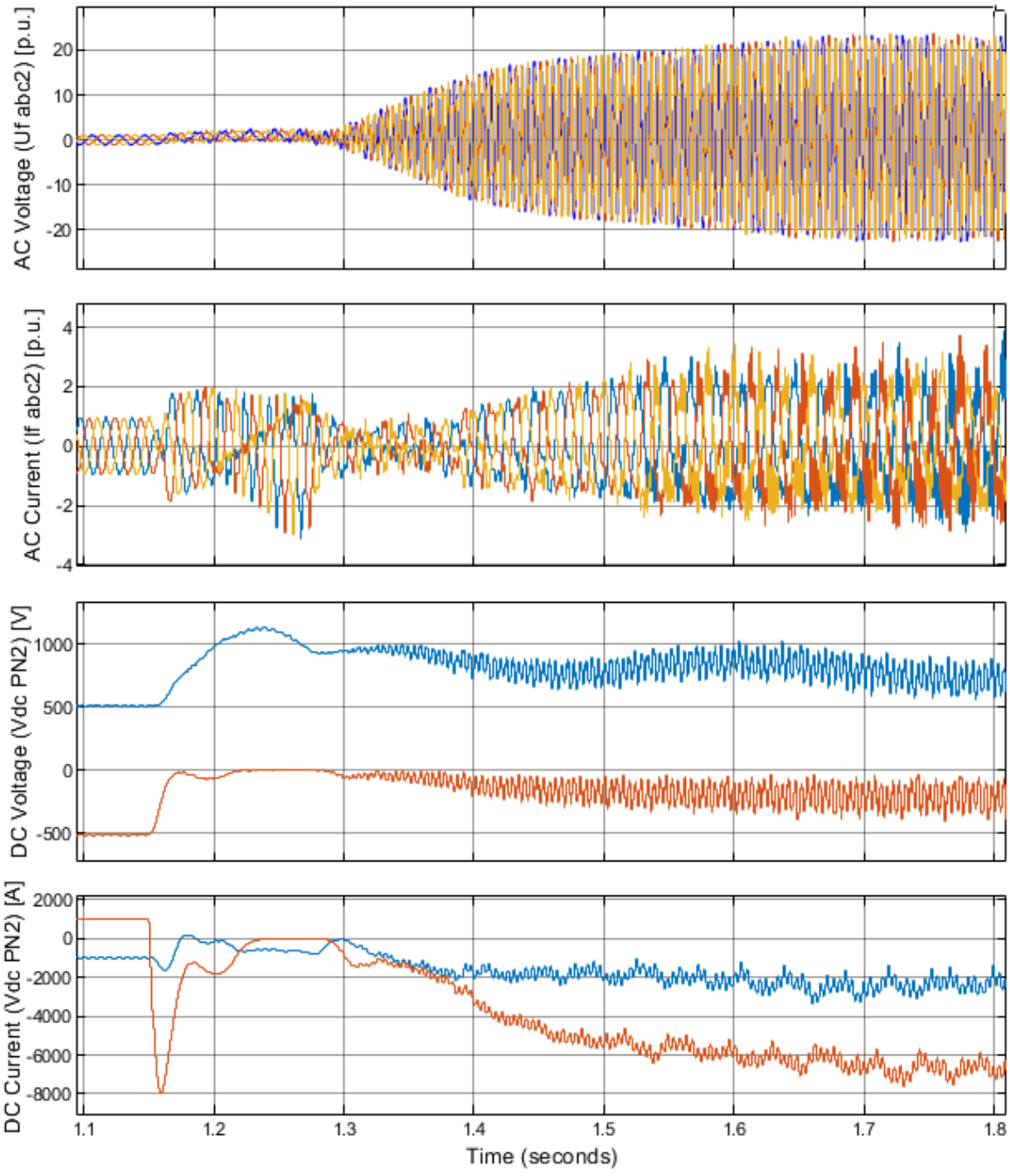
AC Voltage (Uf abc2) [p.u.]
AC Current (If abc2) [p.u.]
DC Voltage (Vdc PN2) [V]
DC Current (Vdc PN2) [A]
Time (seconds)

(b)

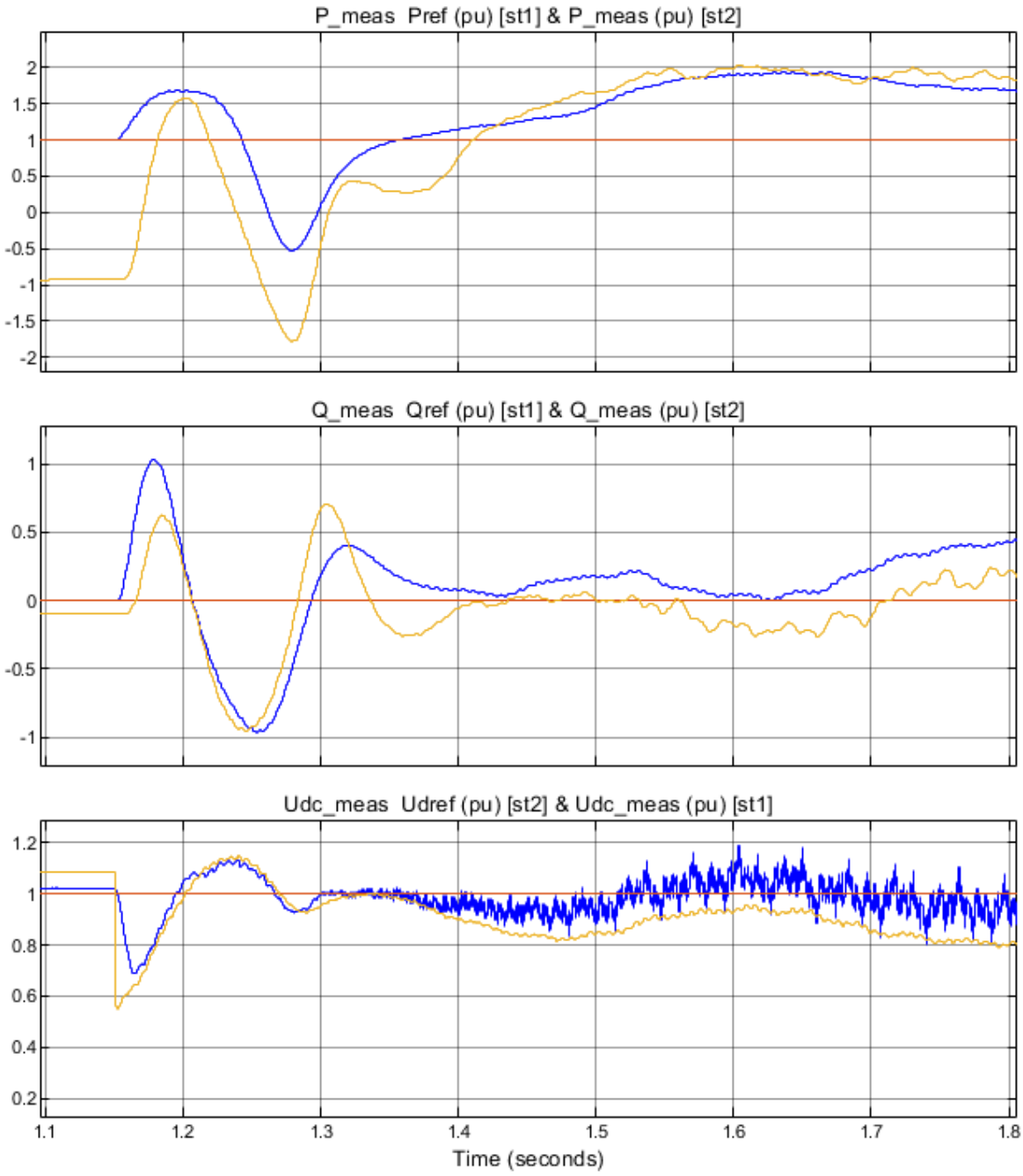

(c)

Figure 5.10 – Short circuit between negative pole and ground (a) Rectifier side (b) Inverter side (c) Power response

Short Circuit at DC Side Capacitor: In this case, a short circuit occurs across the DC side capacitors of rectifier at a time (t = 1.15 sec). The DC bus voltage drops to zero but a huge amount of short circuit current flows in DC bus (±8000 amps) for a time period of 500 msec. However, the AC side voltages decrease to 0.75 p.u. and short circuit current reaches to 5.2 p.u., respectively, as seen in figure 5.11 (a).

However, the inverter side AC voltage decreases linearly and reaches 0.75 p.u. and a peak of 3.5 p.u. in AC current has observed. The DC side voltage reaches zero after 500 milliseconds and the transient of ±8000 amps are seen in DC side current, as seen in figure 5.11(b).

Active power reaches zero after the fault, but the reactive power of 2.7 p.u. is flowing in the system, as seen in figure 5.11(c).

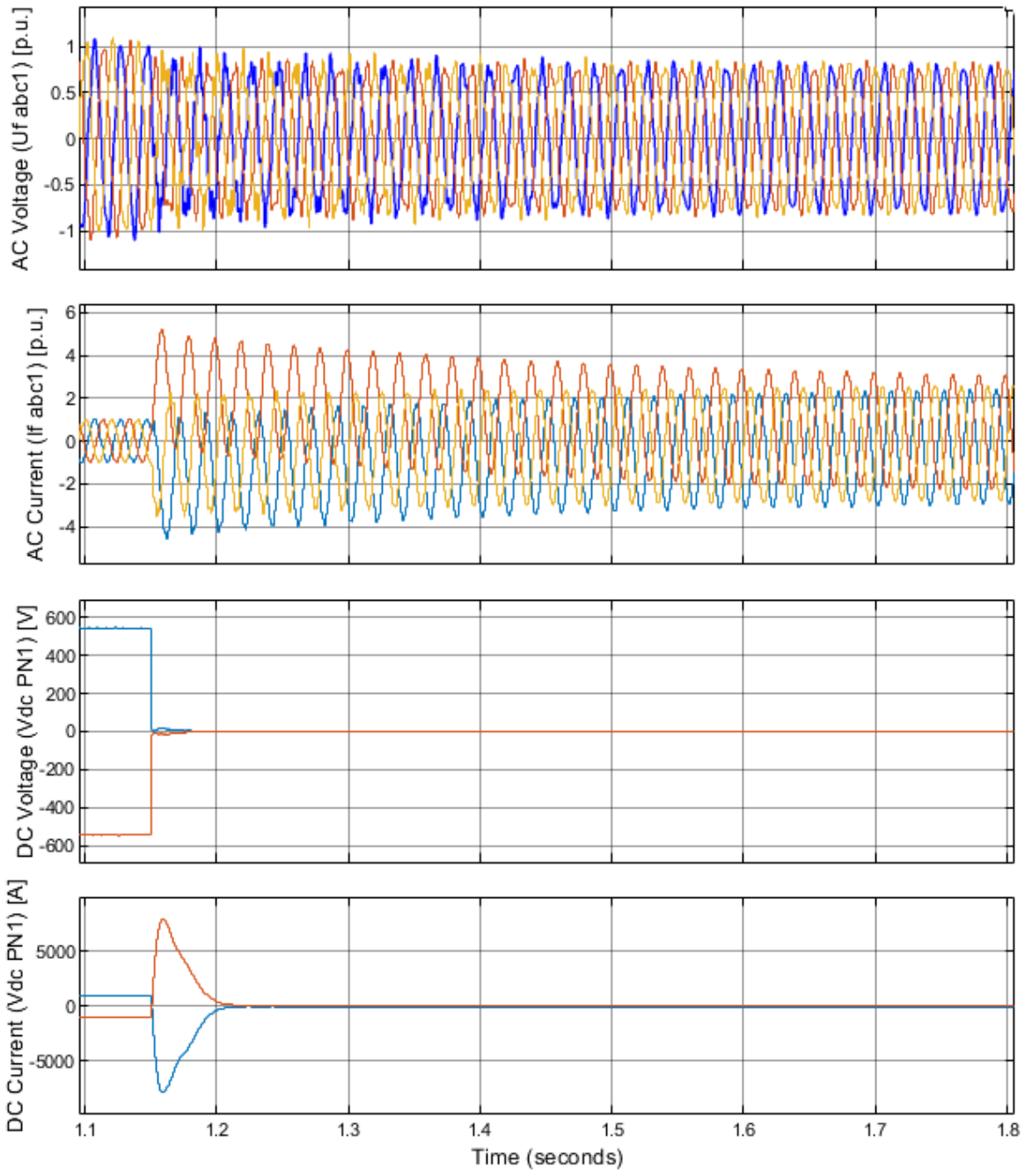
AC Voltage (Uf abc1) [p.u.]
AC Current (If abc1) [p.u.]
DC Voltage (Vdc PN1) [V]
DC Current (Vdc PN1) [A]
Time (seconds)

(a)

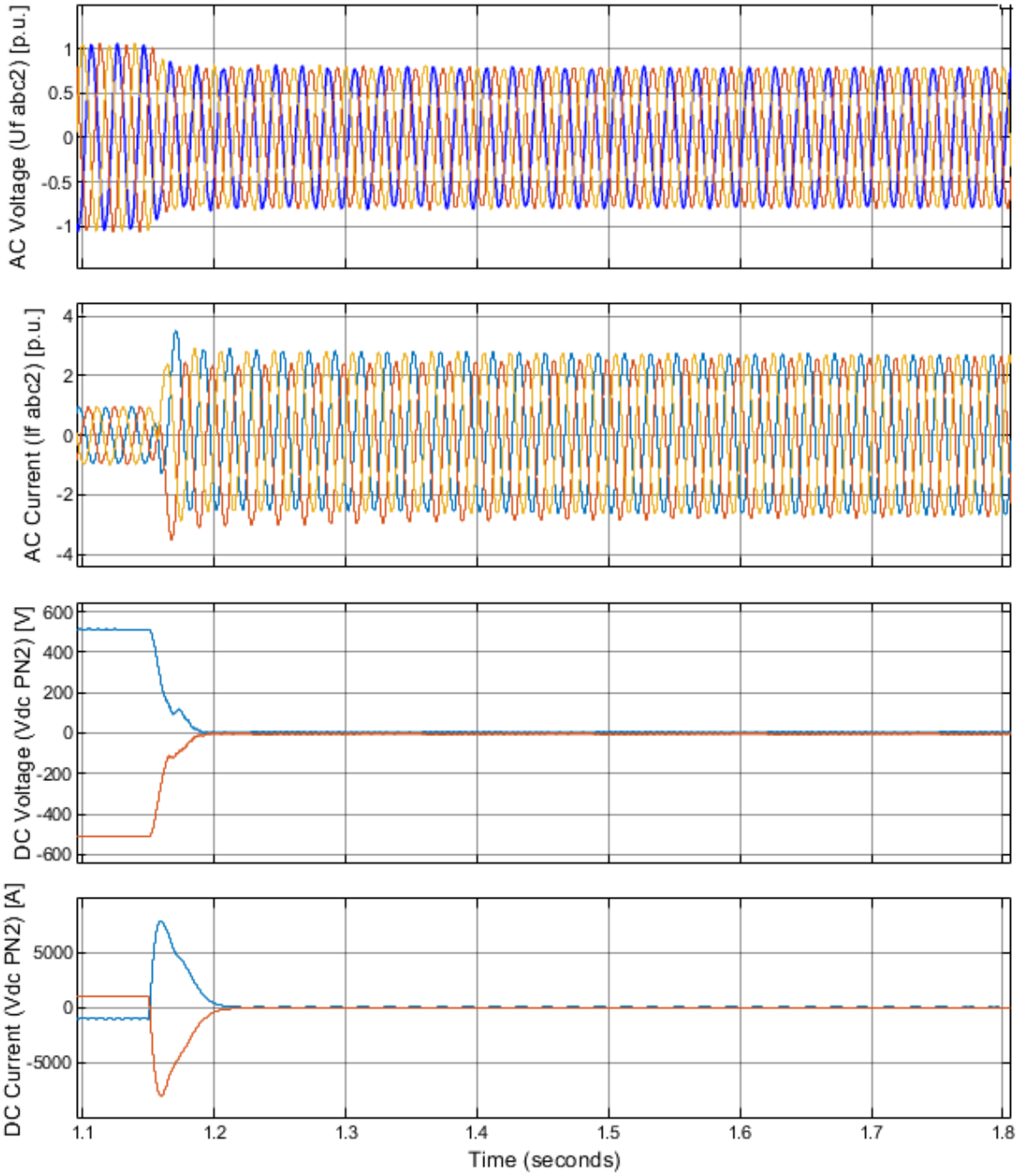
AC Voltage (Uf abc2) [p.u.]
1
0.5
0
-0.5
-1
AC Current (If abc2) [p.u.]
4
2
0
-2
-4
DC Voltage (Vdc PN2) [V]
600
400
200
0
-200
-400
-600
DC Current (Vdc PN2) [A]
5000
0
-5000
1.1
1.2
1.3
1.4
1.5
1.6
1.7
1.8
Time (seconds)

(b)

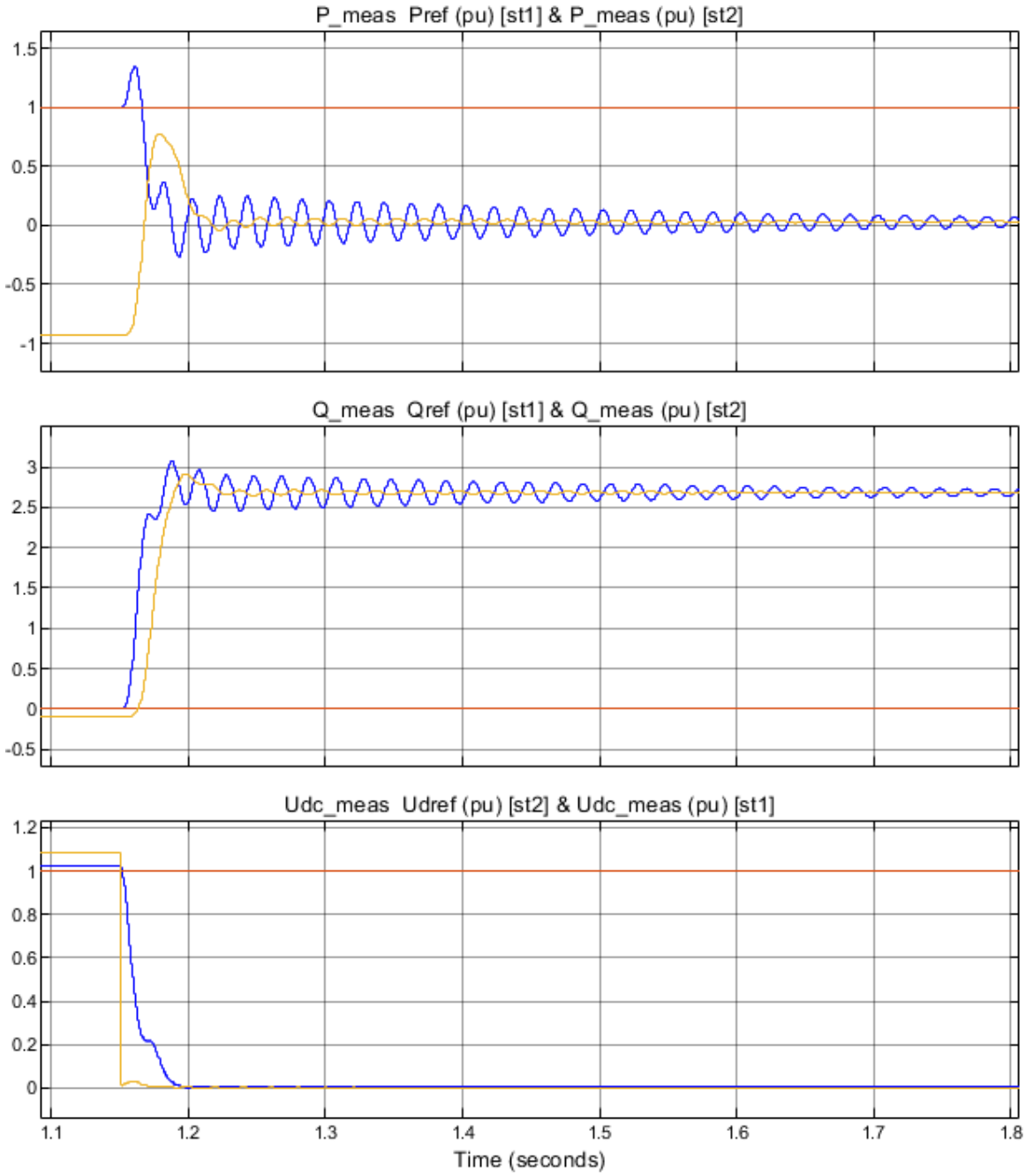

(c)

Figure 5.11 – Short circuit at DC side capacitor (a) Rectifier side (b) Inverter side

(c) Power response

Three-Phase to Ground Fault at Inverter AC Side Bus: As seen in figure 5.12(c), during the three-phase to ground fault the transmitted DC power is almost halted, and the DC voltage tends to increase since the DC side capacitance is being excessively charged. Hence, the DC side voltage reaches to a very high value of 1250 Vdc (2.5 p.u.).

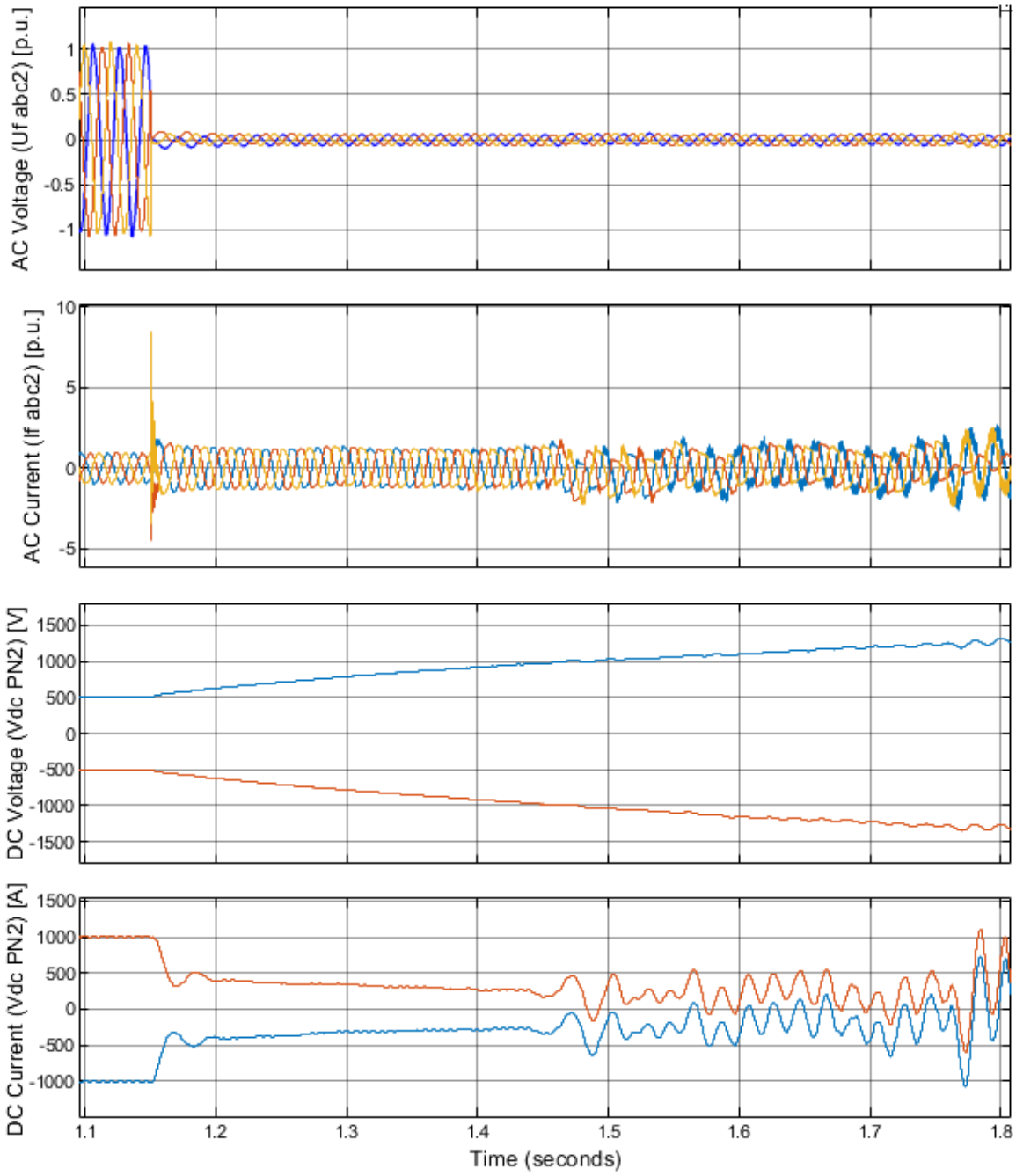

(a)

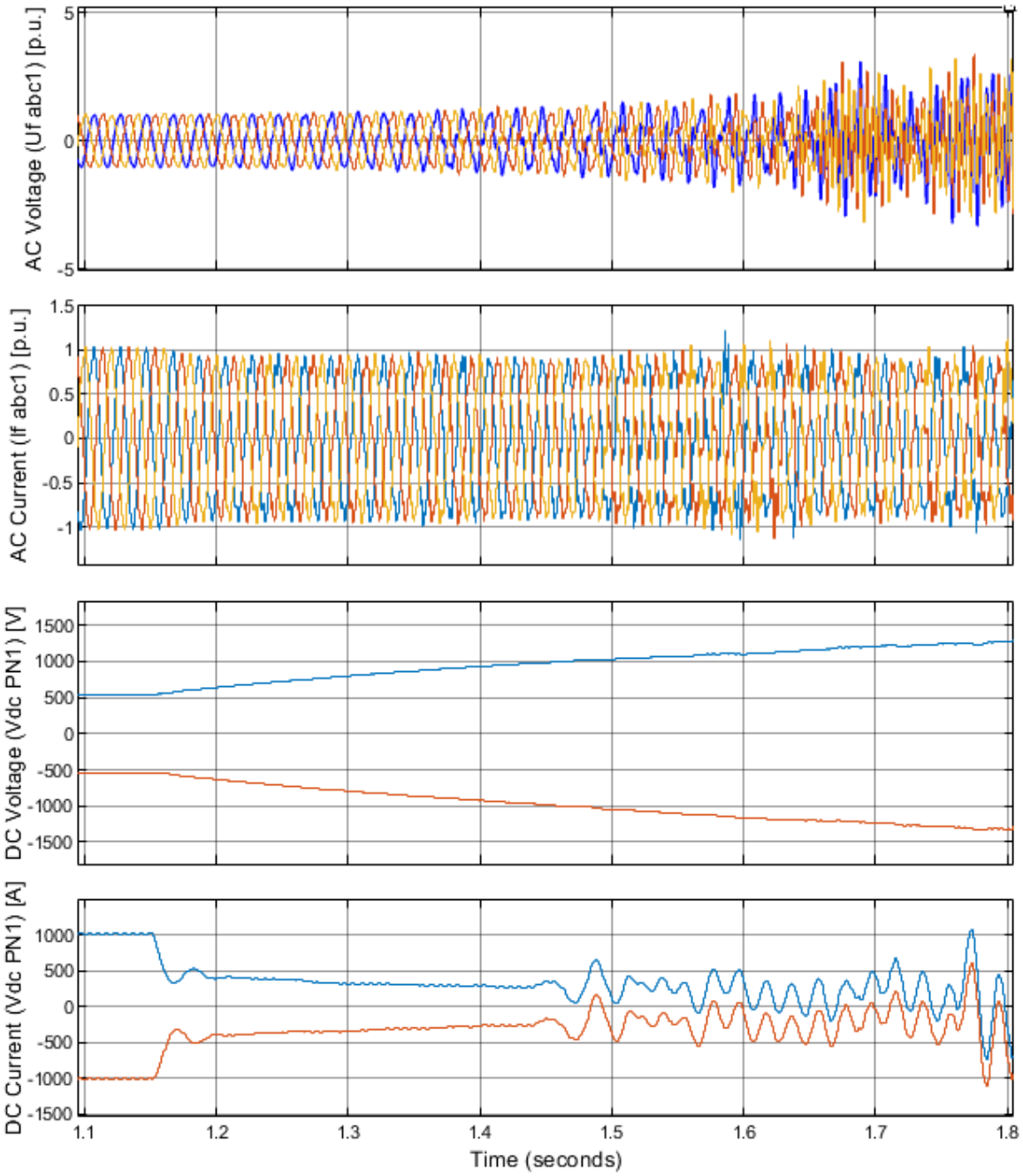
AC Voltage (Uf abc1) [p.u.]
AC Current (If abc1) [p.u.]
DC Voltage (Vdc PN1) [V]
DC Current (Vdc PN1) [A]
Time (seconds)

(b)

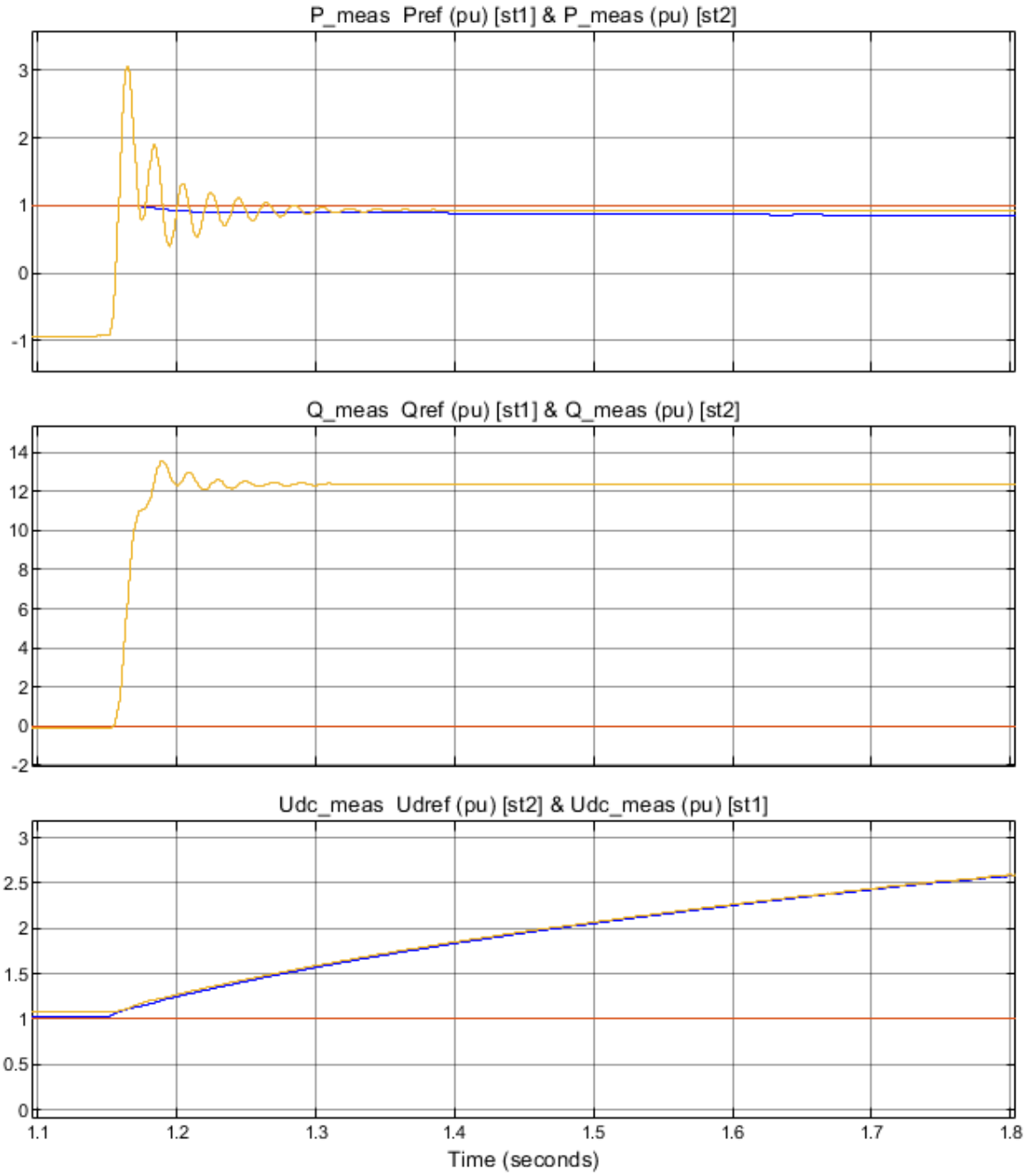

(c)

Figure 5.12 – Three-phase to ground fault at inverter AC side bus (a) Inverter side (b) Rectifier side (c) Power response

As seen in figure 5.12(c), the DC bus voltage reaches at a very high value (2.5 p.u.) 1250 Vdc. To limit the DC voltage within a fixed range, a special function (DC Voltage Control Override) in the active power control (in station 1) has implemented. As a result, the DC bus voltage is limited to (1.15 p.u.) 600 Vdc, as seen in figure 5.13(a).

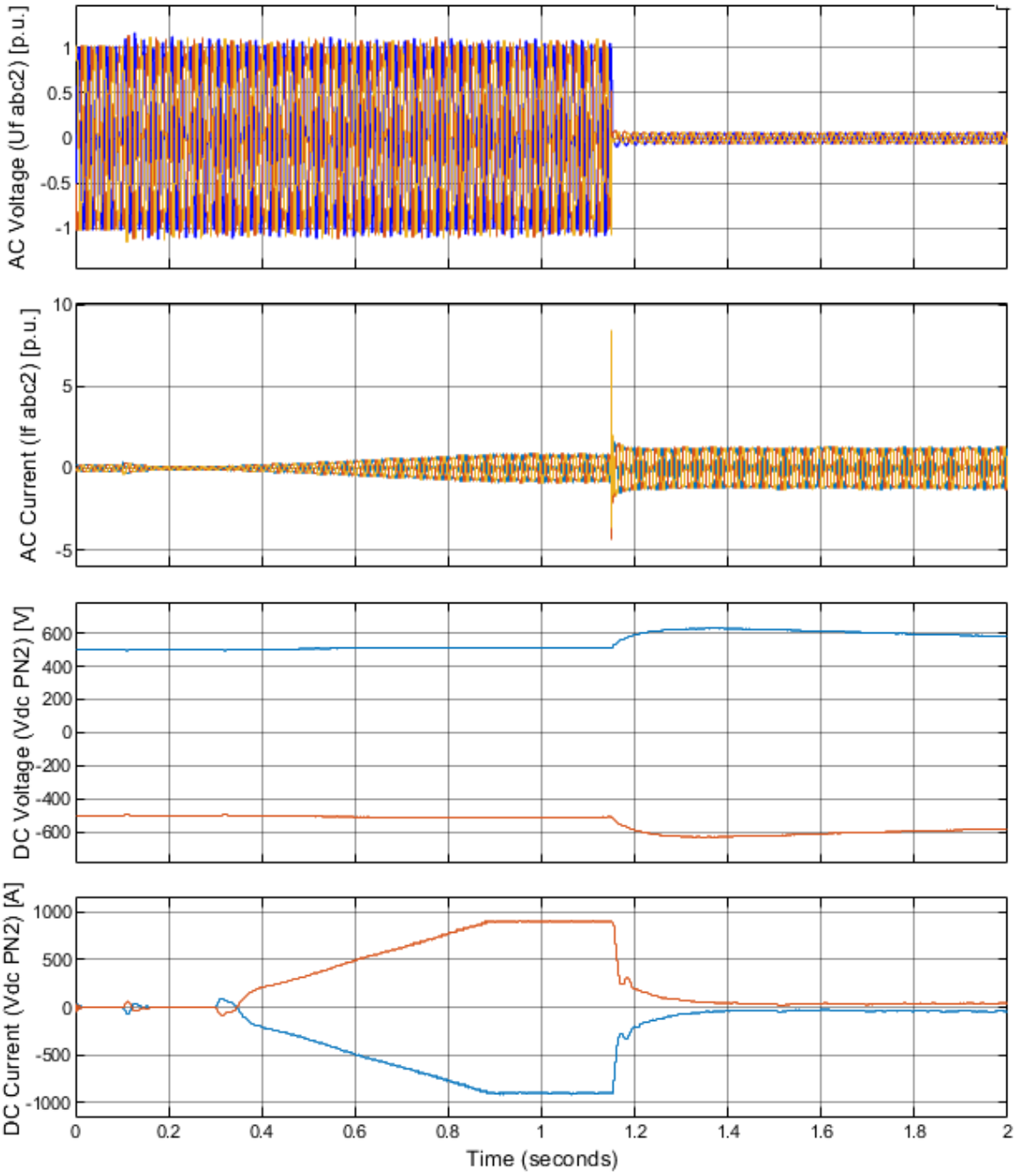

(a)

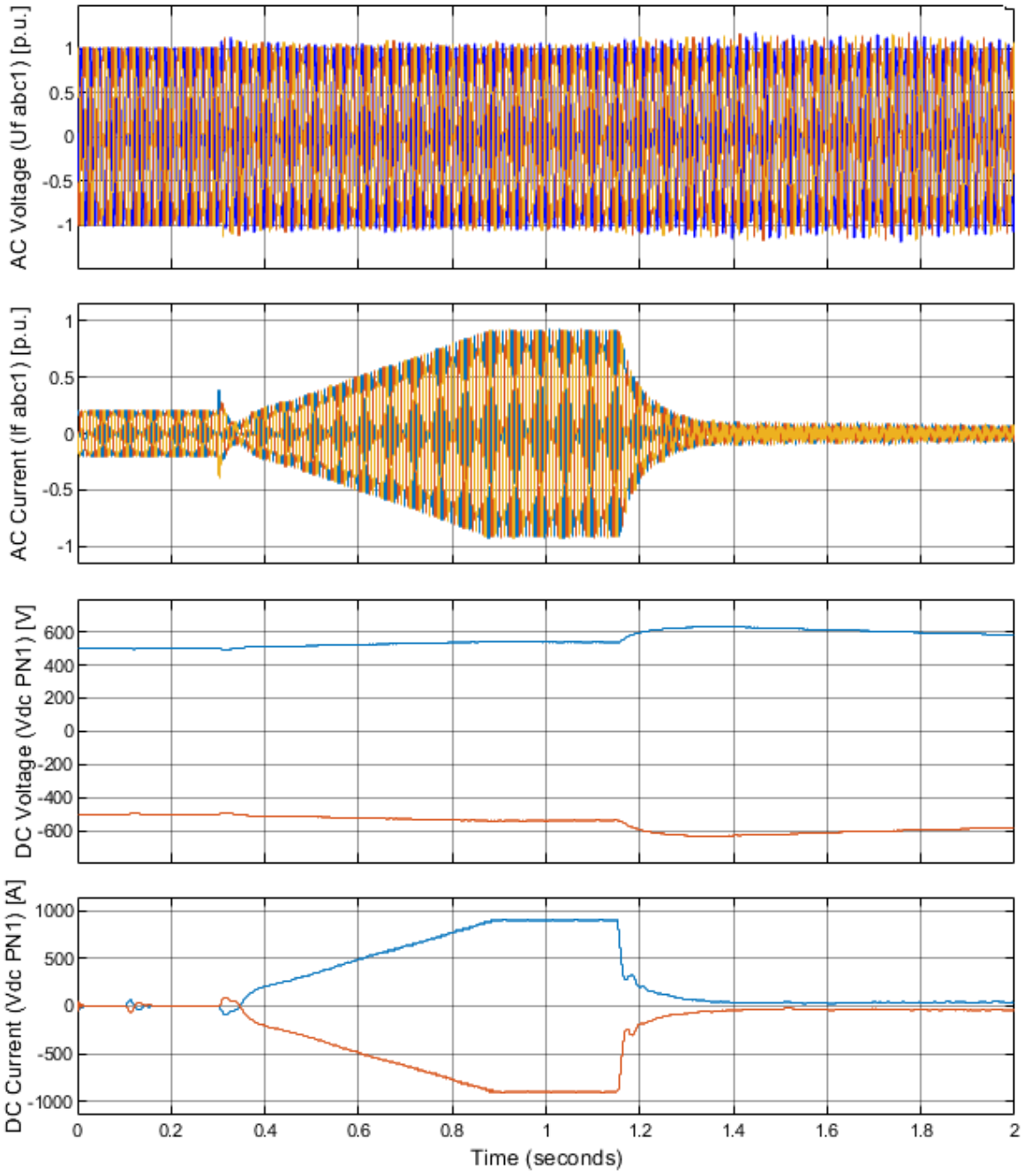
AC Voltage (Uf abc1) [p.u.]
AC Current (If abc1) [p.u.]
DC Voltage (Vdc PN1) [V]
DC Current (Vdc PN1) [A]
Time (seconds)

(b)

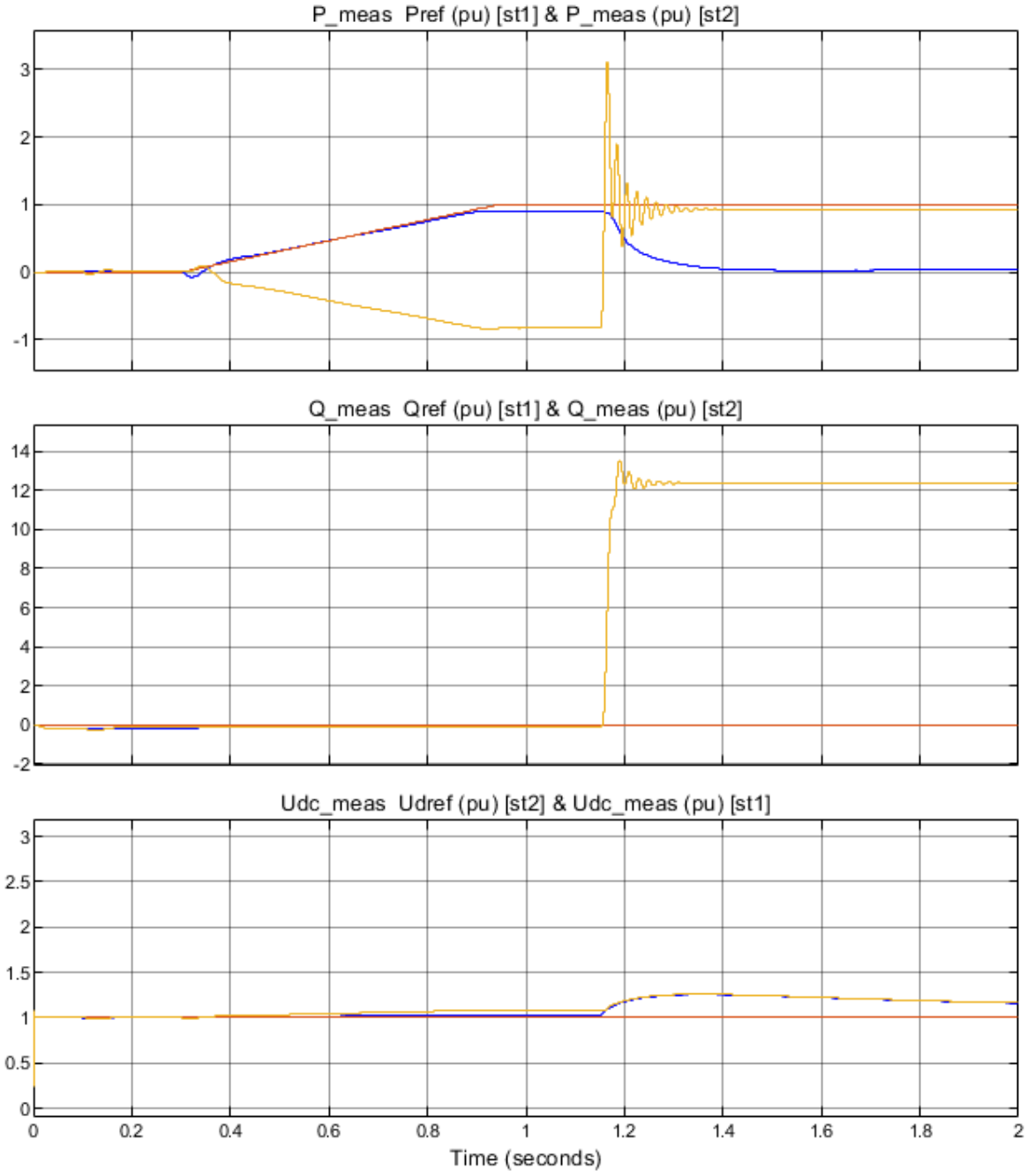

(c)

Figure 5.13 – Three-phase to ground fault at inverter AC side bus with DC voltage override control (a) Inverter side (b) Rectifier side (c) Power response

Summary & Conclusion

In this section, the main results of the dissertation are summarised. The main objective of the research was the development of the LVDC distribution system. The LVDC distribution system stability, power quality, and faults were evaluated by modeling and actual measurements. The model of the LVDC distribution system and its components were implemented in Simulink environment. With the help of the developed model, the addressed system issues included; the system transient behavior, the DC bus voltage stability, the DC power quality, and harmonic transfer to the AC side of the network. Further, monitoring and control data of the system verified under normal and different fault conditions.

Key Results of the Dissertation

The objective of the study was to analyze certain system-issues by taking a modeling approach. The LVDC distribution system model was developed and actual measurements were validated w.r.t to standards. Therefore, the key results are:

- The Simulink models of the network used for the time-domain transient analysis of the LVDC network.
- For the control and diagnostics purpose, the data acquisition under normal operation and under different fault scenarios were collected from the LVDC model, which used for model verification and comparison of results.

- The transient behavior of the network is stable in both steady-state and during large scale disturbances. Therefore, the author boasts that the dimensioning of the AC and DC components are adequate for a stable network.

The scientific contributions of the dissertation are:

- The work discusses the modeling and computation methodology of the LVDC distribution network.
- The dissertation highlights the harmonic content in the LVDC network and discussed the optimized results.
- The work demonstrates the transient behavior of the LVDC network.
- The dissertation addresses the possible DC voltage instability issues under different fault scenarios and analyses such issues by introducing DC voltage override control.

The limitations of the developed model:

- The harmonics produced by the three-level neutral point clamped converter in the LVDC network is very high. Special filters needed to limit them.
- Half of the pole (positive/negative) to ground current flows through the common point “0” of the converter.
- During a pole to ground (positive pole to the ground and negative pole to the ground) fault, very high current flows in the entire network and system become unbalanced. Further, the overvoltage observed in the AC side of the customer-end inverter.

Suggestions for Future Research

The suggestions for the most important topics of further research are:

- Higher harmonics are observed in the proposed model; therefore, the author proposed the implementation of Modular Multi-level Converter (MMC) for future work.
- As the middle point is solidly ground, during the normal operation, high (half of the pole to the ground) circulating current flows from the middle point to

the ground. Hence, the middle point can be connected to ground with an adequate impedance to limit the current.

- Development and integration of the distributed energy resource into the existing model for small-scale PV generation.
- Further development of the model to allow demand response and energy storage integration studies in LVDC networks and an analysis of the cost-efficiency benefits.

Glossary

DG --- Distributed Generation

PHEV--- Plug-in hybrid electric vehicle

DER --- Distributed Energy Reserves

LVDC --- Low Voltage Direct Current

VSC --- Voltage Sourced Converter

FFT --- Fast Fourier Transform

DC --- Direct Current

PCC --- Point of Common Coupling

AC --- Alternating Current

PV --- Photovoltaic

MV --- Medium Voltage

HVDC --- High Voltage Direct Current

LVAC --- Low Voltage Alternating Current

ESS --- Energy Storage System

LV --- Low Voltage

CEI --- Customer End Inverters

TN-S --- In TN-S DC system, the negative pole and enclosure is directly connected with the ground via protective earth (PE) wire

TN-C --- In TN-C DC system, the negative pole and enclosure is directly connected with the ground via protective earth (PE) wire

TT --- In TT DC system, the negative pole and enclosure is directly connected with the ground

IT --- In IT DC system, the negative pole is connected via resistance and enclosure directly connected with the ground

HV --- High Voltage

XPLE --- Cross-Linked Polyethylene

PEC --- power electronic converters

BESS --- battery energy storage system

Pref --- Active Power Reference

Qref --- Reactive Power Reference

Udref --- DC Voltage Reference

PWM --- Pulse Width Modulation

IGBT --- Insulated Gate Bipolar Transistor

PLL --- Phase-Locked Loop

Uabc1 --- PCC1 Voltage

Uabc2 --- PCC2 Voltage

Iabc1 --- PCC1 Current

Iabc2 --- PCC2 Current

Uf_abc1 --- Rectifier Side Transformer Secondary Voltage

If_abc1 --- Rectifier Side Transformer Secondary Current

Uf_abc2 --- Inverter Side Transformer Secondary Voltage

If_abc2 --- Inverter Side Transformer Secondary Current

Uv_abc1 --- Rectifier AC Side Voltage

Iv_abc1 --- Rectifier AC Side Current

Uv_abc2 --- Inverter AC Side Voltage

Iv_abc2 --- Inverter AC Side Current

VdcPN1 --- Rectifier DC Side Voltage

IdcPN1 --- Rectifier DC Side Current

VdcPN2 --- Inverter DC Side Voltage

IdcPN2 --- Inverter DC Side Current

Bibliography

[1] Keon-Woo Park, Chul-Hwan Kim, Doo-Ung Kim, Gi-Hyeon Gwon, Yun-Sik Oh, and Joon Han, "A Study on the Fault Characteristics of Line Fault in LVDC Distribution System."

[2] J. Kim, H. Lee, and J. Kim, "Design and Construction of Korean LVDC Distribution System for Supplying DC Power to the Customer," CIRED 23rd International Conference on Electricity Distribution, 2015.

[3] A. Lana, J. Karppanen, P. Nuutinen, T. Kaipia, and J. Partanen, "Consideration on Battery Energy Storage System for an LVDC Distribution System," September 2014.

[4] P. Salonen, T. Kaipia, P. Nuutinen, P. Peltoniemi, and J. Partanen, "An LVDC Distribution System Concept," Nordic Workshop on Power and Industrial Electronics (NORPIE), 2008.

[5] A. LANA, T. KAIPIA, A. MATTSSON, J. KARPPANEN, P. Peltoniemi, and J. Partanen, "Prospects of Development of LVDC Electricity Distribution System Energy Efficiency," 23rd International Conference on Electricity Distribution in Lyon, Paper 1475, 15-18 June 2015.

[6] V. Voutilainen, "Master Thesis: Determining the Possibility of Equivalent Distribution," 2007.

[7] T. Kaipia, A. Mattsson, J. Kim, J. Cho, and J. Karppanen, "Effect of Voltage Level Selection on Earthing and Protection of LVDC Distribution Systems," 2015.

[8] J. Rekola, J. Jokipii, and T. Suntio, "Effect of Network Configuration and Load Profile on Efficiency of LVDC Distribution Network," 2014.

[9] T. Kaipia, P. Salonen, J. Lassila, and J. Partanen, "Possibilities of the Low Voltage DC Distribution Systems," August 2006.

[10] E. Rodriguez-Diaz, F. Chen, J. C. Vasques, J. M. Guerrero, R. Burgos, and D. Boroyevich, "Voltage-Level Selection of Future Two-Level LVdc Distribution Grids," IEEE Electrification Magazine, June 2016, pp. 22–23.

[11] F. Li, W. Qiao, H. Sun, Z. Xu, and P. Zhang, "Smart Transmission Grid: Vision and Framework," IEEE Transactions on Smart Grid, vol. 1, no. 2, pp. 168–177, 2010.

[12] P. Peltoniemi and P. Nuutinen, "Fault Detection Method for Phase-to-Ground Faults in Three-Phase Inverter Applications," in *IECON 2013 - 39th Annual Conference of the IEEE*

Industrial Electronics Society, 2013, pp. 767–772.

[13] P. Nuutinen, "Doctoral Thesis: Power Electronic Converters in Low Voltage Direct Current Distribution Analysis and Implementation," Lappeenranta University of Technology Finland, 2015.

[14] A. Mattsson, A. Lana, A. Pinomaa, M. Luukkanen, and T. Hakala, "LVDC Rules – Technical Specifications for Public LVDC Distribution Network," 24th International Conference & Exhibition on Electricity Distribution (CIRED), no. 1, pp. 293–296, 2017.

[15] L. Li, J. Yong, L. Zeng, and X. Wang, "Investigation on the System Grounding Types for Low Voltage Direct Current Systems," IEEE Electrical Power and Energy Conference (EPEC), 2013.

[16] M. Carminati and E. Ragaini, "Considerations on DC side Grounding Configurations of LVDC Microgrids," 5th International Youth Conference on Energy (IYCE) - Proceedings, 2015.

[17] P. Salonen, P. Nuutinen, P. Peltoniemi, and J. Partanen, "Protection Scheme for an LVDC Distribution System," 20th International Conference on Electricity Distribution (CIRED) in Prague, Paper 0891, 8-11 June 2009., vol. 5.

[18] A. A. S. Emhemed, K. Fong, S. Fletcher, and G. M. Burt, "Validation of Fast and Selective Protection Scheme for an LVDC Distribution Network," IEEE Transactions on Power Delivery, vol. 32, no. 3, pp. 1432–1440, 2017.

[19] Yuliya Khegay, "Master's Thesis: Optimization of the Power Cable for Low Voltage Direct Current (LVDC) Distribution System," Lappeenranta University of Technology, Faculty of Electrical Engineering., 2010.

[20] D. Antoniou, A. Tzimas, and S. M. Rowland, "LVDC Utilization of Existing LVAC Distribution Cables," IEEE Electrical Insulation Conference (EIC) in Ottawa Canada, pp. 518–522, 2013.

[21] T. Kaipia, J. Lassila, and J. Partanen, "Application of Low Voltage DC-Distribution System – A Techno-Economical Study," 19th International Conference on Electricity Distribution (CIRED) in Vienna, Paper 0464, 2007.

[22] A. Lana, "Doctoral Thesis: LVDC Power Distribution System Computational Modeling," Lappeenranta University of Technology, 2014.

[23] J. Barros, M. de Apráiz, and R. Diego, "Power Quality in DC Distribution Networks," Energies (MDPI), vol. 12, 2019.

[24] M. Berman, "All About EMI Filters," Electronic Products, vol. 50, no. 10, pp. 51–53, 2008.

[25] W. Javed, D. Chen, M. E. Farrag, and Y. Xu, "System Configuration, Fault Detection, Location, Isolation, and Restoration: A Review on LVDC Microgrid Protections," Energies

(MDPI), vol. 12, 2019.

[26] M. Hajian, D. Jovcic, and B. Wu, "Evaluation of Semiconductor Based Methods for Fault Isolation on High Voltage DC Grids," IEEE Transactions on Smart Grid, vol. 4, no. 2, pp. 1171–1179, 2013.

[27] A. F. Moreno and E. Mojica-Nava, "LVDC Microgrid Perspective for a High-Efficiency Distribution System," IEEE PES Transmission and Distribution Conference and Exposition, 2014.

[28] D. Salomonsson and A. Sannino, "Low-Voltage DC Distribution System for Commercial Power Systems With Sensitive Electronic Loads," IEEE Transactions on Power Delivery, vol. 22, no. 3, pp. 1620–1627, 2007.

[29] W. Lu and B. T. Ooi, "Multi-terminal LVDC System for Optimal Acquisition of Power in Wind-Farm using Induction Generators," IEEE Transactions on Power Electronics, vol. 17, no. 4, pp. 558–563, 2002.

[30] S. Vazquez, S. M. Lukic, E. Galvan, L. G. Franquelo, and J. M. Carrasco, "Energy Storage Systems for Transport and Grid Applications," IEEE Transactions on Industrial Electronics, vol. 57, no. 12, pp. 3881–3895, 2010.

[31] V. A. Prabhala, B. P. Baddipadiga, P. Fajri, and M. Ferdowsi, "An Overview of Direct Current Distribution System Architectures & Benefits," Energies (MDPI), vol. 11, 2018.

[32] B. E. Rodriguez-Diaz, J. C. Vasquez, and J. M. Guerrero, "Intelligent DC Homes in Future Sustainable Energy Systems: When Efficiency and Intelligence Work Together," *IEEE Consumer Electronics Magazine*, vol. 5, IEEE, pp. 74–80, 2016.

[33] D. Nilsson, "Load Modelling for Steady-State and Transient Analysis of Low-Voltage DC Systems," 39th IAS Annual Meeting, IEEE Industry Applications Conference, vol. 2, 2004.

[34] International Electrotechnical Commission (IEC), "IEC 60479-1 - Effects of Current on Human Beings and Livestock," vol. 1.0, 2018.

[35] R. Dean, P. Marzin, and L. O. N. Cedex, "Grounding Concept Considerations and Recommendations for 400VDC Distribution System," IEEE 33rd International Telecommunications Energy Conference (INTELEC), 2011.

[36] A. Agustoni, E. Borioli, M. Brenna, G. Simioli, and E. Tironi, "LVDC Distribution Network with Distributed Energy Resources: Analysis of Possible Structures," 18th International Conference on Electricity Distribution, 2005.

[37] M. Von, "Discovering DC (A Primer on DC Circuit Breakers, their Advantages, and Design," *IEEE Industry Applications Magazine*, no. 2013.

[38] W. Tschudi, "Edison Redux: 380Vdc Brings Reliability and Efficiency to Sustainable Data Centers," *IEEE Power and Energy Magazine*, vol. 10, IEEE, pp. 50–59, 2012.

[39] P. Inttpat, P. Paisuwanna, and S. Khomfoi, “Capacitor Lifetime Monitoring for Multilevel Modular Capacitor Clamped DC to DC Converter,” 8th Conference - Electrical Engineering/ Electronics, Computer, Telecommunications and Information Technology (ECTI) Association of Thailand, pp. 719–722, 2011.

[40] D. Talapko, “Telecom Datacenter Power Infrastructure Availability Comparison of DC and AC UPS,” International Telecommunications Energy Conference - INTELEC, (Proceedings), 2012.

[41] D. J. Becker and B. J. Sonnenberg, “DC Microgrids in Buildings and Data Centers,” International Telecommunications Energy Conference - INTELEC, (Proceedings), 2011.

[42] V. Sithimolada and P. W. Sauer, “Facility-level DC vs Typical AC Distribution for Data Centers: A Comparative Reliability Study,” IEEE Region 10 Annual International Conference, Proceedings/TENCON, pp. 2102–2107, 2010.

[43] R. J. Hill, “Electric Railway Traction - Part 3 : Traction Power Supplies,” Power Engineering Journal, pp. 275–286, 1994.

[44] ABB, “Technical Application Papers No.5, ABB Circuit-Breakers for Direct Current Applications,” 2011.

[45] Y. Sun, “Thesis: The Impact of Voltage-Source-Converters Control on the Power System : the Stability Analysis of a Power Electronics Dominant Grid,” 2018.

[46] W. Pei, W. Deng, X. Zhang, H. Qu, and K. Sheng, “Potential of Using Multiterminal LVDC to Improve Plug-In Electric Vehicle Integration in an Existing Distribution Network,” IEEE Transactions on Industrial Electronics, vol. 62, no. 5, pp. 3101–3111, 2015.

[47] ABB, “Technical Application Papers No.14, Faults in LVDC Microgrids with Front-End Converters,” 2015.

[48] B. Zahedi and L. E. Norum, “Voltage Regulation and Power Sharing Control in Ship LVDC Power Distribution Systems,” 15th European Conference on Power Electronics (EPE) and Applications, 2013.

[49] ABB, “Technical Application Papers No . 24, Medium Voltage Direct Current Applications,” pp. 10–24, 2017.

[50] ABB, “HVDC Light, It’s Time to Connect,” pp. 1–72, 2012.

[51] ABB, “It’s Time to Connect - Technical Description of HVDC Light Technology,” vol. 39, 2013.

[52] Stamatiou Georgios, “Doctoral Thesis: Converter Interactions in VSC-based HVDC Systems,” Chalmers University of Technology, Sweden, 2015.

[53] N. Flourentzou, V. G. Agelidis, and Georgios D. Demetriades, “VSC-Based HVDC Power Transmission Systems : An Overview,” IEEE Transactions on Power Electronics, vol. 24, no.

3, pp. 592–599, 2009.

[54] H. Krug, E. Gmbh, T. Kume, M. Swamy, and Y. E. America, "Neutral-Point Clamped Three-Level General Purpose Inverter - Features, Benefits, and Applications," 35th Annual IEEE Power Electronics Specialists Conference, 2004.

[55] L. Zeni, T. Haileselassie, G. Stamatiou, K. Uhlen, P. Sørensen, and N. A. Cutululis, "DC Grids for Integration of Large Scale Wind Power," EWEA Offshore, 2011.

[56] S. Namballa, "A Sinusoidal PWM Scheme for Neutral Point Clamped Five-Level Inverter," International Electrical Engineering Journal (IEEJ), vol. 4, no. 1, pp. 918–925, 2013.

[57] G. P. Adam, S. J. Finney, O. Ojo, and B. W. Williams, "Quasi-Two-level and Three-level Operation of a Diode-Clamped Multilevel Inverter using Space Vector Modulation," IET Power Electronics, vol. 5, no. 5, pp. 542–551, 2012.

[58] M. Beza and S. Norrga, "Three-level Converters with Selective Harmonic Elimination PWM for HVDC Application," IEEE Energy Conversion Congress and Exposition (ECCE) - Proceedings, pp. 3746–3752, 2010.

[59] V. S. C. D. Systems and S. G. Johansson, "Power System Stability Benefits with VSC DC-Transmission Systems," International Council on Large Electric Systems (CIGRE), 2004.

[60] P. Ganesan and K. Hatua, "Vector Control Adopted for Single Phase Dual Active Bridge," IEEE International Conference on Power Electronics, Drives and Energy Systems (PEDES), 2016.

[61] A. Egea-Alvarez, S. Fekriasl, F. Hassan, and O. Gomis-Bellmunt, "Advanced Vector Control for Voltage Source Converters Connected to Weak Grids," IEEE Transactions on Power Systems, vol. 30, no. 6, pp. 3072–3081, 2015.

[62] C. J. M. Sr and W. Sunderman, "Distribution System Power Quality Assessment Phase II: Voltage Sag and Interruption Analysis," pp. 113–120, 2005.

[63] S. Bhattacharyya, J. M. A. Myrzik, and W. L. Kling, "Consequences of Poor Power Quality - An Overview," Proceedings of the Universities Power Engineering Conference, 2007.

[64] P. Nuutinen *et al.*, "Research Site for Low-Voltage Direct Current Distribution in a Utility Network-Structure, Functions, and Operation," IEEE Transactions on Smart Grid, vol. 5, no. 5, pp. 2574–2582, 2014.

[65] IEEE, "IEEE Recommended Practices and Requirements for Harmonic Control in Electrical Power Systems," *IEEE std 519-1992*, 1993.

[66] P. Nuutinen, T. Kaipia, A. Lana, and P. Silventoinen, "Start-Up of The LVDC Distribution Network," 21st International Conference on Electricity Distribution (CIRED), Frankfurt, no. 0892, 2011.

[67] J. Do Park and J. Candelaria, "Fault Detection and Isolation in Low-Voltage DC-Bus

Microgrid System," IEEE Transactions on Power Delivery, vol. 28, no. 2, 2013.

[68] D. Salomonsson, L. Söder, and A. Sannino, "Protection of Low-Voltage DC Microgrids," IEEE Transactions on Power Delivery, vol. 24, no. 3, pp. 1045–1053, 2009.

[69] J. Yang, J. E. Fletcher, and J. O'Reilly, "Short-Circuit and Ground Fault Analyses and Location in VSC-Based DC Network Cables," IEEE Transactions on Industrial Electronics, vol. 59, no. 10, pp. 3827–3837, 2012.

[70] W. Leterme, P. Tielens, S. De Boeck, and D. Van Hertem, "Overview of Grounding and Configuration Options for Meshed HVDC Grids," IEEE Transactions on Power Delivery, vol. 29, no. 6, pp. 2467–2475, 2014.

[71] J. Mohammadi, F. B. Ajaei, and G. Stevens, "DC Microgrid Grounding Strategies," Industrial and Commercial Power Systems Technical Conference, 2018.

[72] Y. S. Tzeng and C. H. Lee, "Assessment of Grounding Schemes on Rail Potential and Stray Currents in a DC Transit System," IEEE Transactions on Power Delivery, vol. 21, no. 4, 2006.

[73] G. E. G.Mauthe, E.Ruoss, "Development of High Current HVDC Circuit Breaker with Fast Fault Clearing Capability," IEEE Transactions on Power Delivery, vol. 3, no. 4, 1988.

[74] C. Meyer, M. Kowal, and R. W. De Doncker, "Circuit Breaker Concepts for Future High-Power DC-Applications," IAS Annual Meeting (IEEE Industry Applications Society), pp. 860–866, 2005.

[75] S. Krstic, E. L. Wellner, A. R. Bendre, and B. Semenov, "Circuit Breaker Technologies for Advanced Ship Power Systems," IEEE Electric Ship Technologies Symposium (ESTS), 2007.

[76] M. Callavik and A. Blomberg, "The Hybrid HVDC Breaker: An Innovation Breakthrough Enabling Reliable HVDC Grids," *ABB Grid Systems*, 2012.